UNDERSTANDING PECAM-1-MEDIATED MECHANOTRANSDUCTION: FROM THE PROTEIN TO THE VESSEL

Caitlin Collins

A dissertation submitted to the faculty of the University of North Carolina at Chapel Hill in partial fulfillment of the requirements for the degree of Doctor of Philosophy in the Curriculum of Cell and Molecular Physiology.

Chapel Hill
2013

Approved by:

Ellie Tzima, PhD

Keith Burridge, PhD

Richard Cheney, PhD

Carol Otey, PhD

Rich Superfine, PhD

ABSTRACT

CAITLIN COLLINS: Understanding PECAM-1-mediated mechanotransduction: from the protein to the vessel
(Under the direction of Ellie Tzima)

Hemodynamic forces are critical for endothelial cell (EC) function and vessel health. Platelet endothelial cell adhesion-1 (PECAM-1) has been identified as a critical endothelial mechanosensor that is required for transducing mechanical signals into intracellular signaling events; however, molecular mechanisms of PECAM-1-mediated mechanotransduction remain elusive. This dissertation investigates mechanosignaling and cellular responses directly linked to force transduction via PECAM-1.

In recent years, there has been increasing interest to understand how cells respond to tension on mechanosensitive proteins. Numerous studies investigating force-bearing integrins and have revealed that the cell responds to exogenous force by increasing cell-generated force that is proportional to the applied force. This change in cellular force manifests as an adaptive cellular stiffening response that allows the cell to resist the strain of the applied force. While much work has focused on cellular responses linked to integrins, other mechanosensitive proteins are now being probed. In Chapter II, I demonstrate that tension on PECAM-1 also results in an adaptive stiffening response. Furthermore, I demonstrate that, surprisingly, the PECAM-1-mediated mechanoresponse is not locally restricted to regions proximal to the site of force application, but rather global in nature. These data suggest that, contrary to previous thoughts, a localized mechanical perturbation can globally affect signaling cascades and cellular phenotype.

Mechanosensitive signaling within the endothelium is greatly influenced by the subendothelial matrix composition. In Chapter III, I investigate how the extracellular matrix (ECM) identity influences PECAM-1 mechanosignaling and cellular response to force. I demonstrate that, contrary to cells adherent on fibronectin, adhesion to collagen suppresses mechanical responsiveness to tension on PECAM-1, including adaptive stiffening and focal adhesion growth. I further identify PKA-mediated inactivation of RhoA as critical signaling axis that influences endothelial cell mechanics in response to tension on PECAM-1 and the physiological stimulus of fluid shear stress *in vitro* and *in vivo*. Taken together, the work presented in this dissertation advances our understanding of how endothelial cells integrate mechanical and extracellular matrix-specific cues and provides insight into how these factors may contribute to cellular phenotype *in vivo*.

ACKNOWLEDGEMENTS

First and foremost I would like to thank my advisor, Ellie Tzima, for giving me guidance, support, knowledge, confidence, and opportunities to grow as a scientist. I met Ellie while interviewing at UNC and already knew at that point that I would be lucky to be part of her lab. She has been an excellent role model and mentor for many reasons. I respect her insight, immense enthusiasm for science, willingness to explore new territories, and her genuine care for her students. She has taught me to be confident in my ideas and myself. I am grateful for her support and guidance, both of which helped me mature as a scientist.

I would also like to thank everyone in the Tzima lab, past and present: Zhongming Chen, Chris Givens, Tyler Moser-Katz, Maggie McCormick, Dan Sweet, Meghan Childs, Sruthi Cherkur, Yunhao Liu, and Meredith Brown. They have been great co-workers and wonderful to work with on a daily basis. Dan and Maggie were excellent examples of what a great grad student should be. I consider them to be not only colleagues, but also good friends, despite subjecting me to all things Philly. I would also like to thank Zhongming for not only helping me with studies included in this dissertation, but also for always being kind and for giving me many good laughs. Finally, I want to thank Chris, Sruthi, and Moserkat for always being helpful, enthusiastic, and optimistic. For these reasons, and many others, they have been excellent people to work with on a daily basis.

I have also relied on so many amazing people for their insight, expertise, and kindness during my time at UNC. Much of this work would not have been possible without the help of great collaborators in the Superfine, Burridge, and Hahn labs. I have been very lucky to work with such kind and talented people. The Superfine lab has been a second

scientific home to me during my 5 years at UNC, and I am grateful to Rich and all of his lab members for being extremely welcoming and helpful. Without their help, my project would not have been possible. I would also like to thank Keith Burridge and the Burridge lab members for their kindness and assistance throughout all stages of my graduate studies. While many members of the Superfine, Burridge, and Hahn labs have been extremely helpful, I would particularly like to acknowledge Christophe Guilluy, Luke Osborne, Chris Welch, and Tim O'Brien. All of these people directly contributed to work presented in this dissertation and were a pleasure to work with. I could not have asked for more kind or helpful collaborators. Finally, I would to thank my thesis committee members for their helpful discussions and invaluable insight and the Cell and Molecular Physiology administration team for providing support and assistance over the past 5 years.

I am extremely grateful for the love and support of many great friends, both near and far. I am lucky to have made many new friends during my time in North Carolina, and I'm thankful to those who have contributed to my happiness and well-being during graduate school, particularly Maggie McCormick, Luke Osborne, and Jenny Heppert. I spent nearly every day of the first four years of my graduate studies beside Maggie and formed a unique and lasting bond with her. She is smart and caring, and I'm lucky to have formed a great friendship with her. Luke has both challenged me and shared many laughs with me. I appreciate his thoughtfulness, generosity, humor, and sarcasm more than he knows. Jenny is perhaps the most kind and genuine person I have ever met. She is a brilliant thinker and great listener, and I'm grateful to have run countless miles by her side. My time in Chapel Hill would not have been nearly as memorable without these (and many other) friends. I also want to thank four extremely important people in my life – Anna Wipprecht, Kelly Young, Emily Ross-Teague, and Kristin Lawrence. Although I don't get to see them nearly as much as I would like, their friendship means the world to me.

Finally, I'd like to thank my family for all of their love and support over the past 27 years. My parents, Dave and Barb, have always been my biggest supporters and have given me the confidence to pursue any and all of my dreams. They are two of the most loving and caring people I know, and I am extremely proud to be their daughter. I would not be where I am today without them, and for that, I am eternally grateful. Finally, I'd like to thank my sisters, Emily and Kim, brothers-in-law, Mike and Matt, and the newest addition to our family, my nephew, Owen. I am incredibly lucky to have so many wonderful people in my life and a part of my family.

For the work presented in Chapters II and III, I would like to thank Dr. Robert Bagnell and the UNC Lineberger Cancer Center Microscopy Facility for help with microscopy studies. For the work presented in Chapter II, I would also like to thank Marie Rougié for assistance with FRET experiments and Luke Osborne and Ben Rardin for calculating magnetic forces used in the study. The work presented in this dissertation was supported in part by an NIH grant (HL088632) to E.T, the Dr. Susan Fellner Physiology Graduate Student Research Fellowship (to C.C.) and an American Heart Association Predoctoral fellowship (12PRE119300000) to C.C.

PREFACE

The work presented in Chapter II was previously published in *Current Biology* in November 2012. My roles in this project included designing and performing experiments, analyzing data, and writing the manuscript. Christophe Guilluy performed the Rho pulldowns. Christopher Welch performed the FRET analyses and Tim O'Brien helped with magnetic tweezers experiments. Ellie Tzima was the principal investigator and helped design experiments and write the manuscript.

The citation for the manuscript is as follows: Collins C, Guilluy C, Welch C, O'Brien ET, Hahn KM, Superfine R, Burridge K, and Tzima E. Localized tensional forces on PECAM-1 elicit a global mechanotransduction response via the integrin-RhoA pathway. *Current Biology*, 2012, 22(22):2087-94.

The work described in Chapter III has been submitted for publication. My roles in this project included designing and performing experiments, analyzing data, and writing the manuscript. Luke Osborne performed the passive microbead rheology studies. Christophe Guilluy performed the Rho pulldowns. Ellie Tzima was the principal investigator and helped design experiments and write the manuscript.

Part of the Discussion included in Chapter IV was previously published in a commentary in *Small GTPases* in March 2013. The citation for the manuscript is as follows: Collins, C and Tzima, E. RhoA goes GLOBAL. *Small GTPases*, 2013, 4(2).

TABLE OF CONTENTS

LIST OF FIGURES

LIST OF ABBREVIATIONS

AFM	atomic force microscopy
CL	collagen
EC	endothelial cell
ECM	extracellular matrix
eNOS	endothelial nitric oxide synthase
ERK	extracellular signal-related kinase
ET-1	endothelin-1
FAK	focal adhesion kinase
FG	fibrinogen
FN	fibronectin
FRET	fluorescence resonance energy transfer
GAP	GTPase activating protein
GDI	GDP dissociation inhibitor
GEF	guanine nucleotide exchange factor
GPCR	G-protein coupled receptor
ICAM-1	intracellular adhesion molecule-1
Ig	immunoglobulin
ITIM	immunoreceptor tyrosine-based inhibitory motif
JNK	c-Jun N-terminal kinase
kD	kilodalton
KLF2/4	krüppel-like factor 2/4
LDL	low density lipoprotein
LN	laminin
MSD	mean-squared displacement
NF-κB	nuclear factor kappa-light-chain-enhancer of activated B cells

NO	nitric oxide
oxLDL	oxidized low density lipoprotein
PAK	p21 activated kinase
PDMS	polydimethylsiloxane
PECAM-1	platelet endothelial cell adhesion molecule-1
PI3K	phosphatidylinositol 3-kinase
PKA	protein kinase A
PKC	protein kinase C
pMLC	phospho-myosin light chain
pN	piconewton
ROCK	Rho-associated kinase
RTK	receptor tyrosine kinase
SFK	Src family kinase
TEM	transendothelial migration
VE-cadherin	vascular endothelial cadherin
VCAM-1	vascular cell adhesion molecule-1
VEGFR2	vascular endothelial growth factor receptor 2
VSMC	vascular smooth muscle cell

CHAPTER I.

Introduction

Forces in biology.

Mechanical forces influence nearly all aspects of cell behavior. Because forces are central to a number of biological processes, cells are decorated with numerous mechanosensitive proteins that work in concert to regulate the cellular response to external mechanical stimuli, such as stretch or shear stress. In addition to external forces, cells also generate their own forces via actomyosin-based contractility, and cell-generated forces are required for cellular processes, such as adhesion and maintenance of cell-cell junctions[1, 2]. In light of evidence highlighting the central role of mechanical forces in basic biological processes, much work has focused on understanding cellular response to force on various mechanosensitive proteins.

The best characterized mechanosensors to date are tension-bearing integrins that couple the extracellular matrix (ECM) to the internal actin cytoskeleton. It was first noted that mechanical stress applied to β1 integrins results in force-induced focal adhesion growth and a simultaneous force-dependent stiffening response[3]. Much work over the past twenty years has focused on understanding the molecular mechanisms behind these observations, and it has become apparent that the small GTPase RhoA plays a central role in the regulation of the cellular response to force. RhoA is activated downstream of tension on integrins via two guanine nucleotide exchange factors (GEFs), GEF-H1 and LARG[4]. Activation of the GTPase is required for both the stiffening response[4] and focal adhesion

growth[4, 5]. Other signaling molecules have also been implicated in the cellular response to force, as tension on integrins also elicits activation of Src[6], focal adhesion kinase (FAK)[4], and extracellular-signal related kinase (ERK)[4]. Inhibition of any of these kinases, as well as inhibition of myosin ATPase and Rho-associated protein kinase (ROCK)[7], blocks stiffening, indicating that coordination of numerous signaling molecules is required for the cellular response to force. In addition to activation of molecular signaling cascades, the force response also entails recruitment of signaling and structural proteins to the site of applied stress. Force-dependent stiffening involves the recruitment of focal adhesion proteins such as β1 and β3 integrins that function to reinforce force-bearing adhesions[8]. Other data suggest that changes in gene expression may also contribute to mechanical coupling of integrins with the extracellular matrix, as mRNAs and ribosomes redistribute to sites of mechanically stressed integrin adhesions[9]. In recent years, researchers have begun to probe other mechanosensitive proteins such cadherins[10-12] and platelet endothelial cell adhesion molecule-1 (PECAM-1)[13]. The work in this dissertation contributes to our understanding of the cellular response to tension on PECAM-1.

The endothelium and shear stress.

The endothelium is composed of a single layer of endothelial cells (ECs) that line the lumen of the blood vessel and form the interface between the circulating blood and underlying tissue. Due to their unique location within the vessel wall, ECs are constantly exposed to hemodynamic forces produced by blood. The parallel frictional force of blood flow, termed fluid shear stress, is a critical determinant of vessel health and disease. Because of the importance of hemodynamic forces in vessel health, ECs are equipped with numerous mechanosensitive protective that transduce the physical force of blood flow into various intracellular biochemical signals. Proposed mechanosensors line all surfaces of ECs and include, but are not limited to: G-protein coupled receptors (GPCRs), receptor

tyrosine kinases (RTKs), ion channels, caveolae, integrins, and a mechanosensory complex composed of PECAM-1, vascular endothelial (VE)-cadherin, and vascular endothelial growth factor receptor 2 (VEGFR2)[14]. While only the apical surface of the endothelium is exposed to shear stress, a 'decentralised' model of mechanotransduction has proposed that the shear forces are transmitted to distant cellular sites (such as cell-cell junctions, focal adhesions, and the nucleus) through the actin cytoskeleton[15] (Fig.1.1). Therefore, the actin cytoskeleton also has a well-defined role in mechanotransduction of shear stress. While signaling through many of these mechanosensors likely acts synergistically to influence the EC phenotype, it is important to understand the contributions of individual mechanoreceptors. This dissertation will focus on PECAM-1-mediated mechanotransduction, described in greater detail below.

Endothelial responses to shear stress differ depending on the magnitude and pattern of blood flow. In regions of the vessel where blood flow is low (<5 dyn/cm^2) and disturbed, such as regions of high curvature and vessel bifurcations, ECs exist in a constitutively activated, proinflammatory state. Thus, ECs in these regions display chronic activation of the inflammatory transcription factor nuclear kappa-light-chain enhancer of activated B cells (NF-κB) and augmented expression of cell adhesion molecules such as vascular cell adhesion molecule-1 (VCAM-1) and intracellular adhesion molecule-1 (ICAM-1), which promote leukocyte transendothelial migration (TEM) and development of atherosclerotic plaques[16]. Conversely, ECs in regions of the vessel that experience unidirectional, laminar flow often display an atheroprotective gene expression profile, including expression of anti-inflammatory genes, such as Krüppel-like factors 2 and 4 (KLF 2/4), endothelin-1(ET-1), and elevated production of the vasodilator nitric oxide (NO)[17]. Importantly, these regions of the vasculature also display relatively low incidence of atherosclerotic plaque development. Work from the past several decades has highlighted fluid shear stress as a critical determinant of atherosclerotic plaque development, although many of the molecular

mechanisms of mechanotransduction remain elusive. Thus, identifying molecular signaling cascades activated downstream of specific mechanosensors, such as PECAM-1, may reveal insights into some of the earliest events that contribute to development of disease.

PECAM-1 structure and function.

PECAM-1 is a 130 kilodalton (kD) protein that is expressed in ECs and other vascular cells of hematopoietic lineage, such as leukocytes and platelets. The extracellular domain of the protein contains 6 immunoglobulin (Ig)-like domains that impart adhesive properties to the protein. Ig-like domain 1 and 2 facilitate homophilic binding between PECAM-1 molecules on neighboring cells[18, 19]. However, PECAM-1 has also been shown to function as a heterotypic ligand for other proteins, such as αvβ3[20]. The protein contains a single transmembrane domain and a relatively short cytoplasmic tail that is important for PECAM-1 signaling function (Fig. 1.2). The cytoplasmic tail contains two immunoreceptor tyrosine-based inhibitory motifs (ITIMs) that are phosphorylated upon cellular activation. Src family kinase (SFK)-dependent phosphorylation of tyrosine residues Y_{663} and Y_{686} within the ITIM domains promote recruitment of SH2-containing proteins, such as SHP2, and lead to activation of downstream signaling cascades[21]. Thus, although the protein has no intrinsic catalytic activity, PECAM-1 has been implicated in multiple intracellular signaling cascades by serving as a scaffold for numerous adaptor molecules. Therefore, it is not surprising that PECAM-1 has a multifunctional role in vascular biology. The protein was first identified for its role in leukocyte TEM[22]. Later work also identified roles for PECAM-1 in angiogenesis[23], cell survival[24, 25], junctional integrity[26], immune cell signaling[27, 28], and shear stress signaling[29].

In the past decade, PECAM-1 has come to the forefront as a critical regulator of EC mechanotransduction. Several studies first identified that the protein is rapidly tyrosine phosphorylated upon mechanical perturbation of the plasma membrane by fluid shear

stress[30] or hyperosmotic shock[31], and later work demonstrated that PECAM-1 tyrosine phosphorylation is mediated by the SFK Fyn[32]. Tyrosine phosphorylation of the cytoplasmic tail results in activation of downstream signaling molecules such as ERK1/2, Akt, and endothelial nitric oxide synthase (eNOS)[31, 33]. Work from our lab identified PECAM-1 as part of a mechanosensory complex with VE-cadherin and VEGFR2 that mediates several EC responses to shear stress, including: activation of small GTPases[34], alignment of the actin cytoskeleton in the direction of flow[29], activation of the transcription factor NF-κB[29], and flow-mediated upregulation of cell adhesion molecules VCAM-1 and ICAM-1[35]. PECAM-1 also has clear roles in mechanotransduction *in vivo*, as PECAM-1$^{-/-}$ mice display impaired flow-mediated dilation[36], vascular remodeling[35], arteriogenesis[37], and altered atherosclerotic plaque formation[38-40]. Nevertheless, while studies clearly indicate a role for PECAM-1 in shear stress signaling *in vitro* and *in vivo*, molecular mechanisms of PECAM-1-mediated mechanotransduction remain elusive.

Extracellular matrix specific signaling.

Integrins are transmembrane receptors that couple the ECM to the internal actin cytoskeleton. The mammalian genome encodes 18 α integrin subunits and 8 different β subunits, which give rise to 24 distinct α/β heterodimers. Furthermore, α/β integrin composition dictates the ECM ligand for each heterodimer. Within the endothelium, EC adhesion to the ECM is largely mediated by $\alpha v\beta 3$ and $\alpha 5\beta 1$, which bind to fibronectin (FN), and $\alpha 2\beta 1$, which mediates adhesion to collagen (CL).

In addition to mediating adhesion to the ECM, integrins are also activated and initiate signaling in response to various stimuli, including fluid shear stress[41]. Importantly, shear stress elicits activation of divergent signaling cascades depending on the identity of the underlying ECM, due to signaling through diverse integrin classes. Furthermore, integrins

not in contact with their permissive substrate are actively inhibited due to a mechanism of transdominant inhibition[42]. Thus, fluid shear stress leads to activation of $\alpha v\beta 3$ and $\alpha 5\beta 1$ (while $\alpha 2\beta 1$ is inhibited) in ECs adherent on FN; whereas $\alpha 2\beta 1$ is activated in ECs on CL (while $\alpha v\beta 3$ and $\alpha 5\beta 1$ are actively inhibited). Furthermore, shear-induced integrin activation and ligation with the ECM is required for downstream signaling, such as activation of RhoA and alignment of the actin cytoskeleton[43].

Activation of distinct classes of integrins on disparate ECMs leads to divergent flow-induced signaling downstream of integrins. For instance, ECs adherent on basement membrane proteins such as CL and laminins (LN) display preferential activation of protein kinase A (PKA) and eNOS upon exposure to fluid shear stress when compared to ECs adherent on FN[44, 45]. Conversely, shear stress preferentially activates p21-activated kinase (PAK)[44, 46, 47], c-Jun N-terminal kinase (JNK)[47, 48], and the transcription factor NF-κB when ECs are adherent on FN[37]. Importantly, ECM-specific activation of distinct signaling pathways may not only influence the EC phenotype, but also the overall vessel health. PKA and eNOS (which are activated on CL) are considered anti-inflammatory[44, 49], while JNK and NF-κB have pro-inflammatory properties and have been shown to contribute to vascular diseases such as atherosclerosis[50, 51].

Mechanical and ECM heterogeneity in vivo.

The endothelial microenvironment i*n vivo* is complex and differs in both ECM composition and shear stress patterns, depending on the region of the vasculature (Fig. 1.3). Vessel geometry influences shear stress patterns, which are characterized by direction and magnitude. Regions of the vessel that are straight and unbranched, such as the descending aorta, experience unidirectional laminar shear stress, ranging from 12-70 dyn/cm^2, resulting in net forward movement of blood flow[52]. However, other regions of the vasculature under high curvature or at bifurcations or branch points are subjected to low (<5

dyn/cm^2) and/or disturbed shear stress that is characterized by a change in flow direction without a net forward movement. It has been recognized for decades that shear stress patterns greatly influence overall vessel health and integrity, as vascular disease such as atherosclerosis are highly focal and develop in regions of the vasculature, such as the aortic arch, that experience disturbed shear stress. Thus, ECs in regions of vasculature that experience high laminar flow often display a quiescent and atheroprotective gene expression profile, whereas regions of the vasculature subjected to low and disturbed shear stress exhibit chronic activation of pro-inflammatory signaling pathways, which contribute to local inflammation of the vessel and atherogenesis[52].

In addition to mechanical heterogeneity, the ECM composition also differs in distinct regions of the vessel. Most regions of the vasculature are rich in basement membrane proteins, such as collagen (types I, III, and IV) and laminins. However, provisional matrix proteins, including fibronectin (FN) and fibrinogen (FG), are deposited in regions of disturbed and oscillatory shear stress[51, 53]. As detailed in the previous section, alterations in the ECM composition have profound effects on EC biology and the overall health of the vessel.

Atherosclerosis is a complex and highly focal disease that develops in distinct regions of the vasculature. Evidence suggests that both shear stress patterns and ECM composition contribute to site-specific plaque development, as low and disturbed shear stress and FN are both associated with pro-inflammatory signaling within the endothelium. Furthermore, a direct relationship between shear stress patterns and ECM composition exists, as oscillatory shear promotes FN expression and deposition[51], and increased subendothelial FN content sustains pro-inflammatory signaling within the endothelium in a positive feedback loop[51]. Thus, due to the complex ECM and mechanical microenvironments *in vivo*, there is a need for *in vitro* experiments to dissect the contribution of each factor to EC signaling and understand how cells integrate signals from multiple inputs to regulate

their function. The work described in this dissertation sheds light on how ECs assimilate mechanical and ECM cues to regulate their phenotype *in vitro* and *in vivo.*

EC stiffness and vascular disease.

Several studies have identified a link between EC stiffness and decreased cardiovascular health. For instance, EC stiffness (as well as vessel stiffness) often increases in hypertensive vessels[54] and augmented EC stiffness positively correlates with increased permeability[55]. Furthermore, increased arterial stiffness promotes atherogenic signaling and contributes to development of atherosclerosis[56, 57]. Thus, identifying mechanisms of EC stiffening may have important implications for cardiovascular diseases.

Several stimuli have been show to influence EC stiffness, including shear stress[58]. However, signaling pathways directly linking hemodynamic force to EC stiffening remain elusive. Furthermore, the relationship between shear stress patterns and EC stiffness is complex and measurements of EC stiffness *ex vivo* are lacking. The work in this dissertation identifies mechanisms linking hemodynamic force and EC stiffening responses and may provide insight into complex relationships that influence cardiovascular health *in vivo*.

RESEARCH PRESENTED IN THIS DISSERTATION

As described in the following chapters, the goals of this dissertation are as follows:

CHAPTER II: IDENTIFY THE MOLECULAR MECHANISMS MEDIATING THE CELLULAR RESPONSE TO TENSION ON PECAM-1.

PECAM-1 has been identified as a critical regulator of endothelial cell mechanotransduction. However, molecular mechanisms of PECAM-1 mediated mechanotransduction remain elusive. In order to identify the signaling cascades and cellular responses directly linked to PECAM-1 mechanosignaling, I have utilized a magnetic tweezers system to directly apply force to PECAM-1. Previous studies have reported an adaptive stiffening response following force application to other mechanosensitive proteins. Here, I demonstrate that tension on PECAM-1 also initiates an adaptive stiffening response. Furthermore, this chapter will *1) Identify the signaling molecules that mediate the cellular response to tension on PECAM-1,* and *2) Determine the spatial and temporal regulation of the cellular response.* Finally, I demonstrate that localized tension on PECAM-1 elicits a global mechanotransduction response via the integrin-RhoA pathway.

CHAPTER III: DETERMINE HOW THE ECM COMPOSITION INFLUENCES PECAM-1-MEDIATED MECHANOTRANSDUCTION.

ECM-specific signaling is well documented within the endothelium and has profound effects on EC phenotype. In this chapter, I determine how the ECM influences mechanosignaling and cellular responses downstream of tension on PECAM-1. I demonstrate that ECs adherent on CL are less responsive to tension on PECAM-1 and do generate an adaptive stiffening response. I further identify that the lack of force response is due to force-dependent PKA activation and subsequent inactivation of RhoA. I further extend these findings to the physiological context of fluid shear stress and demonstrate that

force-dependent PKA activation influences EC stiffness and focal adhesion dynamics *in vitro* and *in vivo*.

CHAPTER IV: CONCLUSIONS AND PERSPECTIVES

In this Chapter, I address questions raised by the work presented in Chapters II and III. Furthermore, I discuss the significance of my findings in the fields of cell and cardiovascular biology. Finally, I elaborate on how my findings may relate to observations seen in the aortic endothelium *in vivo*.

Figures

Figure 1.1 Model of decentralised mechanotransduction of endothelial shear stress

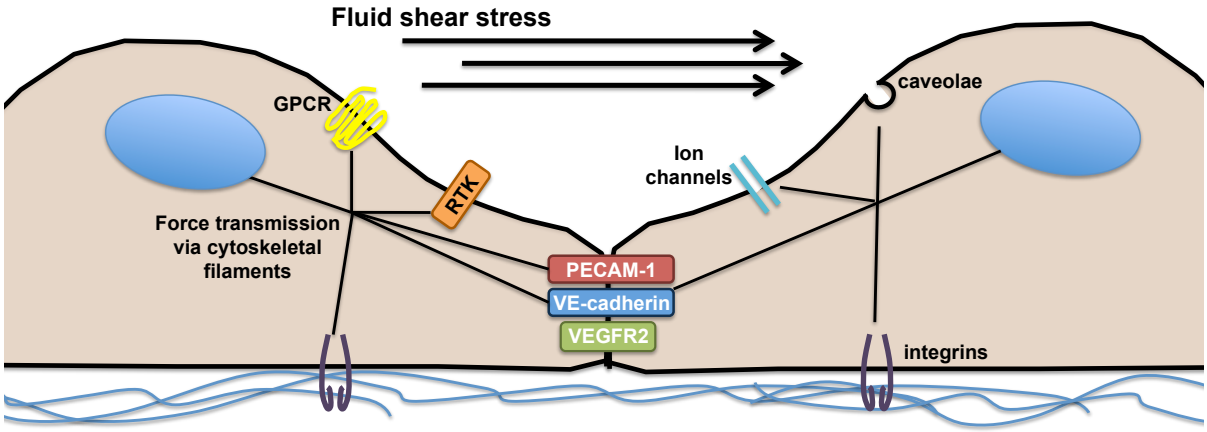

Deformation of the luminal surfaces of ECs can directly activate apical mechanosensors such as GPCRs, RTKs, ion channels and caveolae. Transmission of force through cortical and/or filamentous actin activates mechanosensors at distal sites, such as cell-cell junctions and/or integrins attached to the subendothelial matrix.

Figure 1.2 Important domains in PECAM-1 biology

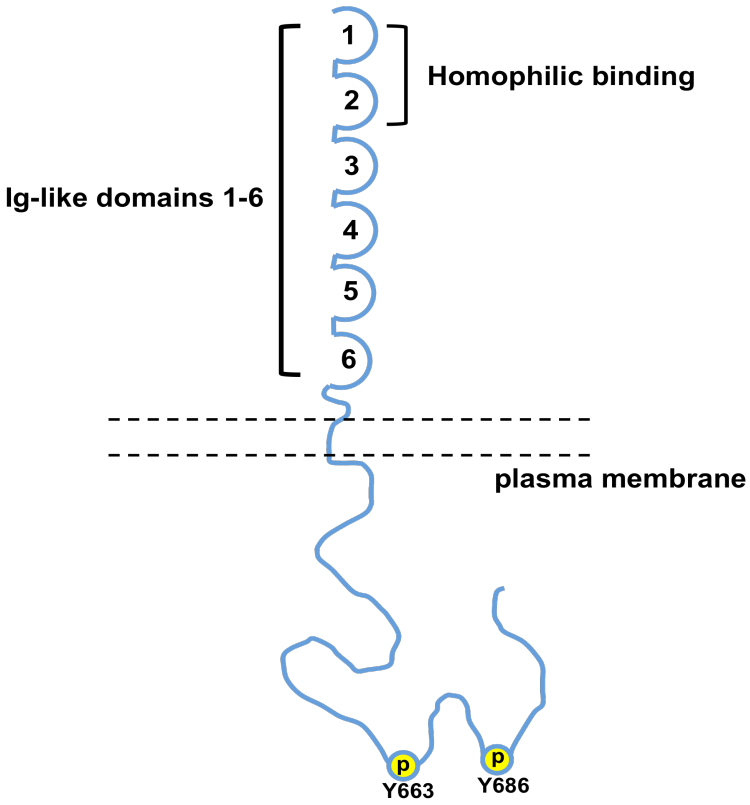

A cartoon representing domains important for PECAM-1 function. The protein has 6 extracellular Ig-like domains, a single pass transmembrane domain, and a relatively short cytoplasmic tail. Tyrosine residues Y663 and Y686 within intracellular ITIM domains are phosphorylated upon cellular activation and are critical for downstream signaling.

Figure 1.3 Mechanical and ECM heterogeneity *in vivo*.

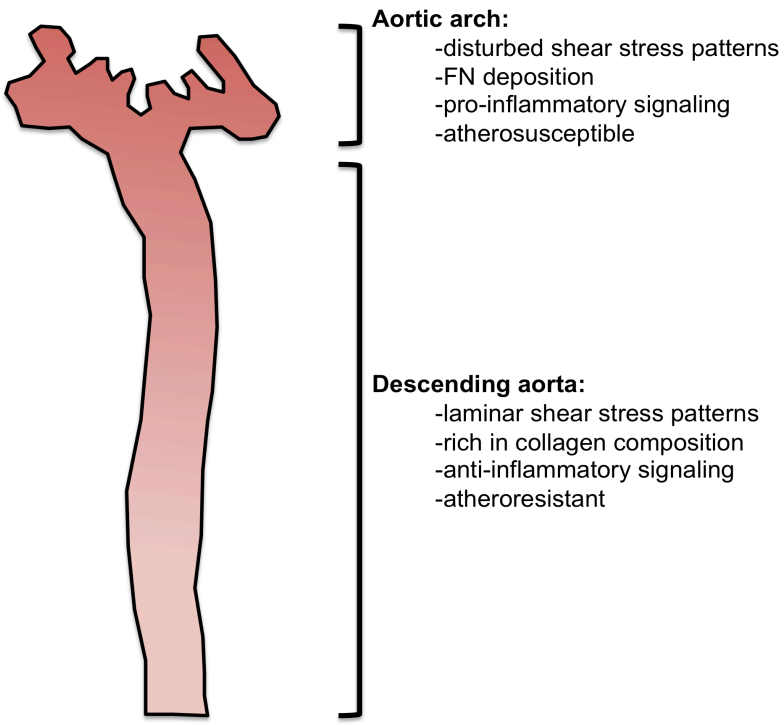

A summary of mechanical and ECM properties in the aortic arch and descending aorta. Both mechanical stimuli and ECM composition influence EC signaling cascade and phenotypes.

CHAPTER II.

Localized tensional forces on PECAM-1 elicit a global mechanotransduction response via the integrin-RhoA pathway

Overview

Background: Mechanical forces regulate cell behavior and function during development, differentiation, and tissue morphogenesis. In the vascular system, forces produced by blood flow are critical determinants not only of morphogenesis and function, but also pathological states such as atherosclerosis. Endothelial cells (ECs) have numerous mechanotransducers, including platelet endothelial cell adhesion molecule-1 (PECAM-1) at cell-cell junctions and integrins at cell-matrix adhesions. However, the processes by which forces are transduced to biochemical signals and subsequently translated into downstream effects are poorly understood.

Results: Here, we examine mechanochemical signaling in response to direct force application on PECAM-1. We demonstrate that localized tensional forces on PECAM-1 result in, surprisingly, global signaling responses. Specifically, force-dependent activation of phosphatidylinositol 3-kinase (PI3K) downstream of PECAM-1 promotes cell-wide activation of integrins and the small GTPase RhoA. These signaling events facilitate changes in cytoskeletal architecture, including growth of focal adhesions and adaptive cytoskeletal stiffening.

Conclusions: Taken together, our work provides the first evidence of a global signaling event in response to a localized mechanical stress. In addition, these data provide a possible mechanism for the differential stiffness of vessels exposed to distinct hemodynamic force patterns *in vivo*.

Introduction

Mechanical forces are involved in nearly all aspects of biology [59]. Within the vascular system, hemodynamic forces produced by blood flow play a critical role in EC biology and maintenance of the vascular homeostasis. Cells respond to mechanical stresses on mechanosensitive proteins, such as integrins, by employing an adaptive cellular stiffening response in an effort to resist increased tensile strain [3, 7, 60]. Adaptive cellular stiffening requires the coordination of mechanically activated signaling cascades, including the small GTPase RhoA and its effectors, which mediate local changes in focal adhesion growth and actomyosin contractility [5, 7, 61].

Within the vascular system, ECs lining the lumen of blood vessels are positioned to experience constant force as a result of the shear stress of blood flow. Hemodynamic forces influence EC biology and play an integral role in determining the health and integrity of the vessel. To this regard, ECs are decorated with numerous mechanosensors that function to convert mechanical forces into defined biochemical signaling cascades. We have previously identified PECAM-1 as a key endothelial mechanosensor that influences vessel physiology and pathology [29, 38, 39], yet insights into cellular responses directly linked to PECAM-1-dependent force transduction are lacking.

Here, we use a magnetic tweezers system and a permanent ceramic magnet to investigate cellular responses to mechanical tension on PECAM-1. We reveal a mechanotransduction pathway that involves integration of signaling between two mechanosensors at distinct cellular sites. Specifically, force transduction via PECAM-1 promotes integrin-dependent RhoA activation, leading to focal adhesion growth and adaptive cellular stiffening. Furthermore, we provide evidence that local mechanical stimulation of PECAM-1 can initiate a global cellular response, providing new insights into the spatial regulation of mechanochemical signaling cascades.

Results

Tensional forces on PECAM-1 result in adaptive cellular stiffening and mechanosignaling

In order to investigate mechanoresponses downstream of PECAM-1, we applied tensional forces, using magnetic tweezers [62], to paramagnetic beads bound to endogenous PECAM-1 on ECs adherent on fibronectin (FN) (Fig. S2.1A). Brief force application (~100pN) revealed a typical viscoelastic-creep response similar to those seen with bead-integrin linkages [7] (Figure S2.1B). Application of successive pulsatile forces on PECAM-1 resulted in a significant decrease in pulse-to-pulse bead displacement in latter pulses, indicative of force-dependent adaptive stiffening (Fig. 2.1A). Furthermore, average bead displacement decreased approximately 40% by the end of the 2-minute time course, indicating a 40% increase in cell stiffness with a calculated time constant of 39.93 seconds (Fig. S2.1C). Notably, bead displacement decreased without significant displacement of cellular organelles, such as the nucleus (Fig. S2.1D), and analysis of bead recovery following each pulse of force revealed a 90-95% recovery from each pulse of force (Fig. S2.1E), suggesting that baseline drift in bead recovery is negligible in the adaptive response. Importantly, adaptive stiffening was specific to anti-PECAM-1-coated beads, as force application to poly-lysine-coated beads did not initiate a mechanical response (Supplementary Fig. S2.1F). Previous work demonstrated activation of PI3K downstream of PECAM-1[29]. In order to examine PI3K activation in response to localized tensional forces on PECAM-1, magnetic beads bound to ECs expressing a GFP-PH fusion protein (which serves as a sensor for PI3-lipids) were subjected to force using a permanent ceramic magnet. Brief force application was sufficient to induce PI3K activation around anti-PECAM-1-coated beads (Fig. 2.1B). Recruitment around the bead was specific to PECAM-1 and not due to perturbation of the membrane, as ECs transfected with GFP alone (Fig. S2.1G) or ECs incubated with poly-lysine-coated beads (Fig. S2.1H) did not display recruitment in

response to force. In order to examine if PI3K activation is required for adaptive cytoskeletal stiffening, pharmacological inhibitors were used to block PI3K activation. Pretreatment of ECs with PI3K inhibitors, LY294002 (Fig. 2.1C) and wortmannin (data not shown), or inhibition of actin polymerization with Cytochalasin D (Fig. 2.1C), abolished adaptive stiffening, suggesting a requirement for both biochemical signaling and cytoskeletal remodeling. In addition to an impaired response to mechanical force on PECAM-1, cells pretreated with Cytochalasin D also exhibited a decrease in basal cell stiffness, indicated by a significant increase in absolute bead displacement during the first pulse of force (Fig. S2.1I).

PECAM-1-mediated adaptive stiffening is an integrin-dependent process

Growing evidence suggests that the integrin-extracellular matrix (ECM) adhesions function as sites of mechanotransduction, where upon application of external forces on integrins, an intracellular response is activated that leads to local focal adhesion assembly and associated cytoskeletal strengthening [3, 4, 60]. We therefore examined if integrin ligation with the underlying ECM plays a role in force transmission via PECAM-1. We used a blocking (16G3) or nonblocking (11E5) antibody to inhibit new integrin-FN connections without disrupting existing adhesions [43]. Inhibition of force-induced integrin engagement with the FN blocking antibody attenuated PECAM-1-mediated adaptive stiffening, whereas the nonblocking antibody had no effect (Fig. 2.2A). These data suggest that new integrin-FN connections are required for adaptive stiffening, and indicate that the mechanical response requires input from more than one mechanosensor. Next, we tested the possibility that new integrin-FN connections are required for force-induced PI3K activation. To this regard, inhibition of new integrin-FN connections had no effect on force-dependent PI3K activation (Fig. 2.2B), as ECs subjected to force showed similar levels of activation in

the presence of the blocking and nonblocking antibodies. These data suggest that PI3K activation is upstream of integrin ligation with the underlying ECM.

Tensional forces on PECAM-1 activate the RhoA pathway via GEF-H1 and LARG

Local activation of the small GTPase RhoA has been implicated in adaptive cellular stiffening in response to mechanical stresses on integrins [4, 7]. To investigate the role of the RhoA pathway in adaptive stiffening downstream of PECAM-1, ECs were pretreated with C3 transferase or Y27632, Rho and ROCK inhibitors, respectively, prior to force application. Inhibition of either Rho or ROCK attenuated adaptation to force (Fig. 2.3A), suggesting a role for the RhoA pathway in adaptive stiffening. We therefore hypothesized that tensional forces on PECAM-1 lead to RhoA activation, which is required for cytoskeletal adaptation to force. To test this hypothesis, we performed Rho pulldown assays to detect levels of active RhoA. ECs were incubated with anti-PECAM-1-and stimulated with continuous force (~10pN) using a permanent magnet for biochemical analyses. Indeed, ECs subjected to tensional force on PECAM-1 displayed robust and sustained RhoA activation in response to force, as levels of GTP-loaded RhoA increased at 5 minutes of force application and remained elevated at 30 minutes of sustained force (Fig. 2.3B). Force-induced RhoA activation was specific to PECAM-1, as poly-lysine-coated beads did not increase levels of active RhoA in response to force (Fig. S2.2). Interestingly, PECAM-1-mediated RhoA activation was integrin-dependent, as inhibition of new integrin-FN connections quenched force-induced RhoA activity (Fig. 2.3C).

We next sought to identify the guanine nucleotide exchange factors (GEFs) that mediate force-induced RhoA activation by performing affinity pulldowns with a nucleotide-free RhoA mutant (G17A) [63]. Analysis revealed a force-dependent increase in GEF-H1 and LARG activity, while the activity of other GEFs, such as Dbl, Vav, and Net1 were unaffected (Fig. 2.4A). Interestingly, these GEFs also mediate RhoA activation in response to tensional

forces on FN-binding integrins [4]. It was also reported that mechanical activation of GEF-H1 relies on activation of a FAK/ERK pathway. Previous studies have demonstrated force-dependent activation of ERK downstream of PECAM-1 [31, 32, 64]. In agreement with previous reports, in response to tensional forces on PECAM-1, we observed a force-dependent increase ERK activation, as well as FAK phosphorylation (Fig. 2.4B). Furthermore, inhibition of FAK or ERK activity with pharmacological inhibitors (FAK 14 or U0126, respectively), attenuated force-induced GEF-H1 activation, while LARG activity was unaffected (Fig. 2.4C). These data suggest a common pathway employed for GEF activation in response to tension on diverse adhesion molecules, and, therefore, may represent a conserved mechanosensitive pathway. In order to confirm a role for GEF-H1 and LARG in PECAM-1-mediated RhoA activation, siRNAs were used to knockdown these GEFs in ECs. Depletion of GEF-H1 and LARG with specific siRNAs attenuated RhoA activation and adaptive cellular stiffening in response to tensional forces on PECAM-1 (Fig. 2.4D,E), further supporting a role for these GEFs in PECAM-1-dependent stiffening.

Localized tensional forces on PECAM-1 a global mechanotransduction response

Our data suggest that force-induced RhoA activation downstream of PECAM-1 is integrin-dependent (Fig. 2.3C). In order to assay integrin activation in response to tensional force on PECAM-1, ECs were immunostained for ligated β_1 integrin (Fig. 2.5A). Unexpectedly, we observed a global increase in β_1 integrin ligation, rather than a local response confined to the region proximal to the bead under tension. This result was surprising, as previous studies applying tensional forces on other adhesion receptors demonstrated a local cellular response restricted to the site of mechanical stress [60]. Cells were assayed for the ratio of “global” versus “local” integrin activation, where “local” was defined as the region with a 5 micron radius from the site of bead attachment and the rest of the cell was deemed “global.” As seen in Supplementary Figure S2.3, while total intensity of

activated integrin staining increased with force, the ratio of local to global integrin activation did not significantly change. These data suggest that all areas of the cell can activate integrins to a similar level and indicate that there is no preferential localization of integrin activation.

PI3K has been implicated in integrin activation in numerous cell types, including ECs in response to shear stress. To this regard, pharmacological inhibition of PI3K attenuated PECAM-1-mediated integrin ligation with the ECM (Fig. 2.5B), suggesting that PI3K activation is required for global integrin activation. We hypothesized that soluble lipid products produced by activated PI3K may promote cell-wide integrin activation. Previous studies have employed the overexpression of a GFP-PH construct to sequester cellular phospholipid messengers [65], as overexpression of GFP-PH restricts the mobility of cellular lipid messengers and affects downstream signaling. In order to test the hypothesis that mobility of PI3K lipid products is required for global integrin activation, we applied force to PECAM-1 on ECs overexpressing GFP-PH and assayed integrin-ECM ligation. Overexpression of the PH domain (which sequesters PI3K-mediated lipids) inhibited global integrin activation (Fig. 2.5C). This effect was specific, as overexpression of GFP alone did not affect force-induced β_1 integrin activation. These data suggest that activation of PI3K and production of a soluble second messenger promotes global integrin activation at sites remote from the applied force.

In light of our data indicating global integrin activation in response to a localized force on PECAM-1, we next tested if downstream RhoA activation was also a global response using a RhoA biosensor that detects RhoA activation via fluorescence resonance energy transfer (FRET) [66]. ECs transfected with the biosensor were subjected to force for the indicated times and fixed for subsequent FRET analysis. Importantly, fixation did not significantly affect the FRET signal intensity or localization (Fig. S2.4A). Consistent with our biochemical assays, we detected a statistically significant increase in RhoA activation after 5

minutes of force (Fig. 2.6A). A trend for increased RhoA activation remained at 30 minutes, but was no longer significant, as 30% of the population had returned to basal levels by this time point. These results are not surprising, as it has been demonstrated that, under chronic force, ECs dampen activated signaling networks to maintain homeostasis. Importantly, a significant increase in FRET was exclusive to anti-PECAM-1-coated beads, as poly-lysine-coated beads did not display increased activation in response to force. In agreement with the ligated β_1 integrin immunostaining, ECs also displayed a remarkable cell-wide increase in RhoA activity in response to force on PECAM-1 (Fig. 2.6A), as RhoA activity increased equally in local and global regions of the cell (Fig. S2.4B). In contrast to PECAM-1, tensional forces on FN-binding integrins did not induce global RhoA activation (data not shown).

Adaptive cellular stiffening is mediated, in part, by a local increase in focal adhesions at the site of mechanical stress that function to resist the applied force [5, 8, 67]. To further explore the possibility that localized force on PECAM-1 could lead to a global cellular response, we assessed focal adhesion growth by immunostaining for the focal adhesion marker vinculin. Remarkably, ECs exhibited a cell-wide increase in focal adhesion number, as well as individual focal adhesion size in response to tensional forces on PECAM-1 (Fig. 2.6B). These results further support the notion that a local force on PECAM-1 promotes a global signaling and cytoskeletal response.

Discussion

The present study provides insights into a mechanochemical signaling pathway downstream of PECAM-1 that relies on signals from multiple inputs, including mechanosensors at other transduction sites, such as integrins (Fig. 2.6C). We propose that force application on PECAM-1 results in PI3K activation, which leads to global activation of integrins and subsequent global RhoA activation via GEF-H1 and LARG. Activation of the

GTPase promotes changes in cytoskeletal organization, including adaptive stiffening of the cytoskeleton and a cell-wide growth of focal adhesions. Using pharmacological inhibitors, we show that numerous signaling molecules work in concert to facilitate adaptive cellular stiffening. Interestingly, cells treated with cytoskeletal inhibitors (Cytochalasin D, C3, and Y27632) are immediately impaired and cannot respond to force (pulses 2-11, Figs. 2.1C, 2.3A), whereas inhibition of new FN-integrin connections does not impair the mechanical response until latter pulses (pulses 5-11, Fig. 2.2A). These data suggest that pre-existing tension within the cytoskeleton is required for the immediate response to force, while new FN-integrins interactions are required for strengthening of adhesions and adaptive stiffening. At the present time it is difficult to determine if adaptive stiffening is a cell-wide phenomenon or a local event that occurs proximal to the site of force application. However, a global increase in focal adhesion size and number suggests that regions of the cell distal from the site of mechanical stress are responsive to exogenous force.

Previous studies probing integrins reported rapid mechanosignaling propagated through tensile cytoskeletal elements to remote cytoplasmic locations away from the site of mechanical stress [6, 68, 69]. However, these signals were not global and diffuse, but rather confined to distinct foci that corresponded with sites of cytoskeletal deformation. Thus, we provide the first evidence of a global signaling event in response to a localized mechanical stress.

While PECAM-1 has not been shown to directly interact with the cytoskeleton, indirect association via cytoplasmic interactions with β-catenin and γ-catenin have been proposed[70, 71]. Although we cannot rule out that mechanical signaling through tensile cytoskeletal elements may contribute to PECAM-1-mediated mechanotransduction, our data suggest that chemical signaling (via activated PI3K) is required for a global cellular response, such as integrin activation. We also observed a delayed cellular stiffening response following force application on PECAM-1 compared to the immediate stiffening

response reported when probing integrins [4, 7]. This delayed response further suggests involvement of a chemical signaling component, as an exclusively mechanical response would be expected to occur on a millisecond timescale. Future studies with PECAM-1 cytoplasmic tail truncation mutants may provide insight into the relative contributions of mechanical and chemical signaling components in adaptive stiffening.

Our study also highlights cooperation of two mechanosensors (PECAM-1 and integrins) in the EC response to force. Previous studies have highlighted a complex relationship between PECAM-1 and integrins. PECAM-1/PECAM-1 homophilic engagement can upregulate function of β_1 integrins in numerous cell types. Crosslinking of PECAM-1 on specific subsets of T-lymphocytes increases β_1–mediated adhesion [72]. In addition, engagement of PECAM-1 on platelets increases integrin-dependent adhesion and aggregation [73]. Our data suggest that PECAM-1-mediated mechanosensing may also promote β_1–mediated adhesion in ECs, as tension on PECAM-1 initiates β_1 ligation with the underlying extracellular matrix. Furthermore, β_1 integrin engagement has also been shown to mediate tyrosine dephosphorylation of the cytoplasmic tail of PECAM-1, which may influence PECAM-1-mediated signaling [74]. Therefore, it is possible that a complex feedback loop may be present in our system. Importantly, a complex relationship between PECAM-1 and $\alpha_v\beta_3$ also exists. $\alpha_v\beta_3$ serves as a heterotypic ligand for PECAM-1, and interaction between these proteins may be important for endothelial functions such as leukocyte transendothelial migration and angiogenesis [20]. While we focus on the β_1 integrin subtype, $\alpha_v\beta_3$ integrins may also contribute to the EC response to force. At the present time, we cannot differentiate the contribution of the different FN-binding integrin subtypes to the cellular response to tension on PECAM-1. However, previous studies have implicated a role for $\alpha_5\beta_1$ clustering in the formation of adhesions that experience strong matrix forces, while $\alpha_v\beta_3$ integrin heterodimers strengthen integrin-cytoskeleton linkages in a talin-dependent

manner [75]. Therefore, it is likely that multiple integrin subtypes may also be involved in PECAM-1-mediated mechanotransduction.

Atomic force microscopy (AFM) studies have revealed that ECs in regions of the vasculature that experience disturbed hemodynamics, and are thus predisposed to development of atherosclerotic plaques, exhibit increased stiffness when compared to ECs in healthy regions of the vessel [76]. Interestingly, regions of disturbed shear stress are also rich in FN deposition [53, 77], which, we now show, promotes a stiffer cellular phenotype. Therefore, our work may provide insights into early signaling events that contribute to cellular stiffening and plaque development.

Figures

Figure 2.1 Tensional forces on PECAM-1 result in adaptive cellular stiffening and PI3-kinase activation.

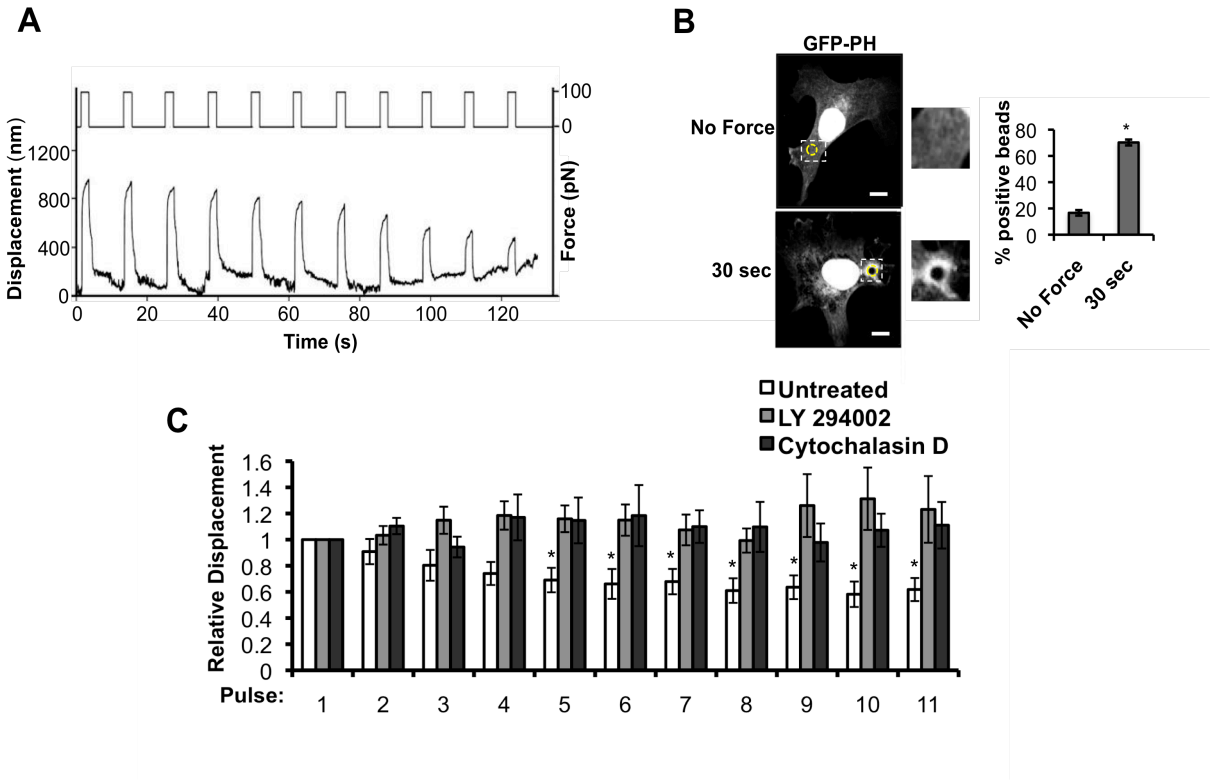

(A) Schematic of experimental design. Two-second pulses of force (~100 pN) separated by 10-second intervals over a 2-minute time course. Representative example of bead displacement in response to the pulsatile force regimen. Stiffening is indicated by decreased displacement during latter pulses. (B) ECs expressing GFP-PH were incubated with anti-PECAM-1-coated magnetic beads and subjected to force with a permanent ceramic magnet for the indicated times. Cells were fixed and scored for GFP-PH recruitment around the bead (box). Location of the bead is highlighted by the yellow circle (n > 50 cells/condition from 3 independent experiments; scale bar = 10μm). (C) Average

relative anti-PECAM-1 bead displacements induced by the pulsatile force regimen. In some experiments, cells were pretreated with LY294002 (30μM for 20 min) or Cytochalasin D (10μM for 30 min) prior to incubation with magnetic beads. Average displacements were calculated relative to the first pulse of force. (n >15 beads/condition from 3 independent experiments). Error bars represent s.e.m., *$p<0.05$.

Figure 2.2 PECAM-1-mediated adaptive cellular stiffening, but not PI3K activation, is integrin-dependent.

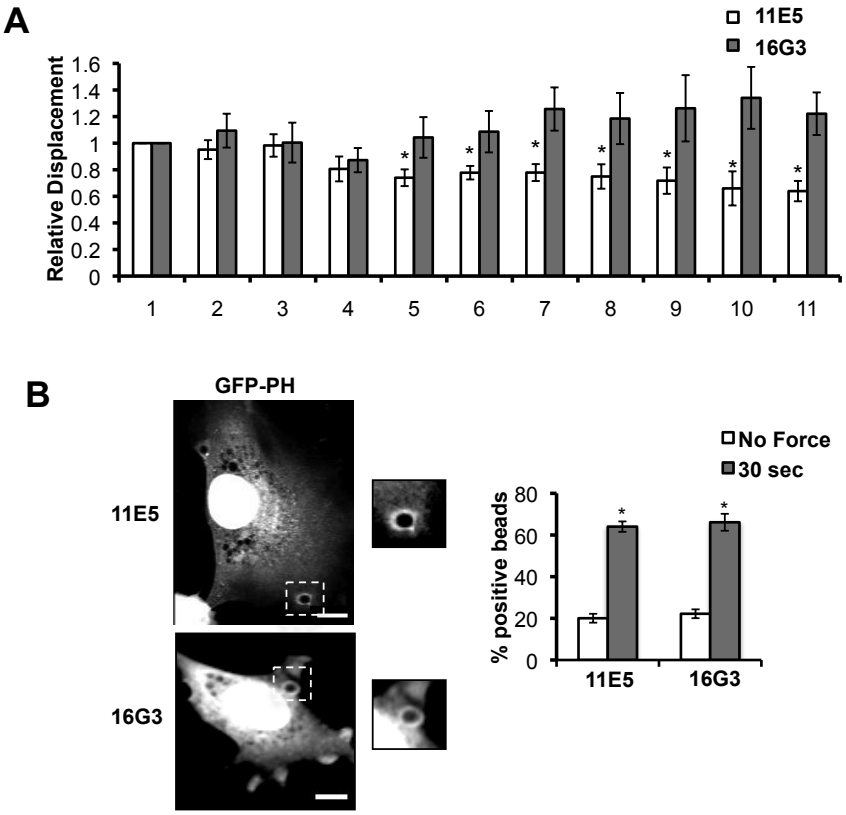

(A) ECs were incubated with 20μg/ml of FN blocking (16G3) or nonblocking antibody (11E5) for 20 min prior to force application. Average displacements were calculated relative to the first pulse of force to anti-PECAM-1-coated beads (n > 15 beads/condition from 3 independent experiments) (B) ECs expressing GFP-PH were incubated with 16G3 or 11E5 (20μg/ml, 20min) antibodies prior to being subjected to force with a permanent ceramic magnet. Cells were fixed and scored for GFP-PH recruitment around the bead (n > 50 cells/condition from 3 independent experiments; scale bar = 10μm). Error bars represent s.e.m., *p<0.05.

Figure 2.3 Tensional forces on PECAM-1 activate the RhoA pathway.

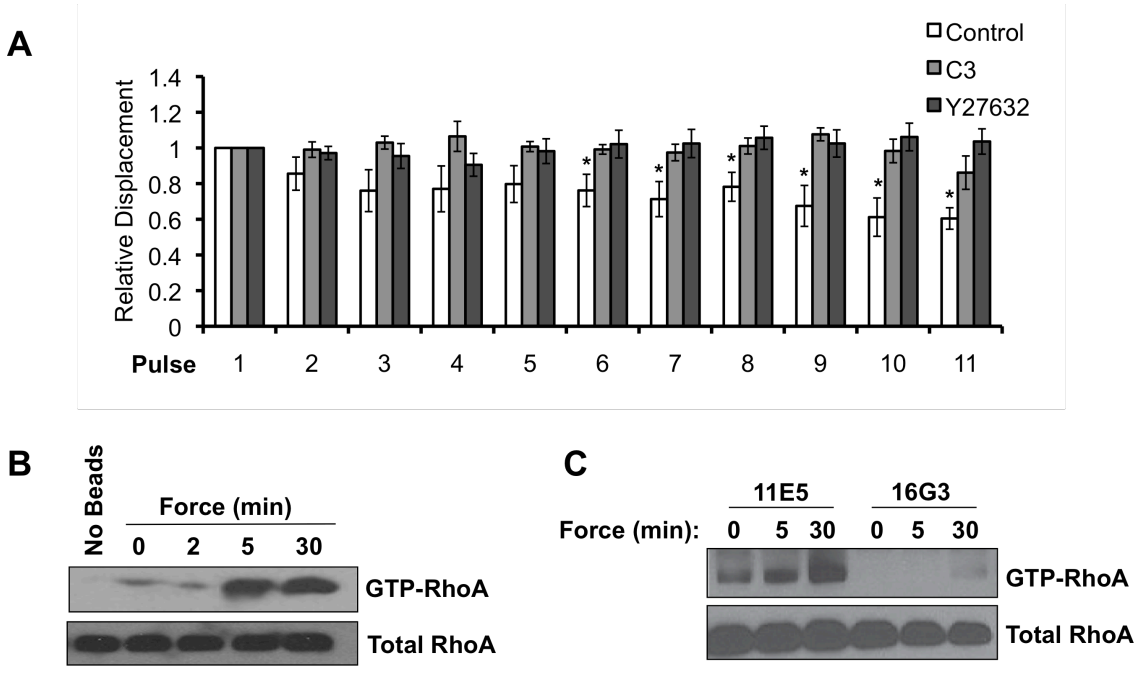

(A) Adherent ECs were incubated with anti-PECAM-1-coated magnetic beads and subjected to pulsatile tensional forces. For some conditions, cells were pretreated with C3 (2.0μg/ml, 2hrs) or Y27632 (5μM, 10min) prior to force application. Average displacements were calculated relative to the first pulse of force. (n>15 cells/condition from 3 independent experiments). Error bars represent s.e.m., *p<0.05. (B-C) ECs were incubated with anti-PECAM-1-coated beads and subjected to force with a permanent ceramic magnet for the indicted times (B) Active RhoA (RhoA-GTP) was isolated with GST-RBD and analyzed by western blot (n=5). (C) ECs were incubated with 20μg/ml of FN blocking (16G3) or nonblocking antibody (11E5) for 20 min prior to force application. Active RhoA (RhoA-GTP) was isolated with GST-RBD and analyzed by western blot (n=3). Blots (B, C) are representative of at least 3 independent experiments.

Figure 2.4 Tensional forces on PECAM-1 elicit RhoA activation and adaptive cellular stiffening via GEF-H1 and LARG.

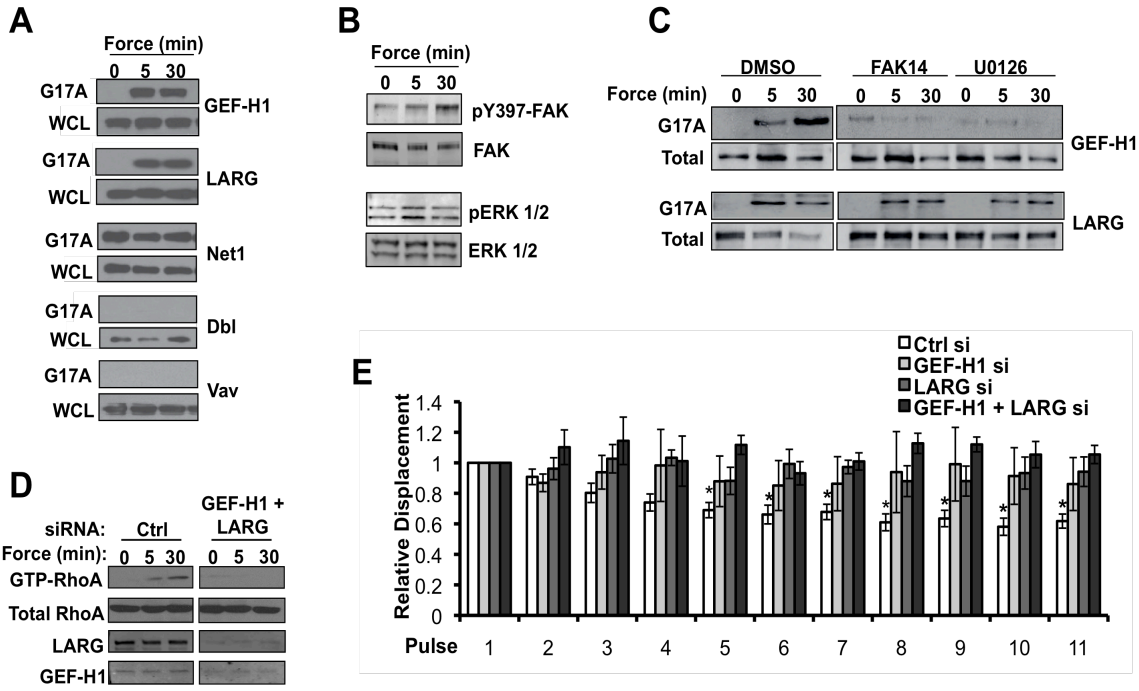

(A-D) Cells were incubated with anti-PECAM-1 coated magnetic beads and tension was applied for the indicated times using a permanent ceramic magnet. (A) Cells were lysed and active GEFs were precipitated with GST-(G17A)RhoA and analyzed by western blot (n=3), (B) Cells were lysed, subjected to SDS-PAGE, and immunoblotted with indicated antibodies. Blots are indicative of 3 independent experiments. (C) Cells were lysed and active GEFs were precipitated with GST-(G17A)RhoA and analyzed by Western blot (n=3). For some conditions, cells were pretreated with FAK inhibitor 14 (5μM, 30min) or U0126 (5μM, 30min) to inhibit FAK and ERK, respectively (n=3). (D,E) siRNA-transfected ECs were incubated with anti-PECAM-1-coated beads and subjected to force for the indicated times. Active RhoA was isolated with GST-RBD and analyzed by western blot (n=3). All blots (A-D) are indicative of at least 3 independent experiments. (E) siRNA-transfected ECs

on FN were incubated with anti-PECAM-1-coated magnetic beads and subjected the pulsatile force regimen using magnetic tweezers. Average displacements were calculated relative to the first pulse of force (n >15 beads/condition from 3 independent experiments, *$p<0.05$).

Figure 2.5 Local tensional forces on PECAM-1 elicit global β_1 integrin activation.

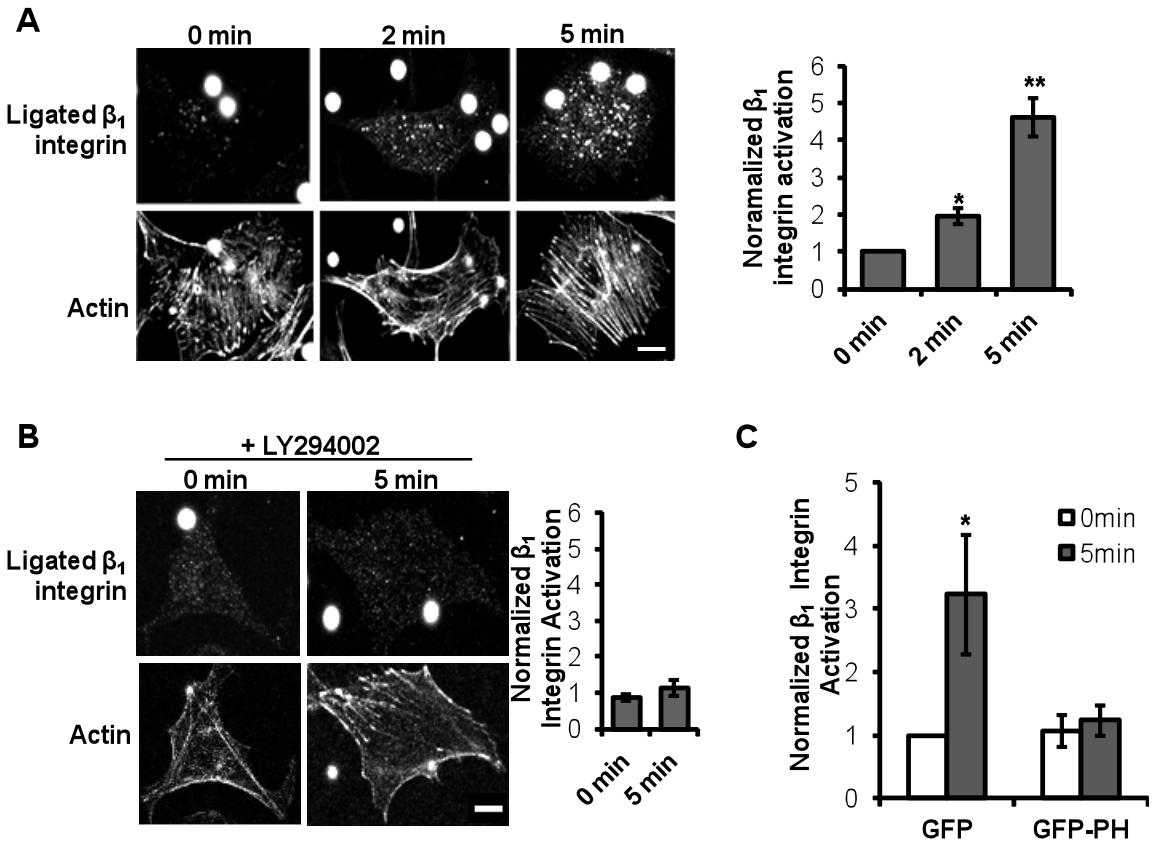

(A) ECs were incubated with anti-PECAM-1-coated beads (4.5μm) and subjected to force with a permanent ceramic magnet for the indicated times. ECs were fixed and stained with HUTS-4, which recognizes ligated β_1 integrin, and phalloidin to mark the actin cytoskeleton. (n > 30 cells/condition from 3 independent experiments; scale bar = 10μm, *p<0.05, **p<0.02). (B) ECs were incubated with anti-PECAM-1-coated beads (4.5μm) and subjected to force for the indicated times. ECs were fixed and stained for activated β1 integrins and the actin cytoskeleton. Cells were pretreated with LY294002 (30μM, 20min) to inhibit PI3K activation prior to force application (n > 25 cells/condition from 3 independent experiments; scale bar = 10μm, *p<0.05). (C) ECs overexpressing GFP or GFP-PH were incubated with anti-PECAM-1-coated beads (4.5μm) and force was applied. ECs were fixed

and stained for activated β1 integrins (n > 25 cells/condition from 3 independent experiments, *p<0.05). For all panels, integrin activation was quantified using thresholded images and ImageJ software. Values were normalized to the “No Force” condition. Error bars represent s.e.m.

Figure 2.6 Local tensional forces on PECAM-1 elicit global RhoA activation and adhesion growth.

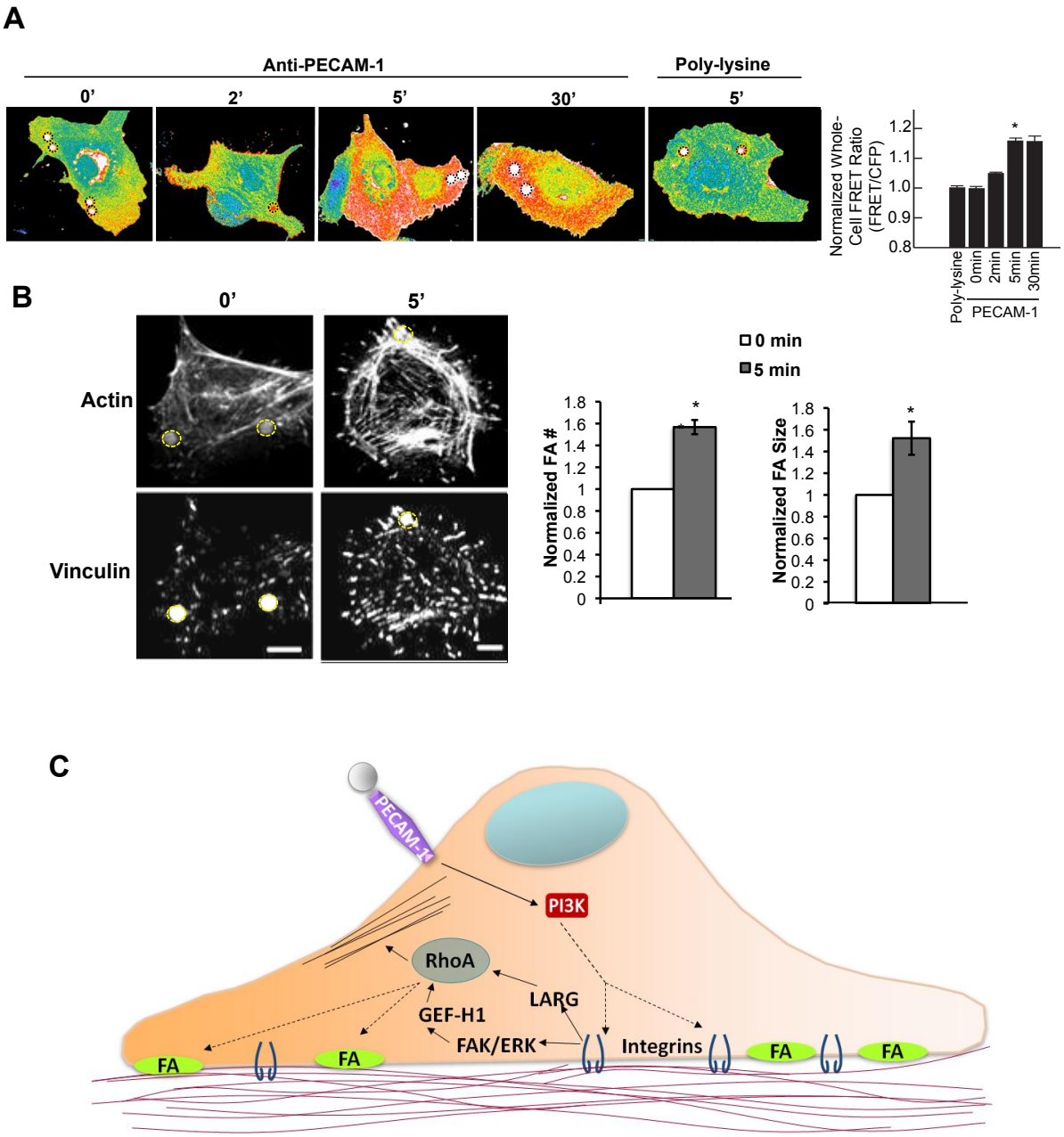

(A) ECs expressing the RhoA biosensor were incubated with poly-lysine or anti-PECAM-1-coated beads (4.5μm) and subjected to force with a permanent ceramic magnet for the indicated times. Cells were fixed and analyzed for FRET. Whole cell FRET ratios were

calculated for each condition. Autofluorescent beads are highlighted in black dotted circles (n > 45 cells/condition from 4 independent experiments, *p < 0.05). (B) Adherent ECs on FN were incubated with anti-PECAM-1-coated magnetic beads and subjected to force for the indicated times. ECs were fixed stained with phalloidin and an anti-vinculin antibody to mark focal adhesions. Focal adhesion number and size were quantified using NIH ImageJ software. Values were normalized to the "No Force" condition. Location of the beads are highlighted in yellow circles (n > 30cells/condition from 3 independent experiments, *p < 0.05, scale bar = 10μm). (C) Model of PECAM-1-mediated mechanotransduction. Local tensional forces on PECAM-1 results in global mechanosignaling and changes in cytoskeletal architecture.

Experimental Procedures

Cell culture, reagents, and antibodies. Bovine aortic endothelial cells were maintained in Dulbecco's modified Eagle's medium (DMEM, CellGro) with 10% fetal bovine serum, and 1% penicillin/streptomycin solution. Cells were plated on fibronectin (10μg/ml) 4 hours prior to experiments. LY294002, Cytochalasin D, wortmannin, and Y27632 were purchased from Calbiochem. Cell permeable C3 transferase was purchased from Cytoskeleton. The PECAM-1 antibody (PECAM 1.3) was a generous gift from D.K. Newman (BloodCenter of Wisconsin). Integrin blocking (16G3) and nonblocking (11E5) antibodies were kindly provided by K. Yamada (NIH). The LARG antibody was a generous gift from Kozo Kaibuchi (Nagoya University, Japan). Antibodies to RhoA (26C4) and Dbl (sc-89) were purchased from Santa Cruz Biotechnologies. The GEF-H1 was from Cell Signaling and the antibody to Vav was from BD Transduction. The antibody to Net1 was obtained from Abcam and the vinculin antibody was purchased from Sigma. The HUTS-4 antibody (which recognizes ligated β_1 integrin) was purchased from Millipore.

Transfections and RNA interference. For GFP-PH and FRET experiments, cells were seeded at 50% confluence and transfected with 2.5μg of the GFP-PH construct or RhoA biosensor using Effectene reagents (Qiagen) according to the manufacturer's protocol and experiments were performed 48 hours after transfection. For RNA interference experiments, control (Dharmacon siGLO RISC-free control siRNA), GEF-H1, or LARG siRNAs (Dharmacon) were transfected into cells using DharmaFECT4 (Dharmacon), according to the manufacturer's instructions. Cells were plated on FN 72 hours post-transfection and experiments were performed. The following siRNA sequences were used in this study: GEF-H1: 5'- AGACAGAGGAUGAGGCUUAUU -3'; and LARG: 5'-GGGAAUAUGGAGAGAAUUAUU- 3'.

Preparation of beads. Tosyl-activated paramagnetic beads (2.8 or 4.5 micron, Invitrogen) were washed with PBS and coated with an anti-PECAM-1 antibody (PECAM 1.3) or poly-lysine solution (Sigma) according to the manufacturer's instructions. Beads were quenched in 0.2M Tris prior to use to remove any remaining tosyl group and resuspended in DMEM containing 10% fetal bovine serum and 1% penicillin/streptomycin solution. Immediately before experiments ECs were incubated with beads (2-6 beads/cell) for 30 min at 37°C. Cells were briefly washed with fresh media to remove unbound beads prior to force application.

Pulsatile force application. The UNC 3D Force Microscope (3DFM) was used to apply controlled pulsatile forces (~100pN) to anti-PECAM-1-coated magnetic beads (2.8μm diameter). Bead displacements were recorded with a high-speed video camera (Pulnix, JAI) and tracked using Video Spot Tracker (Center for Computer Integrated Systems for Microscopy and Manipulation). Cells were monitored for changes in morphology, movement of the nucleus, cell edges, and particulates. No significant changes in cell morphology or movement of organelles were noticeable.

Permanent force application. For all immunostaining and biochemical analyses, continuous force (~10pN) was applied to anti-PECAM-1-coated beads (4.5μm diameter) using a permanent ceramic magnet (K&J Magnetics) parallel to the culture dish surface at a distance of 1cm from the adherent cells. No significant changes in cell morphology or movement of the nucleus, cell edges, or organelles was noticeable.

Immunofluorescence. To examine activation of PI3K, GFP-PH-transfected cells subjected to force (permanent magnet, 4.5μm beads) were fixed for 20 min in PBS containing 2% formaldehyde and mounted in Vectashield mounting medium (Vector laboratories). For all

other experiments, cells were fixed for 20 min in PBS containing 2% formaldehyde, permeabilized with 0.2% Triton X-100, and blocked with PBS containing 10% goat serum for 1hr at room temperature. Antibody incubations were performed as previously described [62] and mounted in Vectashield mounting medium. Images were acquired using a confocal microscope (Olympus FV500) with a 63× oil lens.

GST-RBD and GST-RhoA(G17A). Adherent cells were incubated with anti-PECAM-1-coated beads (4.5 micron, Invitrogen) for 30 min and subjected to force for indicated times. Active RhoA pulldowns were performed as previously described[78]. Briefly, following force application, cells were lysed in 50mM Tris (pH 7.6), 500mM NaCl, 1% Triton X-100, 0.1% SDS, 0.5% deoxycholate, 10mM $MgCl_2$, and protease inhibitors. Anti-PECAM-1-coated magnetic beads were removed from lysates with a magnetic separator. Lysates were centrifuged for 5min and supernatants were transferred to a new tube and incubated at 4° with 80μg of purified (GST-RBD) bound to glutathione-sepharose beads. Bead pellets were washed in 50mM Tris (pH 7.6), 150mM NaCl, 1% Triton X-100, 10mM $MgCl_2$, and protease inhibitors, and subsequently resuspended in Laemmli sample buffer and subjected to SDS-PAGE. Precipitation of active GEFs with the nucleotide-free RhoA mutant (G17A) were performed as previously described[63]. Briefly, following force application cells were lysed in 20mM HEPES (pH 7.6), 150mM NaCl, 1% Triton X-100, 5mM $MgCl_2$, and protease inhibitors. Lysates were incubated at 4°C for 45 minutes with 100μg of purified GST-G17A RhoA bound to glutathione-sepharose beads. Pelleted beads were then wash in lysis buffer, resuspended in Laemmli sample buffer, and subjected to SDS-PAGE.

FRET analysis. RhoA activation was measured by FRET in fixed cells by monitoring the ratio of FRET (ECFP excitation and Citrine emission) to ECFP emission (ECFP excitation

and emission) as previously described[51,64]. Cells were chosen for similar, low expression levels. Single-frame images were acquired on an inverted epifluorescence microscope (model IX81; Olympus), using a 40X UPlan FLN 1.3 N/A DIC lens (Olympus), a CCD camera (CoolSnapESII; Roper Industries), and MetaMorph software (Universal Imaging). For emission ratio imaging, the following filter sets were used (Chroma Technology Corp.): CFP: D436/20, D470/40; FRET: D436/20, HQ535/30; YFP: HQ500/20, HQ535/30. A dichroic mirror was custom-manufactured by Chroma for compatibility with all of these filters. Cells were illuminated with a 100 W Hg arc lamp through an ND 1.0 neutral density filter. At each time point, three images were recorded with the following exposure times: CFP (1.2 s) and FRET (0.6 s)

Metamorph software was used to perform image analysis. All images were first shading-corrected and background-subtracted. The FRET image, because it had the largest signal-to-noise ratio and therefore provided the best distinction between the cell and the background, was thresholded to generate a binary mask with a value of zero outside the cell and a value of one inside the cell. After multiplication by this mask, the FRET image was divided by the CFP image to yield a ratio image reflecting RhoA activation throughout the cell. A linear pseudocolour lookup table was applied, and the ratio values were normalized to the lower scale value which was chosen to exclude the bottom 5% of the total histogram distribution, thereby avoiding spurious low intensity pixels. In each experiment, all images were inspected to verify that all portions used to create the ratio image had a sufficiently high signal-to-noise ratio. We targeted at least 300 gray level values (12-bit dynamic range) above background in the lowest intensity regions within the cell ($S/n > 3$). This was especially important in thin parts of the cell where fluorescence was low. The ratio was corrected for bleaching.

Whole-Cell FRET Analysis. To calculate whole-cell average FRET ratio for the determination of the effects of mechanical force on RhoA activation, FRET ratio (FRET/CFP) images acquired and processed as described above were loaded into Metamorph, thresholded to generate masks for each cell, and regions were drawn around each cell using the mask. From these regions, a number of parameters, including average pixel intensity, could be measured and recorded. Average FRET ratio intensity was calculated for each image for at least 10 cells per condition and averaged for each treatment condition.

Quantification of integrin activation and focal adhesions. ECs stained for ligated β_1 integrin- or vinculin were analyzed with NIH ImageJ software. Confocal image planes at the basal surface of the cell were chosen for analysis and RGB images were converted to 8-bit black and white images. Activated integrins and focal adhesions were defined by setting an intensity threshold to remove any background signal. Integrin activation and focal adhesion size and number were analyzed using the 'Analyze particles' function.

Statistical analysis. Data are presented as means ± s.e.m. p-values were determined using a two-tailed unpaired Student's *t*-test.

Supplemental Figures

Supplementary Figure 2.1 Characterization of the cellular response to tension on PECAM-1.

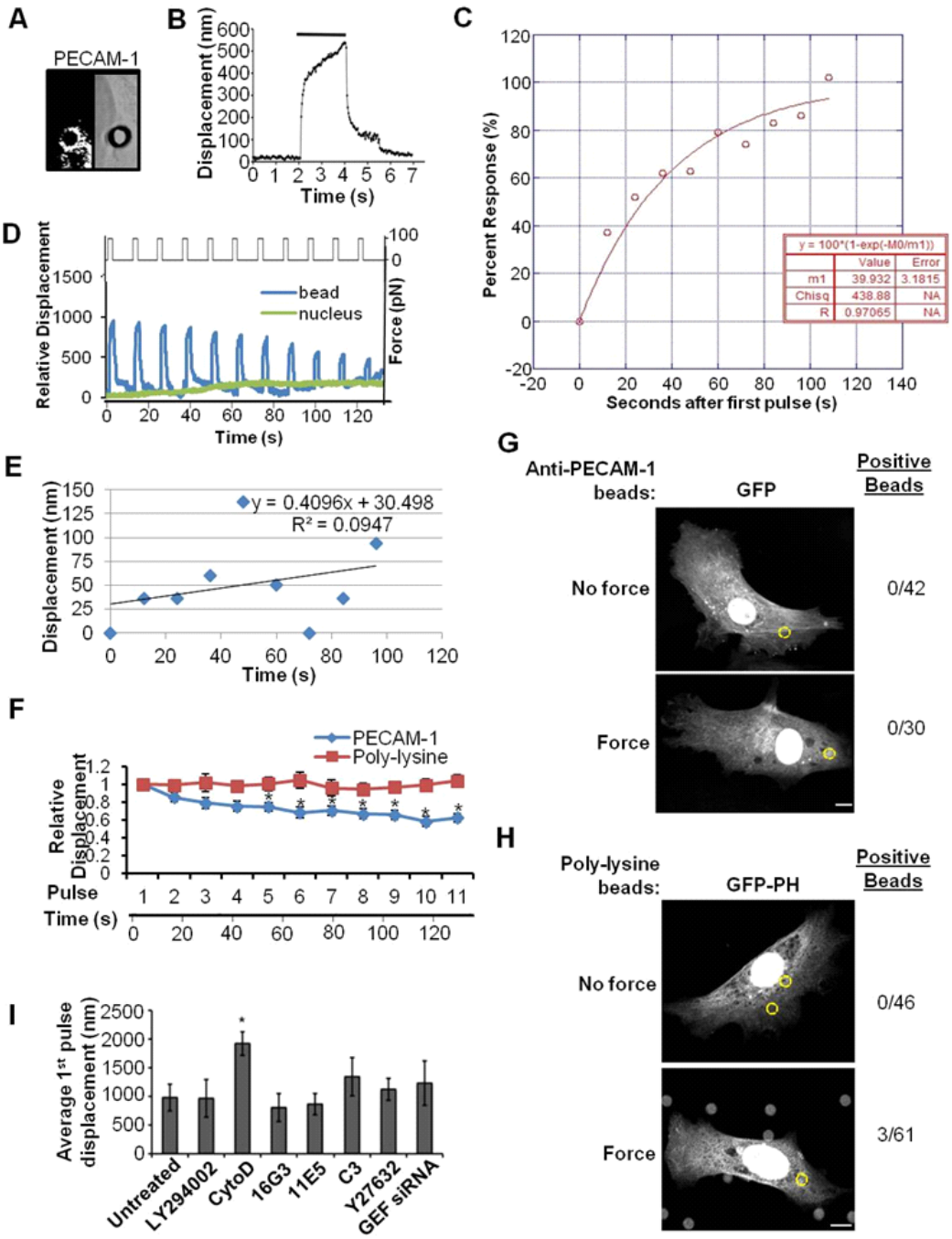

(A) A representative image of endogenous PECAM-1 trapped around an anti-PECAM-1-coated bead. ECs were fixed and stained for PECAM-1 to visualize recruitment of endogenous PECAM-1 around the bead. (B) Representative bead displacement of an anti-PECAM-1 coated bead during a 100pN, 2 second pulse of force (black line). (C) The PECAM-1-mediated stiffening response time constant was calculated by fitting the percent of maximum response to the exponential function 1-e^(-t/T). Maximum response was taken to be a 40% reduction in displacement relative to the first pull. (D) Nuclei of cells with PECAM-1-coated beads under tension were analyzed for movement over a 2-minute time course using Video Spot Tracker software. Average movement of 20 nuclei during the experiment (green) is not significant or pulsatile when compared to a representative PECAM-1-coated bead (blue). (E) ECs were incubated with PECAM-1-coated beads. Two-second pulses of force (~100 pN) separated by 10-second intervals over a 2-minute time course. Recovery from each pulse of force was calculated and plotted over time. Fitted line indicates a 90-95% recovery from each pulse of force and negligible baseline drift in bead movement. (F) Adherent ECs were incubated with anti-PECAM-1-coated or poly-lysine-coated magnetic beads and subjected to pulsatile tensional forces. Average displacements were calculated relative to the first pulse of force. (n>15 cells/condition from 3 independent experiments). Error bars represent s.e.m., *p<0.05. (G) ECs expressing GFP were incubated with anti-PECAM-1-coated magnetic beads and subjected to force for the indicated times. Cells were fixed and scored for GFP recruitment around the bead. Bead location is indication by dotted yellow circle (n > 30 cells/condition from 3 independent experiments; scale bar = 10μm). (H) ECs expressing GFP-PH were incubated with poly-lysine-coated magnetic beads and subjected to force for the indicated times. Cells were fixed and scored for GFP-PH recruitment around the bead. Bead location is indicated by dotted yellow circle (n > 45 cells/condition from 3 independent experiments; scale bar = 10μm). (I) Average displacements of anti-PECAM-1-coated beads. ECs in each

experimental condition were incubated with anti-PECAM-1-coated beads and subjected to pulsatile force. Bead displacement during the first pulse of force was calculated for each condition. Error bars represent s.e.m., n > 15 cells/condition, and *p<0.05.

Supplementary Figure 2.2 Force-induced RhoA activation is specific to PECAM-1.

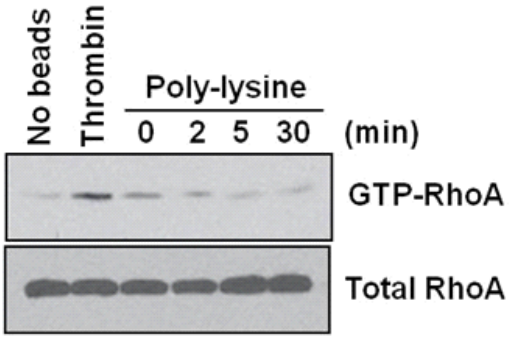

ECs were incubated with poly-lysine-coated beads and subjected to force for the indicted times. Some cells were treated with thrombin as a positive control. Active RhoA (RhoA-GTP) was isolated with GST-RBD and analyzed by western blot. Blot is representative of 3 independent experiments.

Supplementary Figure 2.3 Characterization of the global integrin activation.

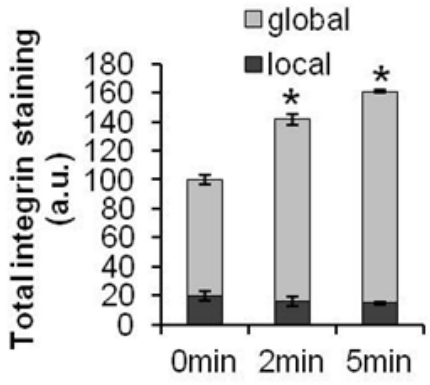

ECs were incubated with anti-PECAM-1-coated beads and subjected to force for the indicated times. ECs were fixed and stained for activated β1 integrins. Images acquired at the cell-ECM interface were analyzed using ImageJ software. Staining within a 5um radius from the site of bead attachment was deemed “local”, while the remaining cell area (more than 5um away from the bead) was classified as “global.” ($n > 15$ cells per condition from 3 independent experiments; error bars represent s.e.m.; $p < 0.05$)

Supplementary Figure 2.4 Characterization of global RhoA activation.

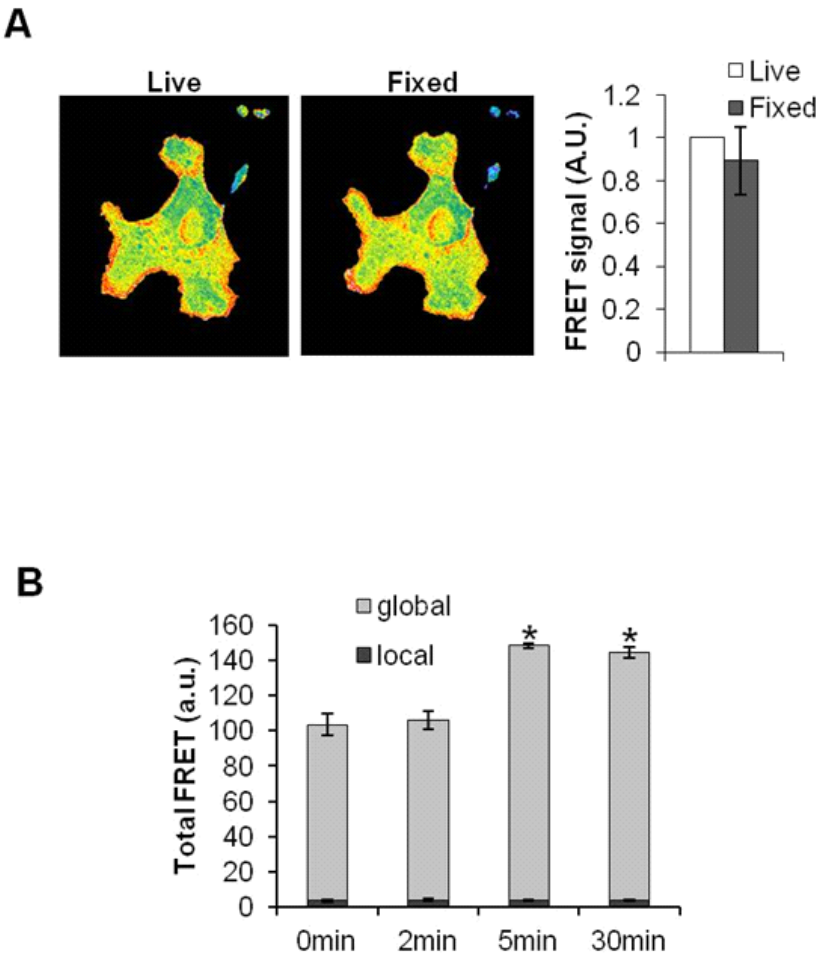

(A) Images were acquired and analyzed for FRET in living ECs expressing the RhoA biosensor. Cells were fixed and subsequently analyzed for FRET post-fixation. Whole cell FRET ratios were calculated for each condition (n=8 cells). Images are representative of a cell pre- and post-fixation. Relative whole cell FRET ratios before and after fixation were calculated. Errors bars are representative of s.e.m. (B) ECs expressing the RhoA biosensor were incubated with PECAM-1-coated beads and subjected to force for the indicated times. Cells were fixed and analyzed for FRET. Whole cell FRET ratios were calculated for each condition. FRET intensity was determined using ImageJ software.

Signal within a 5um radius from the site of bead attachment was deemed “local”, while the remaining cell area (more than 5um away from the bead) was classified as “global.” ($n > 15$ cells per condition from 3 independent experiments; error bars represent s.e.m.; $p < 0.05$).

Supplemental Experimental Procedures.

Cell culture, reagents, and antibodies. Bovine aortic endothelial cells were maintained in Dulbecco's modified Eagle's medium (DMEM, CellGro) with 10% fetal bovine serum, and 1% penicillin/streptomycin solution. Cells were plated on fibronectin (10μg/ml) 4 hours prior to experiments. The HUTS-4 antibody (which recognizes ligated β_1 integrin) was purchased from Millipore.

Transfections and RNA interference. For GFP-PH and FRET experiments, cells were seeded at 50% confluence and transfected with 2.5μg of the GFP-PH construct or RhoA biosensor using Effectene reagents (Qiagen) according to the manufacturer's protocol.

Preparation of beads. Tosyl-activated paramagnetic beads (Invitrogen) were washed with PBS and coated with a PECAM-1 antibody or poly-lysine solution (Sigma) according to the manufacturer's instructions. Beads were resuspended in DMEM containing 10% fetal bovine serum and 1% penicillin/streptomycin solution. Immediately before experiments ECs were incubated with beads (2-6 beads/cell) for 30 min at 37°C. Cells were briefly washed with fresh media to remove unbound beads prior to force application.

Pulsatile force application. The UNC 3D Force Microscope (3DFM) was used to apply controlled pulsatile forces (~100pN) to anti-PECAM-1-coated magnetic beads (2.8μm diameter). Bead displacements were recorded with a high-speed video camera (Pulnix, JAI) and tracked using Video Spot Tracker (Center for Computer Integrated Systems for Microscopy and Manipulation). Cells were monitored for changes in morphology, movement of the nucleus, cell edges, and particulates. No significant changes in cell morphology or movement of organelles were noticeable.

Permanent force application. For all immunostaining and biochemical analyses, continuous force (~10pN) was applied to anti-PECAM-1-coated beads (4.5μm diameter) using a permanent ceramic magnet (K&J Magnetics) parallel to the culture dish surface at a distance of 1cm from the adherent cells. No significant changes in cell morphology or movement of the nucleus, cell edges, or organelles was noticeable.

Immunofluorescence. To examine activation of PI3K, GFP-PH or GFP-transfected cells subjected to force were fixed for 20 min in PBS containing 2% formaldehyde and mounted in Vectashield mounting medium (Vector laboratories). Antibody incubations were performed as previously described [62] and mounted in Vectashield mounting medium. Images were acquired using a confocal microscope (Olympus FV500) with a 63× oil lens.

Calculation of the time constant. The response time constant was calculated by fitting the percent of maximum response to the exponential function 1-e^(-t/T). Maximum response was taken to be a 40% reduction in displacement relative to the first pull. Time in seconds was the time after the beginning of the first pull. Curve fitting was done using the Levenberg-Marquardt algorithm in KaleidaGraph (Synergy Software). Tau was determined to be 39.9 s. This corresponds to a $t_{1/2}$ of 27.7 sec.

GST-RBD. Adherent cells were incubated with PECAM-1 coated beads (4.5 micron, Invitrogen) for 30 min and subjected to force for indicated times. Active RhoA pulldowns were performed as previously described[78]. Briefly, following force application, cells were lysed in 50mM Tris (pH 7.6), 500mM NaCl, 1% Triton X-100, 0.1% SDS, 0.5% deoxycholate, 10mM $MgCl_2$, and protease inhibitors. Anti-PECAM-1-coated magnetic beads were removed from lysates with a magnetic separator. Lysates were centrifuged for 5min and supernatants were transferred to a new tube and incubated at 4° with 80μg of purified

(GST-RBD) bound to glutathione-sepharose beads. Bead pellets were washed in 50mM Tris (pH 7.6), 150mM NaCl, 1% Triton X-100, 10mM $MgCl_2$, and protease inhibitors, and subsequently resuspended in Laemmli sample buffer and subjected to SDS-PAGE.

FRET analysis. RhoA activation was measured by FRET in live and fixed cells by monitoring the ratio of FRET (ECFP excitation and Citrine emission) to ECFP emission (ECFP excitation and emission) as previously described[51,64]. Cells were chosen for similar, low expression levels. Single-frame images were acquired on an inverted epifluorescence microscope (model IX81; Olympus), using a 40X UPlan FLN 1.3 N/A DIC lens (Olympus), a CCD camera (CoolSnapESII; Roper Industries), and MetaMorph software (Universal Imaging). For emission ratio imaging, the following filter sets were used (Chroma Technology Corp.): CFP: D436/20, D470/40; FRET: D436/20, HQ535/30; YFP: HQ500/20, HQ535/30. A dichroic mirror was custom-manufactured by Chroma for compatibility with all of these filters. Cells were illuminated with a 100 W Hg arc lamp through an ND 1.0 neutral density filter. At each time point, three images were recorded with the following exposure times: CFP (1.2 s) and FRET (0.6 s) Metamorph software was used to perform image analysis. All images were first shading-corrected and background-subtracted. The FRET image, because it had the largest signal-to-noise ratio and therefore provided the best distinction between the cell and the background, was thresholded to generate a binary mask with a value of zero outside the cell and a value of one inside the cell. After multiplication by this mask, the FRET image was divided by the CFP image to yield a ratio image reflecting RhoA activation throughout the cell. A linear pseudocolour lookup table was applied, and the ratio values were normalized to the lower scale value which was chosen to exclude the bottom 5% of the total histogram distribution, thereby avoiding spurious low intensity pixels. In each experiment, all images were inspected to verify that all portions used to create the ratio image had a sufficiently high signal-to-noise ratio. We targeted at least 300 gray level

values (12-bit dynamic range) above background in the lowest intensity regions within the cell (S/*n* > 3). This was especially important in thin parts of the cell where fluorescence was low. The ratio was corrected for bleaching using a method.

Whole-Cell FRET Analysis. To calculate whole-cell average FRET ratio for the determination of the effects of mechanical force on RhoA activation, FRET ratio (FRET/CFP) images acquired and processed as described above were loaded into Metamorph, thresholded to generate masks for each cell, and regions were drawn around each cell using the mask. From these regions, a number of parameters, including average pixel intensity, could be measured and recorded. Average FRET ratio intensity was calculated for each image for at least 10 cells per condition and averaged for each treatment condition.

Analysis of β_1 integrin localization. ECs stained for ligated β_1 integrin were analyzed with NIH ImageJ software. Confocal images at the basal surface of the cell were chosen for analysis and RGB images were converted to 8-bit black and white images. Integrin activation was defined by setting an intensity threshold to remove background signal. Integrin activation was analyzed using the 'Analyze particles' function. To calculate "global" versus "local" integrin activation, signal within a 5um radius from the site of bead attachment was deemed "local", while the remaining cell area (more than 5um away from the bead) was classified as "global." Fluorescence intensity in each region of the cell was quantified using ImageJ software.

Analysis of RhoA FRET localization. ECs expressing the RhoA biosensor were analyzed using NIH ImageJ software. Images acquired with an epifluourescence microscope (Olympus Ix81) were converted to 8-bit black and white images. To calculate "global" versus "local" RhoA FRET, signal within a 5um radius from the site of bead attachment was

deemed “local”, while the remaining cell area (more than 5um away from the bead) was classified as “global.” Fluorescence intensity in each region of the cell was quantified using ImageJ software.

CHAPTER III.

Hemodynamic and extracellular matrix cues regulate the mechanical phenotype and stiffness of endothelial cells

Overview

Mechanical forces produced by blood flow influence blood vessel physiology and pathology. Endothelial cell (ECs) lining the lumen of the blood vessel are decorated with numerous mechanoreceptors, including platelet endothelial cell adhesion molecule-1 (PECAM-1), that function to convert mechanical force to intracellular biochemical signals. While it is accepted that mechanical stresses and the mechanical properties of the cells regulate vessel health, the relationship between force and biological response remains elusive. Here, we show that cells integrate external mechanical force and ECM cues to dynamically modulate their own mechanical properties. Using a magnetic tweezers system, we demonstrate that the cellular response to mechanical tension on PECAM-1 depends on the identity of the ECM. While some responses are common, ECs adherent on collagen display divergent stiffening and focal adhesion dynamics compared to ECs on fibronectin. Mechanistically, this is due to collagen-dependent mechanosensitive PKA activation, Ser188 RhoA phosphorylation, and inhibition of RhoA. We further extend these studies and show that this pathway regulates focal adhesion dynamics in ECs *in vitro* in response to shear stress and *in vivo* in the hemodynamic environment of the vessel. Finally, passive microbead rheology studies suggest that the PKA pathway is responsible for maintaining low EC stiffness in the descending aorta and, thus, may serve as an atheroprotective mechanism that maintains endothelial barrier function.

Introduction:

Mechanical forces influence nearly all aspects of cell behaviour, including apoptosis, transcription and translation, differentiation and cell migration[9, 11, 79-81]. The mechanical environment of a cell consists of both cell-generated (endogenous) and applied (exogenous) forces. Endogenous forces are generated when a cell pulls on its extracellular matrix (ECM) or its neighbours via its cytoskeleton. Examples of exogenous forces include the mechanical force of shear stress applied on endothelial cells (ECs) due to blood flow, as well as the stretching of vascular cells due to blood pressure. It is now well accepted that mechanical stresses determine the mechanical properties of cells, which, in turn, influence cell function in both physiology and disease. Nevertheless, the relationship between force and biological response remains elusive.

Various methods have been used to apply exogenous forces to cells[7, 82, 83]. These studies have revealed that when force is applied to mechanosensitive proteins, the cells respond by increasing their stiffness. This is a physiological response that is required in order to resist the applied force; however, increased stiffness is also associated with pathologies such as cardiovascular disease and cancer[55, 84, 85]. We and others have demonstrated that the stiffening response requires the coordination of numerous signaling cascades, including activation of the small GTPase RhoA[7, 13, 82]. Effectors downstream of the GTPase coordinate changes in the actin cytoskeleton and focal adhesions in an effort resist the applied force[13].

While much work has focused on integrin-mediated force transduction, recent work has highlighted other mechanosensitive proteins, such as cadherins and PECAM-1[10-13]. PECAM-1 is a critical mechanosensor in the endothelium that activates a number of intracellular signaling cascades in response to the hemodynamic force of shear stress[29]. We recently reported that ECs adherent on fibronectin (FN) generate an adaptive stiffening response when tension is applied to PECAM-1[13]. Interestingly, this response is dependent

on integrin ligation with the underlying ECM. Integrin heterodimers differ in their ECM specificity based on their α/β subunit composition, and therefore bind to distinct extracellular matrix proteins. Several studies have reported matrix-specific signaling through different integrin subtypes within the endothelium[41, 42, 44]. Throughout most of the vasculature, collagen (CL) and laminins are the predominant ECM proteins. However, distinct regions of the vasculature are rich in FN deposition and therefore differ in matrix composition. Thus, variances in matrix composition permit activation of ECM-specific signaling cascades in localized regions of the vasculature. For instance, fluid shear stress activates protein kinase A (PKA) in ECs adherent on CL, whereas PKA activity is unaffected when ECs adherent on FN are exposed to shear stress[44]. While ECM-specific signaling cascades have been identified, how these divergent signaling pathways affect mechanical signaling and cellular function is not known. Here, we investigate how the ECM identity and signaling through discrete integrin subtypes influences the cellular response to tension on PECAM-1. We identify that CL-dependent activation of PKA in response to mechanical force on PECAM-1 negatively regulates RhoA activity. Furthermore, we show that PKA-mediated inhibition of RhoA modulates the EC force response and focal adhesion dynamics *in vitro* and *in vivo* to, ultimately, dampen EC stiffness in the CL-rich descending aorta.

Results:

The ECM determines the cellular mechanical response to tension on PECAM-1

In order to investigate the role of ECM composition on the mechanical response to tension on PECAM-1, we utilized magnetic tweezers to apply pulsatile force to ECs adherent on FN or CL. ECs incubated with anti-PECAM-1-coated paramagnetic beads were subjected to 2-second pulses of force over a 2-minute time course (Fig. 3.1a). In ECs adherent on FN, application of successive pulses of force on PECAM-1 resulted in a significant decrease in bead displacement during latter pulses (Fig. 3.1b). This observed

reduction in bead displacement is indicative of adaptive stiffening and consistent with previous work[13]. Surprisingly, when ECs adherent on CL were stimulated with the identical force regimen, we could not detect a significant change in pulse-to-pulse bead displacement, suggesting that the cells do not generate a force response in this context (Fig. 3.1b). Interestingly, absolute displacement of anti-PECAM-1 coated beads during the first pulse of force was nearly identical on both FN and CL (Supplementary Fig. S3.1). These results suggest that while ECs adherent on FN or CL have similar basal stiffness, they differ dramatically in their ability to respond to exogenous force application.

Work from our group and others has demonstrated that the adaptive cellular stiffening response is mediated, in part, by an increase in focal adhesions that function to resist the applied force[5, 13]. To this end, we assessed the focal adhesion profile in ECs plated on FN and CL before and after force manipulation. As previously reported, ECs adherent on FN exhibited robust focal adhesion growth in response to force on PECAM-1 (Fig. 3.1c). Conversely, and in agreement with the magnetic tweezers data, focal adhesion size or number did not significantly increase in ECs adherent on CL following force application. Taken together, these data indicate that the ECM composition has a profound effect on the cellular response to tension on PECAM-1. ECs adherent on FN generate an adaptive stiffening response, accompanied by significant focal adhesion growth, whereas ECs adherent on CL do not generate a significant force response or restructure focal adhesions in response to tension on PECAM-1.

Phosphoinositide 3-kinase (PI3K) is a critical regulator of PECAM-1-mediated adaptive stiffening on FN by allowing integrin activation and downstream activation of RhoA[13]. In order to examine PI3K activation in ECs adherent on CL, anti-PECAM-1-coated paramagnetic beads bound to ECs expressing a GFP-PH fusion protein (which serves as a sensor for PI3-lipids) were subjected to force using a permanent ceramic magnet. Brief force application induced rapid PI3K activation around anti-PECAM-1-coated beads

(Supplementary Fig. S2b) at levels similar to those previously reported in ECs adherent on FN[13]. These results suggest that the impaired mechanical response on CL is not due to insufficient PI3K activation. In order to assess force-dependent changes in collagen-binding integrin ($\alpha2\beta1$) activity, ECs adherent on CL were subjected to force and immunostained with an antibody that recognizes ligated $\beta1$ integrins. ECs exhibited transient but robust integrin activation after force application (Supplementary Fig. S3.2b), suggesting that the lack of a mechanical response in ECs adherent on CL may be due to divergent signaling downstream of CL-binding integrins.

Mechanically-induced PKA activity negatively regulates RhoA

Activation of the small GTPase RhoA is known to be important for the cellular stiffening response[7, 13, 82]. Importantly, RhoA activation in response to tension on PECAM-1 requires integrin activation and ligation with the underlying ECM[13]. Although cells on CL exhibited significant integrin activation in response to tensional force on PECAM-1, we next examined if downstream RhoA activation was affected by adhesion to collagen. Tension on PECAM-1 resulted in robust, but transient activation of RhoA, as levels of GTP-bound RhoA increased at 5 min of force, but returned to basal levels by 30 min of force (Fig. 2a). This transient response is in striking contrast to the prolonged RhoA activation that occurs when tension is applied to ECs adherent on FN (Fig. 2b).

Rho GTPases are very tightly regulated in order to allow for proper signaling in response to distinct stimuli, and thus, activity is regulated in three ways: activation (GTP-loading) by a guanine nucleotide exchange factor (GEF), hydrolysis of GTP via a GTPase activating protein (GAP), and inactivation via association with a GDP-dissociation inhibitor (GDI)[86]. Given the transient nature of force-induced RhoA activation on CL, we hypothesized that differential association with GDI might contribute to the decrease in RhoA activity. We considered association with a GDI as an attractive possibility for several

reasons. Inactivation of RhoA (via association with Rho-GDI) is modulated by serine phosphorylation of the GTPase[87-89]. PKA has been implicated as a negative regulator of RhoA activity via phosphorylation of RhoA serine 188[89]. Interestingly, ECs exhibit mechanosensitive and matrix-specific activation of PKA, such that the kinase is activated in ECs adherent on CL in response to the mechanical stimulus of fluid shear stress but not activated in ECs adherent on FN[44]. Therefore, we hypothesized that matrix-specific activation of PKA negatively regulates RhoA activity on CL and inactivates the GTPase by the 30 min time point. In order to test this hypothesis, levels of RhoA serine phosphorylation following force application on PECAM-1 were assessed by immunoprecipitation and immunoblot analysis (Fig. 3.2c). Indeed, ECs exhibited force-induced serine phosphorylation in response to tension on PECAM-1, suggesting that RhoA may be inactivated via serine phosphorylation at later time points. We next sought to determine if PKA is activated following force application on PECAM-1. In agreement with our hypothesis, we detected a force-dependent increase in PKA phosphorylation in ECs on CL, indicating activation of the kinase downstream of PECAM-1 (Fig. 3.2d). Furthermore, mechanical activation of PKA was specific to ECs on CL, as activity of the kinase did not change when ECs adherent on FN were subjected to force (Supplementary Fig. S3.3). In order to test if PKA mediates force-induced serine phosphorylation of RhoA, ECs were pretreated with the PKA inhibitor PKI, prior to mechanical stimulation of PECAM-1. Consistent with our hypothesis, PKA inhibition completely abolished force-dependent RhoA phosphorylation (Fig. 3.2e). Taken together these data suggest that force-induced activation of PKA promotes phosphorylation and inactivation of RhoA in ECs adherent on CL. Thus, we reasoned that abrogation of PKA signaling and therefore, inhibition of RhoA serine phosphorylation should also influence levels of active or GTP-bound RhoA in response to tension on PECAM-1. In agreement with our hypothesis, blockade of PKA signaling resulted in robust and sustained activation of RhoA (Fig. 3.2f). Taken together,

these data indicate that PKA activation modulates RhoA serine phosphorylation and, thus, activity of the GTPase in response to tension on PECAM-1.

Inhibition of PKA confers mechanical responsiveness to ECs on CL

In light of these data, we hypothesized that inhibition of PKA (and prolonged activation of RhoA) may confer the stiffening response to ECs adherent on CL. To address this, we pretreated ECs with the PKA inhibitor prior to stimulating PECAM-1 in the magnetic tweezers system. Control ECs did not respond to tension on PECAM-1 (similar to Fig. 3.1a). In contrast, inhibition of PKA signaling resulted in a rapid and significant adaptive stiffening response (Fig. 3.3a). These data suggest that prolonged activation of RhoA is sufficient to restore mechanical responsiveness to tension on PECAM-1. In order to examine if inhibition of PKA permitted force-induced growth of focal adhesions in cells attached to CL, ECs pretreated with PKI were subjected to force and immunostained for the focal adhesion protein vinculin. In agreement with our magnetic tweezers studies, blockade of PKA signaling resulted in a significant increase in focal adhesion size and number, whereas vehicle-treated ECs did not exhibit significant focal adhesion growth (Fig. 3.3b). Thus, our data indicate that suppression of PKA signaling restores the mechanical response to tension on PECAM-1.

The PKA pathway regulates hemodynamic-induced focal adhesion dynamics in vitro and in vivo

Our data indicates that PKA is responsible for regulating matrix-dependent stiffening and focal adhesion growth in response to applied magnetic forces. However, the hemodynamic force of fluid shear stress is the critical physiological force *in vivo*. Furthermore, ECs subjected to shear stress remodel their focal adhesions in order to resist shear forces[90, 91], and PECAM-1 is part of a mechanosensory complex that influences

cytoskeleton dynamics in ECs subjected to fluid shear stress[29]. Therefore, we extended our studies to investigate the role of the PKA pathway in EC focal adhesion dynamics in response fluid shear stress. ECs plated on CL were subjected to shear stress (12 dyn/cm^2) and immunostained for vinculin to highlight focal adhesions (Fig. 3.4a). ECs subjected to shear stress displayed a 2-fold increase in focal adhesion number (Supplementary Fig. S3.4a), consistent with previous reports[22]. Furthermore, we found that inhibition of PKA signaling significantly augmented shear-induced focal adhesion growth (Fig. 3.4a), similar to the growth of focal adhesions observed when tension was applied on PECAM-1 (Fig. 3.3b). It is important to note that inhibition of PKA did not significantly influence focal adhesion size or number in the absence of shear stress (Supplementary Fig. S3.4b). Thus, these data indicate that PKA regulates focal adhesion dynamics in response to the physiological stimulus of fluid shear stress.

We sought to extend our *in vitro* shear stress studies to an *in vivo* setting. We examined focal adhesions in the descending aorta, as it is rich in collagen composition and experiences relatively uniform shear stress patterns. In order to test if PKA regulates focal adhesion growth *in vivo*, wildtype mice were injected with PKA inhibitor (PKI) or vehicle (DMSO). Two hours after injection, the descending aorta was harvested and *en face* preparations were immunostained with vinculin to highlight focal adhesions in the endothelium. Remarkably, inhibition of PKA signaling *in vivo* resulted in a significant increase in the number of focal adhesions present in the descending aorta (Fig. 3.4b) compared to control, suggesting that the PKA pathway is also a critical regulator of focal adhesion dynamics in ECs in the hemodynamic environment of the vessel.

The PKA pathway modulates hemodynamic-induced aortic endothelial cell stiffness

Several studies have suggested a link between vessel stiffness and cardiovascular disease[55, 84, 85]. However, measurements of EC stiffness *ex vivo* are lacking and the

mechanisms that govern aortic EC stiffness remain largely unexplored. Our *in vitro* data suggest that growth of focal adhesions corresponds with a stiffer EC phenotype and that activation of the PKA pathway exerts a negative effect on active stiffening responses via inhibition of RhoA signaling. In contrast, suppression of PKA signaling restores mechanotransduction in response to tension on PECAM-1 (Fig. 3.3b), shear stress application *in vitro* (Fig. 4a), and in the hemodynamic environment of the blood vessel (Fig. 3.4b). In order to test the direct physiological relevance of these effects, we used external passive microbead rheology[92] to determine whether the PKA pathway is also a determinant of EC stiffness *in vivo*. The descending aorta was freshly isolated from control or PKI-treated mice two hours after injection and prepared *en face* to expose the endothelium for passive microbead rheology measurements. The descending aorta was incubated with FN-conjugated beads in order to establish integrin-mediated attachments with the cortical actin cytoskeleton. Thermal motion of attached beads was tracked and the resulting mean-squared displacements (MSD) were calculated for control or PKI-treated aortas (Fig. 3.5a). Of note, MSD trajectories show a slope less than unity (illustrated by black guide line in Fig 3.5b), indicating a sub-diffusive viscoelastic response consistent with the movements of beads anchored to the actin cytoskeleton via integrins[93]. Ensemble-averaging of the bead populations revealed a significant decrease in MSD magnitude in PKI-treated aortas compared to control aortas (Fig. 3.5b). Furthermore, calculation of the average root mean-squared (RMS) at the 1-second timescale for each condition revealed a significant decrease in the effective radius of bead displacement in PKI-treated aortas (Fig. 3.5c). These data suggest a significant increase in stiffness in the endothelium of PKI-treated aortas compared to control aortas. Thus, the PKA pathway appears to be a significant regulator of EC stiffness in the CL-rich descending aorta.

Discussion:

Here we identify a novel pathway that regulates endothelial mechanical responses and determines aortic EC stiffness, which may contribute to maintenance of blood vessel integrity. We sought out to determine the role of ECM identity in PECAM-1-mediated mechanotransduction and discovered that while some responses are common, ECs adherent on CL display divergent signaling in response to mechanical tension on PECAM-1 compared to ECs adherent on FN. Although tension on PECAM-1 induces PI3K and downstream integrin activation, ECs on do not generate a stiffening response, which may be partially attributed to reduced focal adhesion remodeling. Mechanistically, we demonstrate that mechanical tension on PECAM-1 results in activation of RhoA in cells adherent on CL, which is rapidly deactivated by PKA-dependent Ser188 phosphorylation of RhoA. Inhibition of PKA signaling prolongs force-induced RhoA activation and results in cellular stiffening and focal adhesion growth in response to force (Fig. 3.6). We further extended these findings to the physiological hemodynamic stimulus of fluid shear stress and reveal that PKA negatively regulates focal adhesion dynamics in ECs *in vitro* and in the hemodynamic environment of the vessel *in vivo*. Finally, we highlight PKA as a critical regulator of EC mechanics and demonstrate active regulation of aortic EC stiffness *in vivo*.

PKA is a multifunctional protein that has many roles in cell biology. Within the endothelium, the kinase has well documented roles in anti-inflammatory signaling[15], angiogenesis[94], barrier function[95, 96], and cell migration[97]. Importantly, PKA-mediated RhoA inactivation has been shown to regulate endothelial barrier function *in vitro*[95], and the kinase has been shown to tightly regulate RhoA activity during protrusion-retraction cycles in migrating cells[87, 97]. Here, we demonstrate that PKA inhibition of RhoA signaling also influences EC responsiveness to force and focal adhesion dynamics. PKA can directly phosphorylate RhoA at serine 188, and phosphorylation of this residue inhibits activity of the GTPase[87, 89]. Serine phosphorylation of RhoA increases its association with Rho-GDI and

negatively influences activity by sequestering the GTPase in the cytoplasm[88]. In addition to its role regulating RhoA activity, a complex relationship between PKA and integrin-mediated adhesion also exists. Detachment of cells from the ECM triggers robust, but transient, activation of the kinase[98, 99]. Conversely, integrin-mediated adhesion also stimulates PKA activation and is important for strengthening cell-cell and cell-matrix adhesions in certain cell types[100]. For instance, G-protein-coupled receptor-mediated activation of PKA promotes cell-cell adhesion and inhibits cell migration in a Csk-dependent manner[94].

Our work highlights RhoA as a critical mediator the cellular response to force. While mechanical stimulation of PECAM-1 induces RhoA activation in ECs adherent on CL, activation is transient and insufficient to initiate adaptive stiffening and focal adhesion growth. While we provide evidence for RhoA inactivation via serine phosphorylation, it is possible that force-dependent changes in GEF and GAP activity may also contribute to transient activation of the GTPase. For instance, p190RhoGAP is rapidly phosphorylated in ECs exposed to shear stress, and the GAP is required for flow-mediated changes in the actin cytoskeleton[101]. Therefore, it is possible that force-dependent activation of p190RhoGAP may also influence RhoA activity. In addition, previous work from our lab identified activation of GEF-H1 in response to tension on PECAM-1[13]. Interestingly, others have shown that PKA-dependent phosphorylation of GEF-H1 suppresses its GEF activity[102]. Therefore, it is also possible that force-dependent PKA activation inhibits GEF-H1-mediated GTP-loading at later time points. Nevertheless, our results clearly indicate that PKA regulates RhoA activity and the cellular response to mechanical force.

Our *in vivo* studies suggest that PKA signaling in the descending aorta inhibits focal adhesion growth and promotes a compliant cellular phenotype. The descending aorta is rich in CL composition and, notably, more resistant to atherosclerotic plaque development compared to other regions of the vasculature. Our data indicate that focal adhesion growth corresponds to a stiffer EC phenotype and that the presence of CL suppresses this

phenotype. Interestingly, focal adhesions in other vascular cell types in the vessel have been identified as major contributors to aortic stiffness[103], and our rheology studies suggest that growth of focal adhesions may also contribute to aortic EC stiffness. Interestingly, vessel stiffness positively correlates with EC permeability and leukocyte transmigration[55], and thus, contributes to the development of vascular disease. Therefore, PKA-mediated suppression of RhoA activity and inhibition of focal adhesion growth in the descending aorta may serve as a protective mechanism that maintains endothelial barrier function and regulates permeability.

Overall, our work identifies a unique mechanosensitive and ECM-dependent signaling pathway that regulates EC stiffness and focal adhesion dynamics. Using magnetic tweezers, we show that tension on PECAM-1 initiates an intracellular signaling cascade that regulates the cellular force response and focal adhesion growth. We further demonstrate that PECAM-1-dependent PKA signaling influences focal adhesion dynamics and EC stiffness *in vitro* and *in vivo* and may function as an atheroprotective mechanism in distinct regions of the vasculature.

Figures

Figure 3.1 ECM composition influences the cellular response to tension on PECAM-1

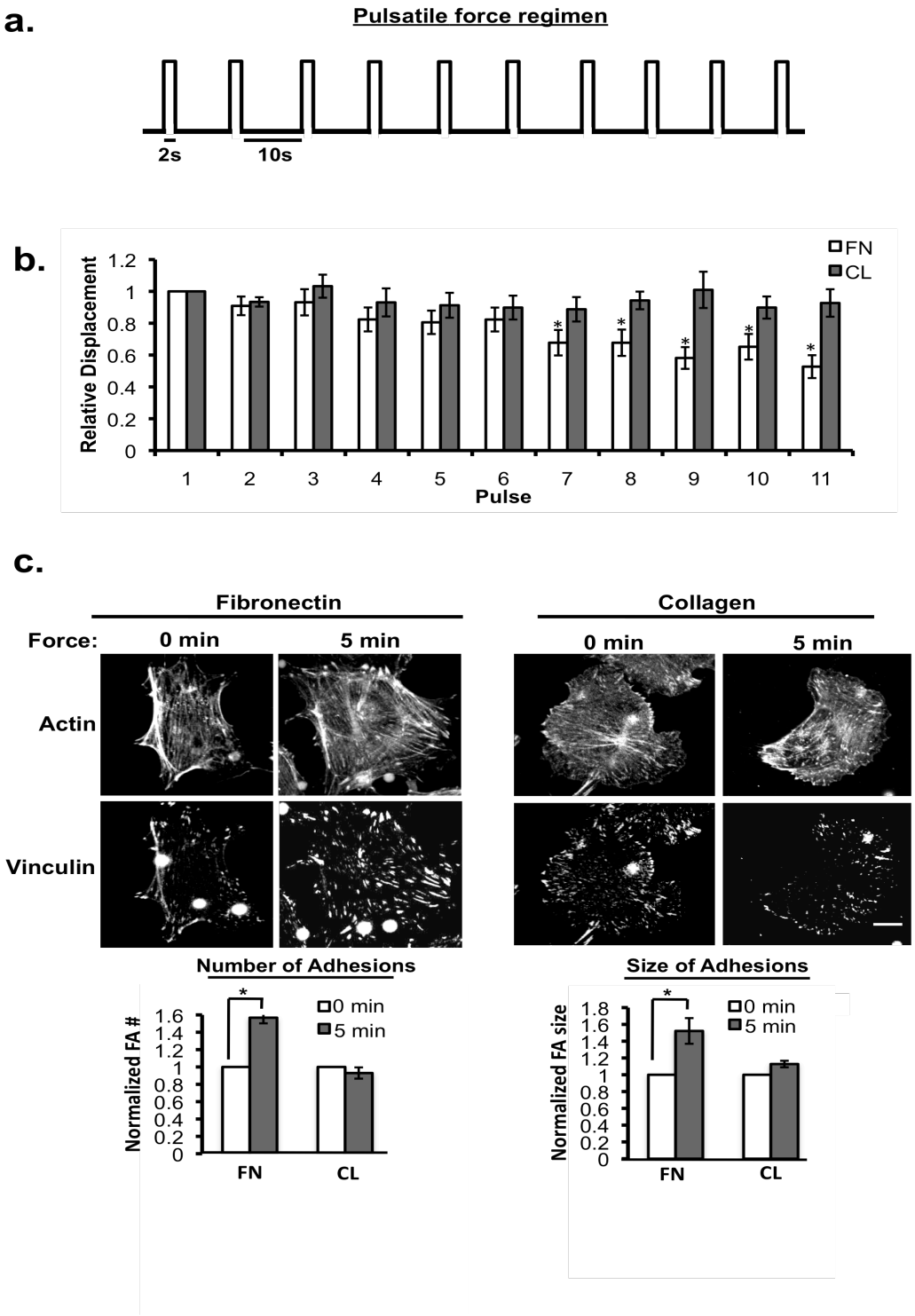

(a) Pulsatile force regimen applied with magnetic tweezers, consisting of a 2 second, 100-pN pulse of force, followed by a 10 second period of rest, repeated over a 2 minute time course. (b) Average relative anti-PECAM-1-coated bead displacements induced by pulsatile force regimen. ECs were seeded on FN or CL 4 hrs prior to incubation with magnetic beads. Average displacements were calculated relative to the first pulse of force. (n >30 beads/condition from 3 independent experiments). Error bars represent s.e.m., *p<0.05. (c) Adherent ECs on FN or CL were incubated with anti-PECAM-1-coated magnetic beads and subjected to force with a permanent magnet for the indicated times. ECs were fixed stained with phalloidin and an anti-vinculin antibody to mark focal adhesions. Focal adhesion number and size were quantified using NIH ImageJ software. Values were normalized to the FN "No Force" condition. Locations of the beads are highlighted in yellow circles (n > 30cells/condition from 3 independent experiments, *p < 0.05, scale bar = 10μm).

Figure 3.2 Mechanically-induced PKA activity negatively regulates RhoA.

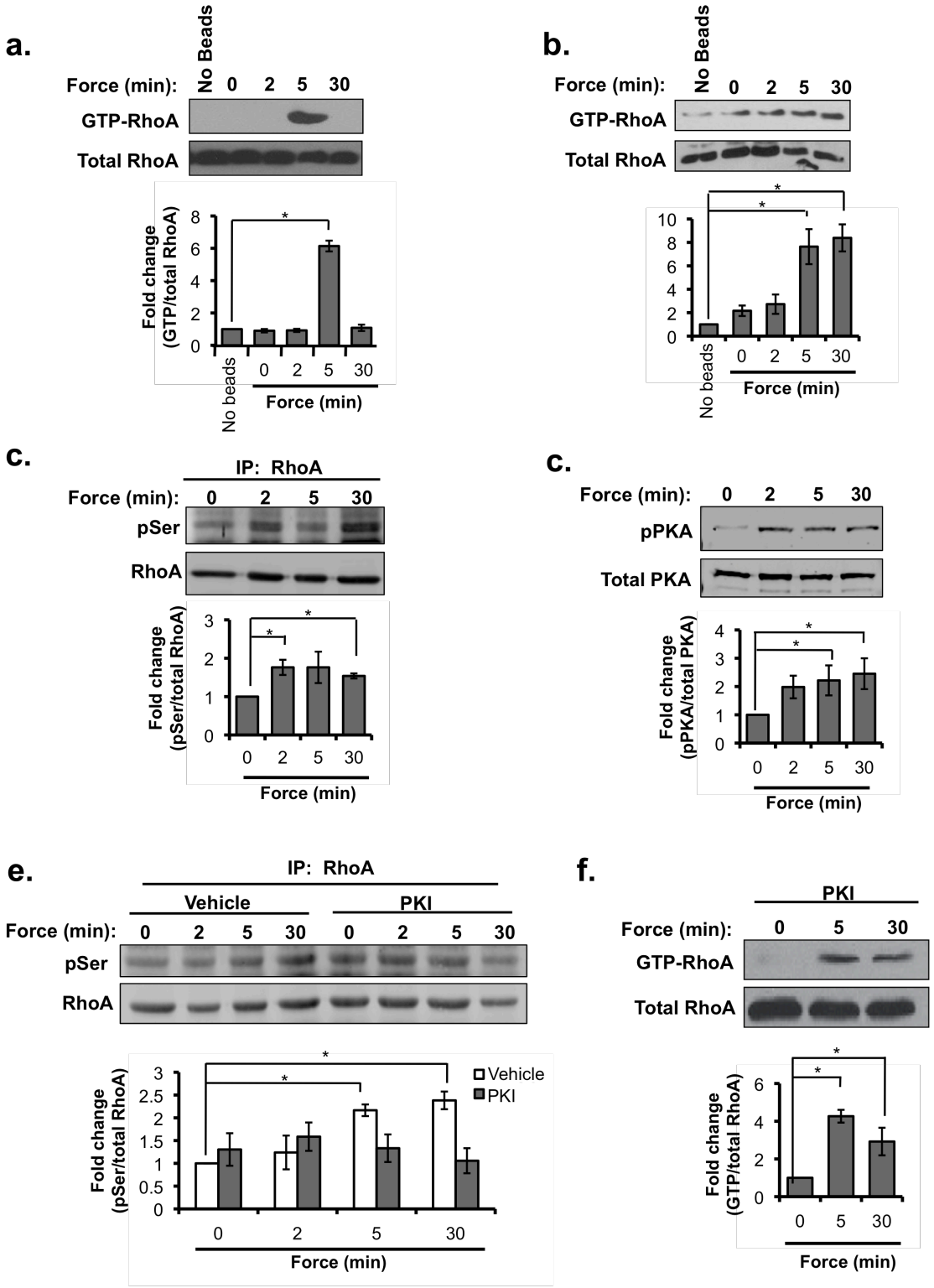

(a-e) Tension was applied to anti-PECAM-1-coated beads using a permanent ceramic magnet for the indicated times, and (a) Active RhoA (RhoA-GTP) was isolated from EC adherent on CL with GST-RBD and analyzed by western blot (n=5). (b) Active RhoA (RhoA-GTP) was isolated from EC adherent on FN with GST-RBD and analyzed by western blot (n=5). (c) Total RhoA protein was immunoprecipitated from cell lysates and immune complexes were subjected to SDS-PAGE, followed by immunoblotting with phosphoserine and RhoA antibodies (n=3). (d) Cell lysates were subjected to SDS-PAGE and immunoblotted for phospho (Tyr497) and total PKA (n=3). (e-f) ECs were treated with PKI (20uM for 1hr) or DMSO and tension was applied to anti-PECAM-1-coated beads using a permanent ceramic magnet for the indicated times. (e) Total RhoA protein was immunoprecipitated from cell lysates and immune complexes were subjected to SDS-PAGE, followed by immunoblotting with phosphoserine and RhoA antibodies (n=3). (f) Active RhoA (RhoA-GTP) was isolated with GST-RBD and analyzed by western blot (n=3). Bar graphs display averages from at least three independent experiments and error bars indicate s.e.m, *$p<0.05$.

Figure 3.3 Inhibition of PKA confers mechanical responsiveness to ECs on CL.

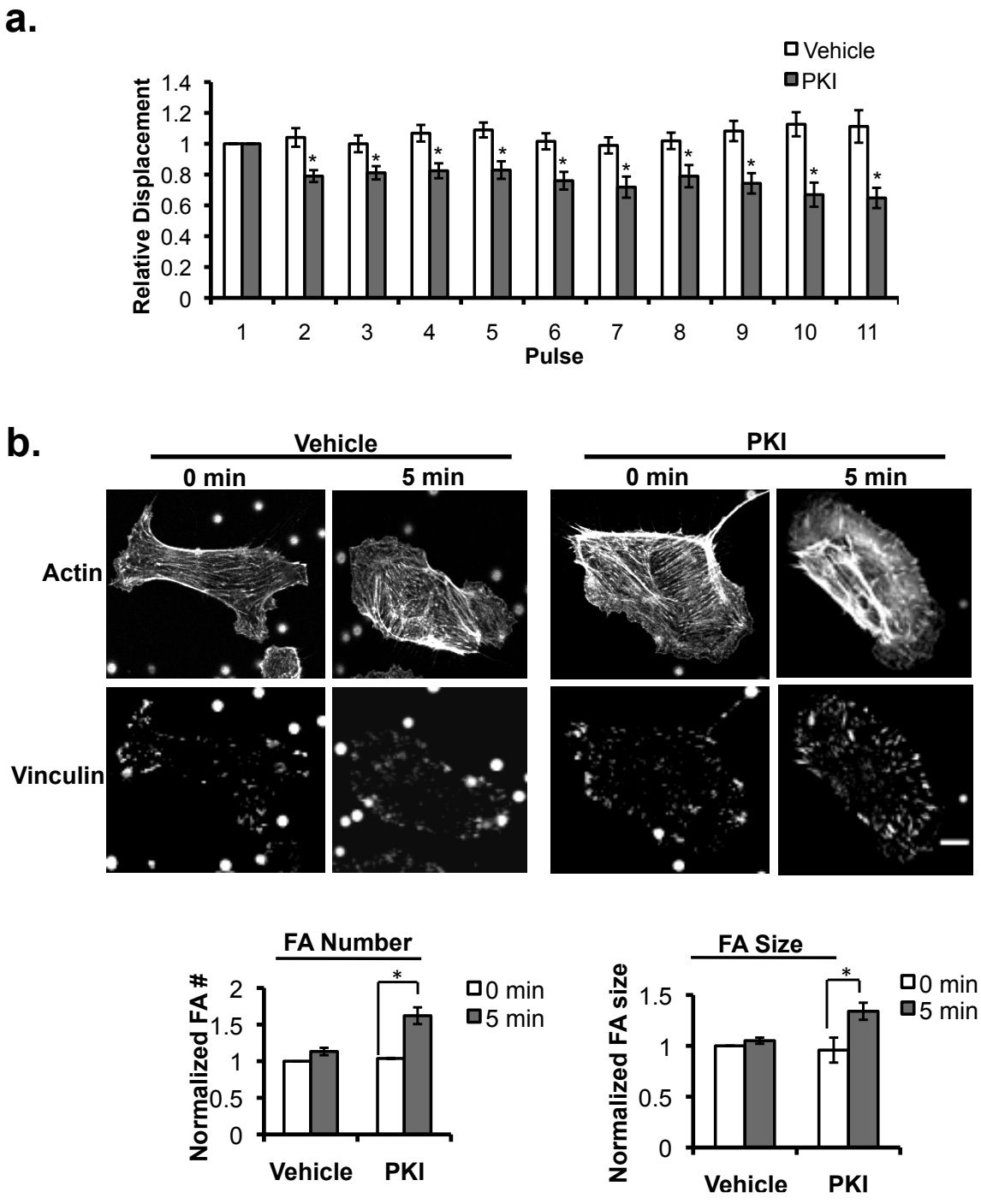

(a-b) ECs were pretreated with PKI (20uM) or vehicle for 1 hr, and (a) Pulsatile forces were applied to PECAM-1 with magnetic tweezers. Average relative anti-PECAM-1-coated bead displacements induced by pulsatile force regimen. Average displacements were calculated relative to the first pulse of force. (n >20 beads/condition from 3 independent experiments). (b) Anti-PECAM-1-coated magnetic beads were subjected to force with a permanent ceramic magnet for the indicated times. ECs were fixed stained with phalloidin and an anti-vinculin antibody to mark focal adhesions. Focal adhesion number and size were quantified using NIH ImageJ software. Values were normalized to the DMSO "No Force" condition. Locations of the beads are highlighted in yellow circles (n > 30cells/condition from 3 independent experiments, *$p < 0.05$, scale bar = 10μm).

Figure 3.4 The PKA pathway regulates hemodynamic -induced focal adhesion dynamics *in vitro* and *in vivo*.

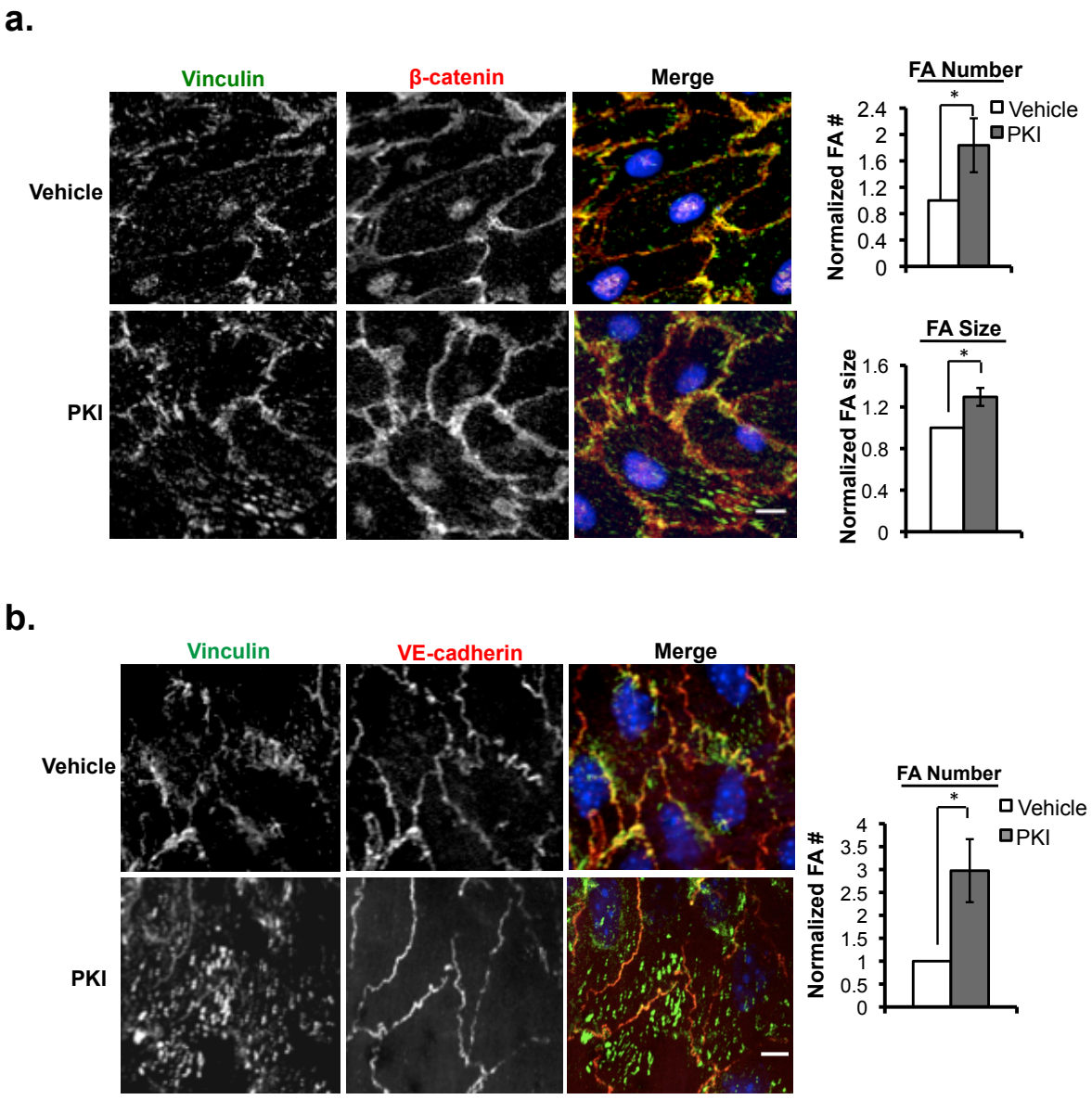

(a) ECs adherent on CL pretreated with PKI (20uM, 1 hr) or vehicle and subjected to shear stress (12 dyn/cm^2 for 30min). Cells were fixed and immunostained with anti-vinculin and anti-β-catenin antibodies. Focal adhesion number and size were quantified using NIH ImageJ software. Values were normalized to the vehicle condition (n=3). (b) Vehicle or PKI

(5nmol) was administered to wildtype mice by retro-orbital injection. Two hrs after injection, aortas were harvested and *en face* preparations were immunostained with anti-vinculin and anti-VE-cadherin antibodies. Focal adhesions were quantified using NIH ImageJ software. Values were normalized to the vehicle (condition for each genotype (n=4 mice/group).

Figure 3.5 The PKA pathway modulates hemodynamic-induced aortic EC stiffness.

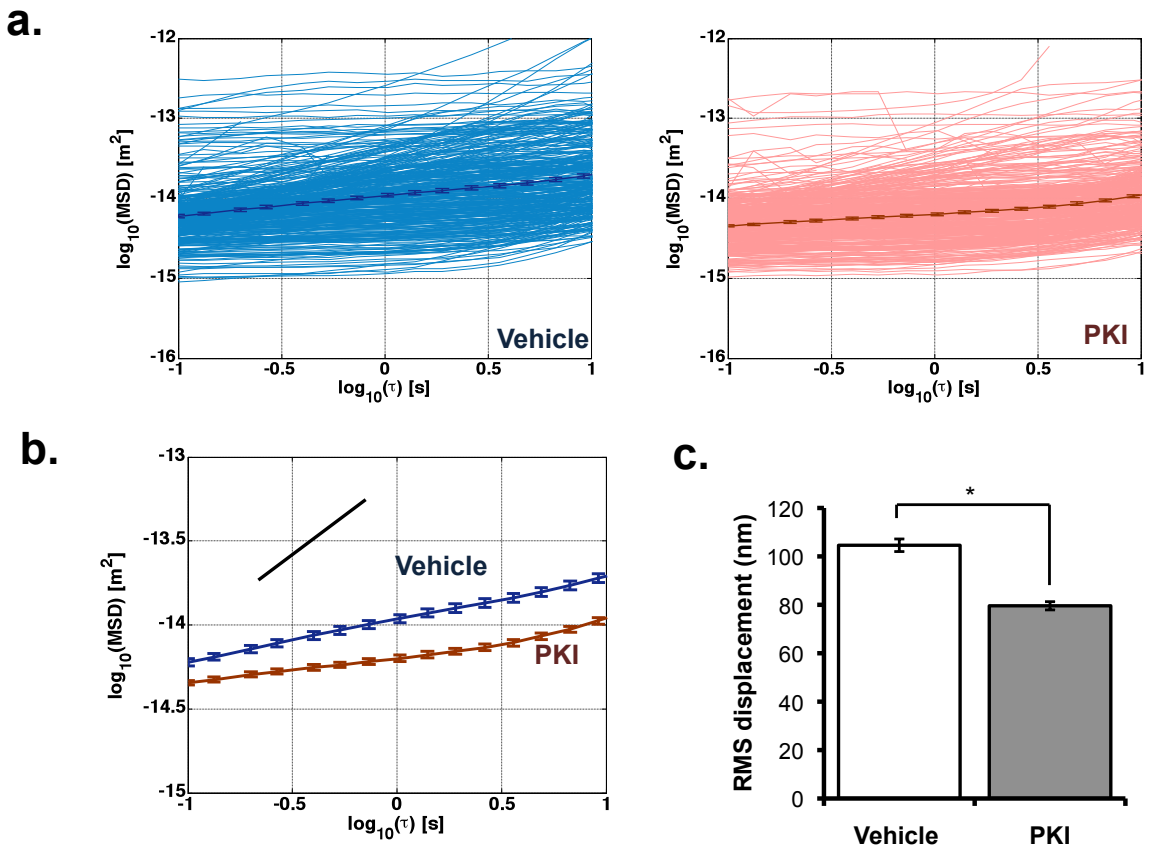

(a) Vehicle or PKI (5nmol) was administered to wildtype mice by retro-orbital injection. Two hrs after injection, aortas were harvested and *en face* preparations were incubated with FN-conjugated beads for external passive microbead rheology. Mean-squared displacement (MSD) trajectories of FN-conjugated, 4.5 μm beads attached to the endothelium of vehicle (blue) or PKI-treated (red) mice. MSDs of individual curves (n > 350 per condition, aggregated from three separate mice for each treatment) are shown in light color and the ensemble-average is represented by the dark curve with s.e.m. shown for indicated timescales. (b) Ensemble-averaged MSDs of beads attached to endothelium of vehicle and PKI-treated mice. Curves show a slope less than unity (illustrated by black guide line),

indicating a sub-diffusive viscoelastic response of beads anchored to the cortical actin cytoskeleton through apical integrin receptors. (c) Root mean-squared (RMS) displacement at the 1-second timescale (τ = 1 s) of beads attached to endothelium of vehicle and PKI-treated mice ($p < 0.0001$).

Figure 3.6 Model of collagen-dependent PECAM-1 mechanosignaling.

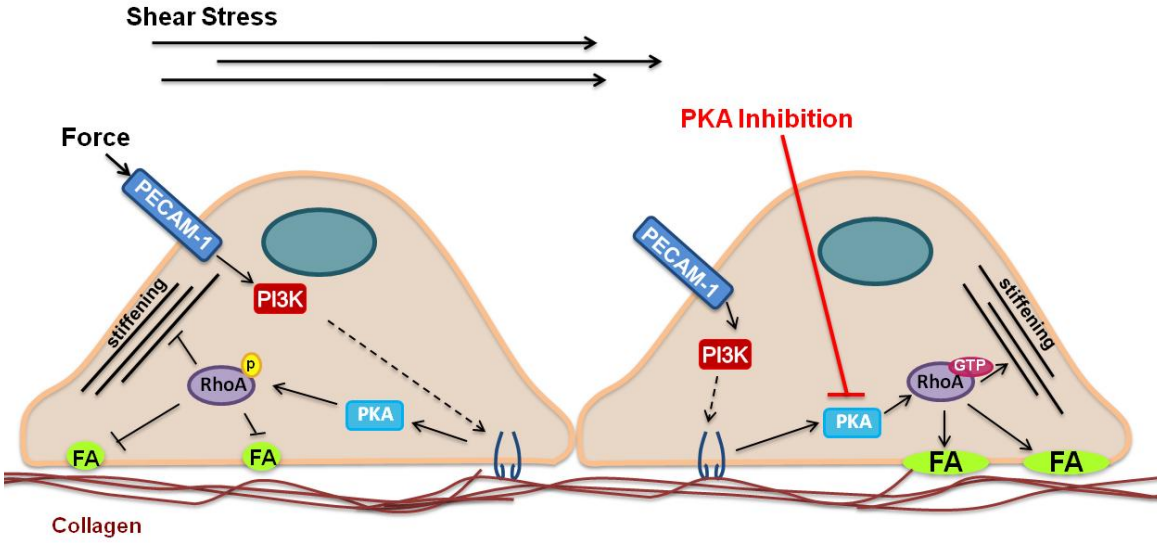

PECAM-1 mechanosignaling through CL-binding integrins results in activation of PKA and subsequent phosphorylation and inactivation of RhoA, which blunts EC responsiveness to force. Inhibition of force-induced PKA activation promotes RhoA activation and is sufficient to restore the cellular response to force, including growth of focal adhesion and increased cellular stiffness.

Experimental Procedures

Cell culture and shear stress. Bovine aortic endothelial cells were maintained in Dulbecco's modified Eagle's medium (DMEM, Cellgro) with 10% fetal bovine serum and 1% penicillin/streptomycin solution. Cells were plated on fibronectin (10μg/ml) or Type I collagen (40μg/ml) 4 hours prior to experiments. For shear stress experiments, endothelial cells were plated on 40 μg/ml collagen in 0.5% FBS. Four hours after plating, cells were slides were loaded onto a parallel plate flow chamber in 0.5% FBS and 12 dynes/cm^2 of shear stress was applied for indicated times.

Reagents, inhibitors, and antibodies. PKI was purchased from Calbiochem. The PECAM-1 antibody (PECAM 1.3) was a generous gift from D.K. Newman (BloodCenter of Wisconsin). The RhoA antibody (26C4) was purchased from Santa Cruz Biotechnologies. The phospho-PKA and total PKA antibodies were from Cell Signaling, and the phospho-serine antibody and rhodamine-phalloidin were from Invitrogen. The vinculin and β-catenin antibodies were obtained from Sigma and the HUTS-4 antibody (which recognizes ligated β1 integrin) was purchased from Millipore. The VE-cadherin antibody was from B.D. Pharminogen.

Preparation of beads. Tosyl-activated paramagnetic beads (2.8 or 4.5um, Invitrogen) were washed with PBS and coated with an anti-PECAM-1 antibody (PECAM 1.3) or purified human fibronectin according to the manufacturer's protocol. Beads were quenched in 0.2M Tris prior to use to remove any remaining tosyl groups and were resuspended in PBS or DMEM containing 10% fetal bovine serum and 1% penicillin/streptomycin solution. Immediately before experiments, ECs were incubated with beads (2-6 bead/cell) for 30min

at 37ºC. Cells were briefly washed with fresh media to remove unbound beads prior to force application.

Pulsatile force application. The UNC 3D Force Microscope (3DFM) was used to apply controlled pulsatile forces (~100pN) to anti-PECAM-1-coated magnetic beads (2.8μm diameter). Bead displacements were recorded with a high-speed video camera (Pulnix, JAI) and tracked using Video Spot Tracker (Computer Integrated Systems for Microscopy and Manipulation, http://cismm.cs.unc.edu/).

Permanent force application. For all immunostaining and biochemical analyses, continuous force (~10pN) was applied to anti-PECAM-1-coated beads (4.5μm diameter) using a permanent ceramic magnet (K&J Magnetics) parallel to the cell culture dish at a distance of 1cm from the adherent cells.

Immunofluorescence. ECs subjected to force (permanent magnet, 4.5μm beads) were fixed for 20min in PBS containing 2% formaldehyde, permeabilized with 0.2% Triton X-100, and blocked with PBS containing 10% goat serum for 1hr at room temperature. Antibody incubations were performed as previously described[13] and mounted in Vectashield mounting medium. Images were acquired using a confocal microscope (Olympus FV500) with a 63x oil lens.

Rho Pulldowns. Adherent cells were incubated with anti-PECAM-1-coated beads (4.5μm, Invitrogen) for 30min and subjected to force for indicated times. Briefly, following force application, cells were lysed in 50mM Tris (pH7.6), 500mM NaCl, 1% Triton X-100, 0.1% SDS, 0.5% deoxycholate, 10mM $MgCl_2$, and protease inhibitors. Anti-PECAM-1-coated

magnetic beads were removed from lysates with a magnetic separator. Lysates were centrifuged for 5min and supernatants were transferred to a new tube and incubated at 4°° with 80μg of purified (GST-RBD) bound to glutathione-sepharose beads. Bead pellets were washed in 50mM Tris (pH 7.6), 150mM NaCl, 1% Triton X-100, 10mM $MgCl_2$, and protease inhibitors, and subsequently resuspended in Laemmli sample buffer and subjected to SDS-PAGE.

Immunoprecipitation and western blotting. Cells were harvested in lysis buffer (20mM Tris (pH 7.4), 150mM NaCl, 50mM NaF, 1% NP-40) supplemented with 10 μg/ml aprotinin, 10 μg/ml leupeptin, 1 mM PMSF, 1 mM Na_3VO_4, 1 mM sodium pyrophosphate, and 1 mM β-glycerophosphate. Lysates were pre-cleared with 15μl protein A/G plus sepharose beads (Santa Cruz) for 1 h at 4°C. Supernatants were then incubated with 30μl protein A/G plus sepharose previously coupled to the primary antibodies for 3 h at 4°C with continuous agitation. The beads were washed three times with lysis buffer supplemented with protease and phosphatase inhibitors and the immune complexes were eluted in 2X SDS sample buffer. Associated proteins were subjected to SDS-PAGE and Western blotting using the appropriate primary antibodies and IRDye-conjugated anti-mouse or anti-rabbit antibodies (Rockland). Images of Western blotting were obtained with an Odyssey infrared scanner system.

Quantification of integrin activation and focal adhesions. ECs stained for ligated β1 integrin (Fig. S2B) or vinculin were analyzed with NIH ImageJ software. Confocal image planes at the basal surface of the cell were chosen for analysis and RGB images were converted to 8-bit black and white images. Activated integrins and focal adhesions were defined by setting an intensity threshold to remove any background signal. Integrin

activation and focal adhesion size and number were analyzed using the 'Analyze particles' function.

Animals and *en face* aorta preparations. 5nmol of PKI or DMSO was administered by retro-orbital injection into 10-12 wk old wildtype. Two hrs after injection, descending aortas were isolated and processed for *en face* immunostaining. Briefly, the aorta was perfusion-fixed and dissected out under dissection microscope. The descending aortas were cut longitudinally and pinned flat with endothelium facing up onto a Surperfrost/Plus glass slide (Fisher Scientific). Tissue sections were stained with anti-vinculin or anti-vinculin antibodies an imaged as described above.

Passive microbead assay for mechanical analysis of aortic endothelium.

The aorta was freshly isolated and prepared *en face* on a coverslip. Briefly, the heart was perfused with PBS containing heparin and nitroprusside and the live aorta was dissected out under a dissection microscope, cut longitudinally, and mounted on a glass coverslip with the endothelium facing up. To anchor the aorta to the coverslip for experiments, a thin sheet (roughly 20 x 40 x 2 mm) of polydimethylsiloxane rubber (PDMS) (Sylgard 184, Dow Corning) was positioned over the tissue. A small section (3 x 5 mm) of the PDMS sheet was removed previous to anchorage to serve as a media reservoir over the descending endothelium (Supplementary Figure S4). The reservoir was immediately filled with Medium 199 containing 10% FBS and 15mM HEPES in order to keep the tissue alive. Fibronectin-conjugated paramagnetic beads (4.5μm, Invitrogen) were incubated over the endothelium for 20 minutes at 37°C. The thermal motion of attached beads was imaged at 40X using an upright reflective microscope (Orthoplan, Leitz) and recorded at 30 frames per second with a high-speed video camera (Pulnix, JAI). Bead motion was monitored for 1 minute and

tracked using Video Spot Tracker software (Computer Integrated Systems for Microscopy and Manipulation, http://cismm.cs.unc.edu/). The time-dependent mean-squared displacement (MSD) of the bead trajectories was computed using $\langle r^2(\tau) \rangle = \langle MSD \rangle = \langle [x(t+\tau) - x(t)]^2 + [y(t+\tau) - y(t)]^2 \rangle$, where t is the elapsed time and τ is the time lag, or timescale. Beads included into analysis were separated from other beads by 3 bead-diameters. Conditions were compared using the ensemble-averaged MSD and the root mean-squared (RMS) displacement.

Statistical analysis. Data are presented as means +/- S.E.M. p-values were determined using a two-tailed unpaired Student's t-test.

Supplemental Figures

Supplementary Figure S3.1 ECM identity does not influence 1st pulse bead displacement.

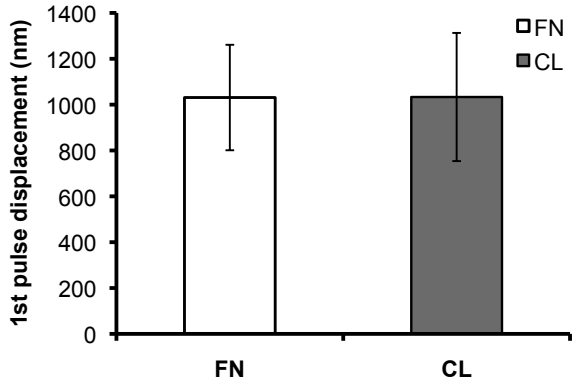

ECs adherent on FN or CL were incubated with anti-PECAM-1-coated beads and subjected to pulsatile force. Bead displacement during the first pulse of force was calculate for each condition. Error bars represent s.e.m., n>15 cells/condition, and $p < 0.05$.

Supplementary Figure S3.2 Force-induced PI3K and integrin activation.

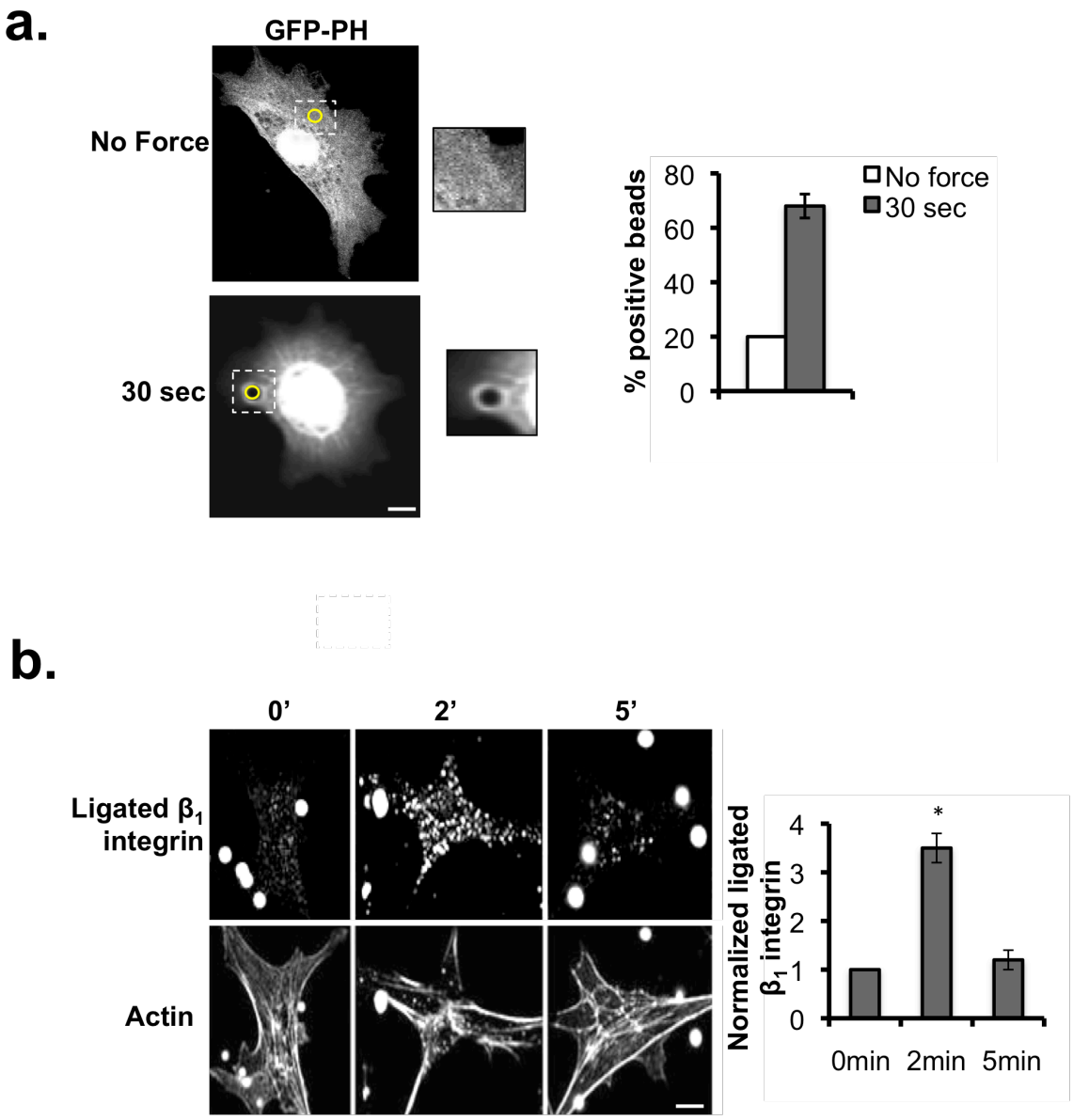

(A) ECs expressing GFP-PH were incubated with anti-PECAM-1-coated magnetic beads and subjected to force with a permanent ceramic magnet for the indicated times. Cells were fixed and scored for GFP-PH recruitment around the bead (box). Location of the bead is highlighted by the yellow circle (n>30 cell/condition for three independent experiments; scale bare = 10μm, $p < 0.05$). (B) ECs were incubated with anti-PECAM-1-coated beads and

subjected to force with a permanent ceramic magnet for the indicated times. ECs were fixed and stained with HUTS-4, which recognizes ligated β1 integrin, and phalloidin to mark the actin cytoskeleton. (n>30 cells/condition from three independent experiments; scare bar = 10μm, $p < 0.05$).

Supplementary Figure 3.3 PKA is not mechanically activated in ECs adherent on FN

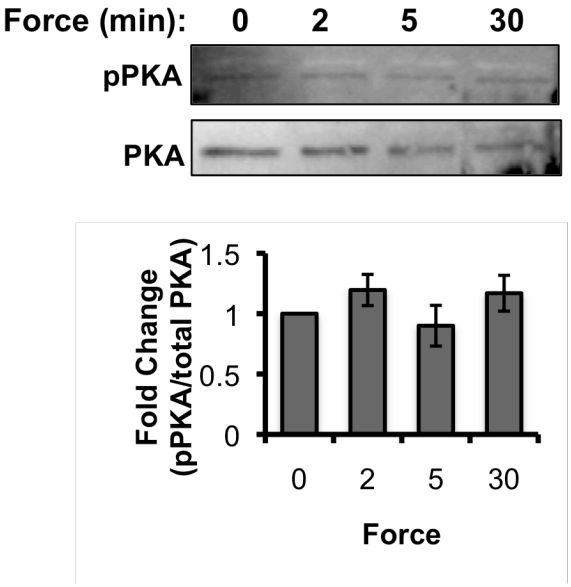

Tension was applied to anti-PECAM-1-coated beads attached to cells adherent on FN using a permanent ceramic magnet for the indicated times. Cell lysates were subjected to SDS-PAGE and immunoblotted for phospho (Tyr497) and total PKA (n=3). Bar graph displays the average fold change in pPKA from at least three independent experiments and error bars indicate s.e.m.

Supplementary Figure S3.4 Regulation of EC focal adhesion profile.

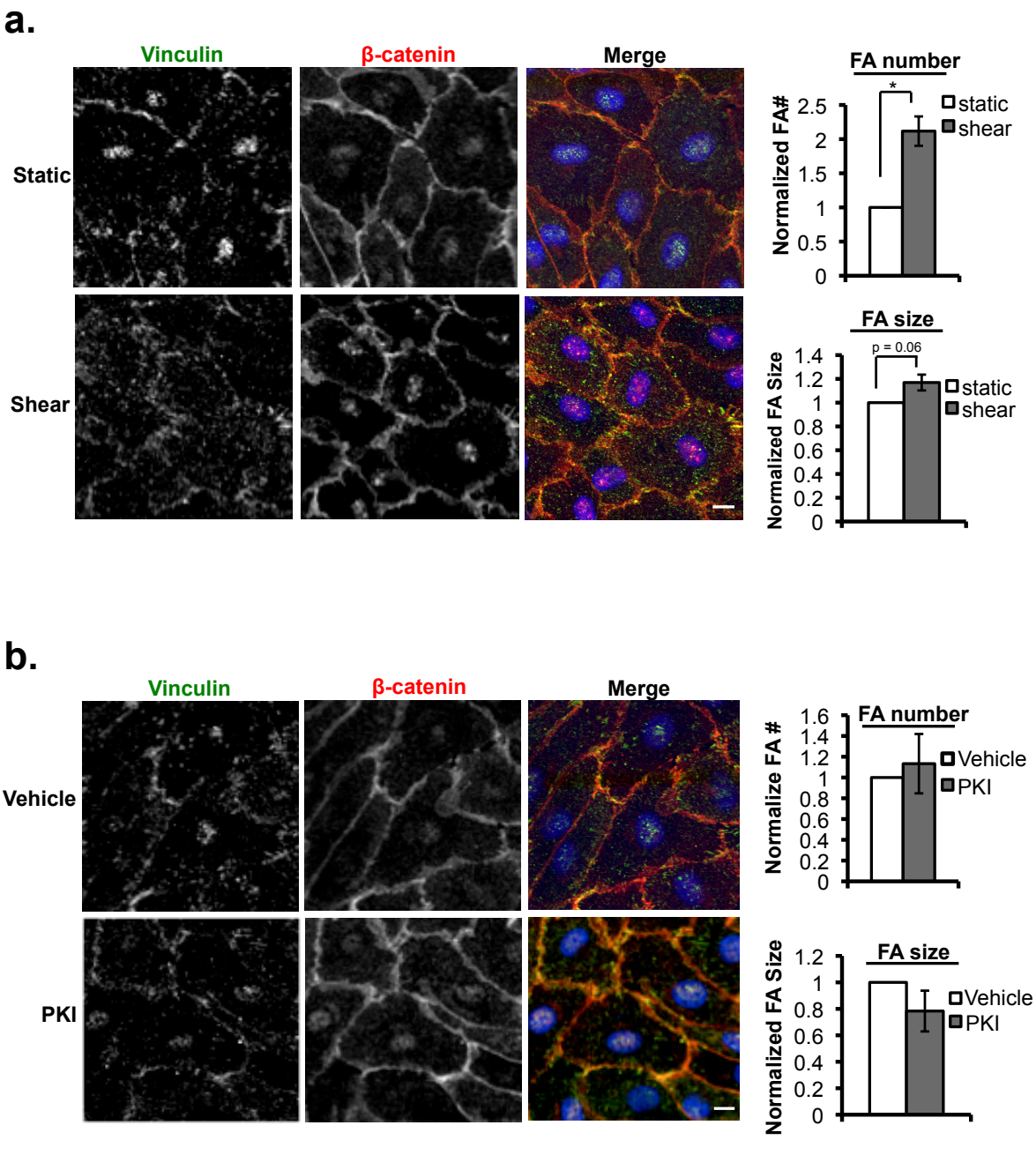

(a) ECs adherent on CL were subjected to shear stress (12 dyn/cm^2 for 30min) or left as static controls. Cells were fixed and immunostained with anti-vinculin and anti-β-catenin antibodies. Focal adhesion number and size were quantified using NIH ImageJ software. Values were normalized to the static condition (n=3). (b) ECs adherent on CL treated with

PKI (20uM, 1 hr) or DMSO. Cells were fixed and immunostained with anti-vinculin and anti-β-catenin antibodies. Focal adhesion number and size were quantified using NIH ImageJ software. Values were normalized to the control (DMSO) condition (n=3). Bar graphs display the averages from three independent experiments and error bars indicate s.e.m., $p<0.05$.

CHAPTER IV.

CONCLUSIONS AND PERSPECTIVES.

OVERVIEW

In Chapters II and III of this dissertation, I have highlighted several new findings that contribute to our understanding of both cell biology and vascular biology. In response to recent evidence highlighting the role of mechanical force in numerous biological processes, there has been a push towards understanding mechanisms of mechanotransduction in recent years. Forces play a pivotal role in vascular biology, as the hemodynamic force of fluid shear stress influences both vessel physiology and pathology. Thus, there is a need to understand how mechanical forces are sensed by ECs and how they are transduced into biochemical signaling pathways that will, ultimately, regulate the EC phenotype and influence vessel health and integrity. The work in Chapter II identified molecular signaling cascades and cellular phenotypes initiated in response to force on the endothelial mechanosensor PECAM-1. The work in Chapter III identified how cells integrate mechanical and extracellular matrix cues to regulate cellular force responses. This work was further extended to the physiological context of shear stress and gave insight into how hemodynamic and extracellular matrix cues influence aortic endothelial stiffness, a critical determinant of vessel integrity.

While Chapters II an III provided novel insights, the research also opened up several new questions. In this Chapter, I will address outstanding questions raised by the research presented in this dissertation and discuss how this work contributes to our understanding of

how complex mechanical and ECM environments regulate EC responses and vessel health *in vivo*.

CHAPTER II: LOCALIZED TENSIONAL FORCES ON PECAM-1 ELICIT A GLOBAL MECHANOTRANSDUCTION RESPONSE VIA THE INTEGRIN-RHOA PATHWAY

In Chapter II, I set out to identify how ECs respond to mechanical force on the mechanosensor PECAM-1. Using a magnetic tweezers system, I showed that ECs respond to force application on PECAM-1 by employing an adaptive stiffening response. This work also identified two interesting findings: 1) a subset of PECAM-1 mechanosignaling is integrin-dependent and therefore, several common mechanotransduction responses between PECAM-1 and integrins exist; 2) localized tension on PECAM-1 elicits a global mechanotransduction response. These intriguing findings are discussed in further detail below.

Common mechanotransduction responses.

A number of experimental approaches used to apply tension on integrins, including optical or magnetic tweezers and electromagnetic microneedles, have shown that cells can sense the applied tension and respond by strengthening their cytoskeletal linkages to oppose the force[3, 7, 60, 82, 104]. Application of tensional forces on anti-PECAM-1-coated beads bound to ECs induces a stiffening response that also depends on the actin cytoskeleton, similar to integrins.

In addition to adaptive stiffening, several other mechanosensitive responses are also shared between PECAM-1 and integrins. Force application to either adhesion receptor results in RhoA activation through two GEFs, GEF-H1 and LARG, via a FAK/ERK signaling

pathway[13, 82]. Interestingly, RhoA activation in response to tensional force on PECAM-1 is integrin dependent, because inhibition of new integrin-ECM connections quenched force-induced RhoA activity[13]. This integrin-dependent RhoA activation might explain the shared GEFs in both systems. Importantly, RhoA-mediated signaling is required for adaptive stiffening downstream of both integrins and PECAM-1, as inhibition of RhoA, its GEFs, or its effectors abolishes the force-dependent stiffening response. Finally, tension on either integrins or PECAM-1 also results in growth of focal adhesions, which mechanically couple the internal actin cytoskeleton to the extracellular matrix[5, 13]. Indeed, the best-defined response of integrin-dependent adhesions to tension is reinforcement of the focal adhesions to counteract the exogenously applied force, as growth of adhesions increases cell generated tension[105]. Similarly, force on PECAM-1 results in growth of focal adhesions. In contrast to the local adhesion growth observed in response to tension on integrins, PECAM-1-mediated adhesion growth is a global phenomenon. This leads us to the important differences in mechanotransduction cascades between these two cell adhesion molecules that will be discussed below.

Differences in mechanotransduction pathways.

Several differences exist when comparing the cellular response to force application on integrins vs. PECAM-1. Closer examination of some of the shared responses, such as adaptive stiffening or RhoA activation, also reveal some notable differences in the cellular responses downstream of each receptor. While mechanical stimulation of either adhesion receptor results in adaptive stiffening, the time course of the response varies between the two proteins. Tension applied to FN-binding integrins results in an immediate stiffening response, as differences in cellular stiffness can be detected immediately following force application. Conversely, while force application on PECAM-1 also elicits adaptive stiffening, the response is delayed and is detectable on a minute, rather than second timescale. This

same trend is also observed when taking a closer look at the time course of RhoA activation. Force application on integrins results in an increase in RhoA activity in as little as 1 min. In contrast, force-induced RhoA activation downstream of PECAM-1 does not increase until 5 min of force. Therefore, it is possible that the delay in the PECAM-1-mediated adaptive stiffening response is a reflection of delayed RhoA activation. Differences in the time course of these events may be attributed to differences in mechanisms of signal transduction. Mechanosensitive signaling pathways may be chemically or mechanically propagated throughout the cell, via diffusion of small chemical messengers or mechanically transmitted through cytoskeletal filaments, respectively. Indeed, mechanical signals can be propagated at a remarkable speed of 30 m/s, whereas biochemical signals diffuse at a mere rate of 2 μm/s [6]. Given integrins' intimate association with the cytoskeleton, it is possible that integrin-mediated mechanotransduction relies more heavily on mechanical transmission of the signaling cascade, while PECAM-1-mediated mechanotransduction is more chemically dependent in nature.

Perhaps the most profound difference between integrin and PECAM-1-mediated mechanosignaling involves the spatial organization of the response. Several studies have revealed that integrin-mediated adaptive stiffening response is mediated, in part, by localized recruitment of focal adhesion proteins (such as β_1 and β_3 integrins, talin, and vinculin), which results in a local growth of adhesions at the site of force application[5, 8]. Similarly, force application on integrins induces localized recruitment of LARG and GEF-H1 to the adhesion complex[4]. Furthermore, mRNA and ribosomes also specifically localize to focal adhesions that form when cells bind to FN-coated microbeads[9]. Surprisingly, our work has revealed that tension on PECAM-1 results in a remarkable cell-wide, or global, mechanotransduction response, as evidenced by a cell-wide increase in focal adhesion growth. This result is especially intriguing, as it is the first documented evidence of a global mechanotransduction event elicited by a localized force. While studies from Ning Wang's

group have reported Src and Rac activation at remote sites away from stress application with RGD-coated beads[6, 68, 106], neither signal displayed cell-wide distribution. Nevertheless, it has been shown that global, cell-wide changes in cytoskeletal structure and mechanics can regulate mechanotransduction, such that the mechanotransduction response is governed by global mechanical cues, including isometric tension (pre-stress) within the cytoskeleton[106, 107].

Globalization of Mechanotransduction.

How does a localized force on PECAM-1 elicit a global response? Phosphoinositide 3-kinase (PI3K) is rapidly activated following application of tension on PECAM-1. Activation of PI3K results in the production of freely diffusible phosphoinositides (such as $PI(3,4,5)P_3$) that act as second messengers to propagate signaling cascades throughout the cell. Experimental evidence suggests that: 1) activation of PI3K, and 2) diffusion of the second messenger $PI(3,4,5)P_3$ is required for the global response downstream of PECAM-1. Localized tension on PECAM-1 not only elicits global focal adhesion formation, but also results in global integrin and RhoA activation. Interestingly, inhibition of PI3K activation, or sequestration of the $PI(3,4,5)P_3$ messenger abolishes the global signaling response. PI3K has been implicated in integrin activation in various contexts and cell types, although the exact mechanism of activation remains elusive[108]. $PI(3,4,5)P_3$ has a documented half-life 60 seconds[109] and a fairly rapid diffusion rate of 0.1-1 $\mu m/s^2$ [110]. Given that ECs are relatively thin cells (generally less that 5μm in height), it is feasible that freely diffusing $PI(3,4,5)P_3$ would be able to globally activate integrins at cellular sites distal to the site of force application. Therefore, the current model of PECAM-1-mediated mechanotransduction suggests that PI3K is rapidly activated downstream of PECAM-1, and $PI(3,4,5)P_3$ promotes global integrin activation. Integrin activation is followed by new binding to the ECM and enlargement of

adhesions. Cell-wide activation of integrins elicits global activation of RhoA via the GEF-H1 and LARG pathway. This is a crucial aspect of the PECAM-1-mediated response, as global activation of the GTPase facilitates global growth of focal adhesions, which contribute to the adaptive stiffening response. This model also highlights cooperation of two mechanosensors in this system: PECAM-1 and integrins. Not only does PECAM-1 lead to activation of integrins, but integrin ligation with the ECM is required for force-induced RhoA activation and adaptive stiffening.

The requirement of PI3K activation and $PI(3,4,5)P_3$ implies that chemical signaling is critical for the global nature of the PECAM-1-mediated response. However, it remains unclear if mechanical propagation of the signal is also required for the global response. Transmission of force through tensile cytoskeletal elements can propagate mechanosensitive signaling away from sites of applied stress. For instance, previous studies probing integrins reported rapid activation of Src and Rac at remote cytoplasmic locations away from the site of mechanical stress [6, 68, 69]. However, these signals were not global in nature, but rather were confined to distinct puncta that corresponded with sites of cytoskeletal deformation. It is also important to note that the integrins' physical association with the cytoskeleton has been well documented. Therefore, it is plausible that tensile cytoskeletal filaments anchored to integrins on opposing sides of the cell could facilitate transmission of a mechanical stimulus across the cell. However, PECAM-1 has not been shown to directly interact with the cytoskeleton, although indirect association via cytoplasmic interactions with β-catenin and γ-catenin have been proposed [70]. Furthermore, the exact of mechanism of PECAM-1-mediated mechanosensing remains unknown. Models of mechanotransduction often involve force-dependent conformational changes in proteins that permit propagation of mechanosensitive signaling cascades. For instance, $\alpha_5\beta_1$ integrin undergoes a force-dependent conformational change[111], which allows chemical crosslinking to FN and recruitment and

activation FAK. While it is appealing to hypothesize that PECAM-1-mediated mechanotransduction may be dependent on a conformational change, a force-dependent change in the protein structure has not yet been identified, and thus, the mechanism of mechanosensing remains elusive. Comprehensive studies investigating the structure of the PECAM-1 cytoplasmic tail may provide insights into the mechanisms of PECAM-1-mediated mechanosignaling and reveal the relative contributions of chemical signaling and mechanical transmission in the global mechanotransduction response.

CHAPTER III: HEMODYNAMIC AND EXTRACELLULAR MATRIX CUES REGULATE THE MECHANICAL PHENOTYPE AND STIFFNESS OF ENDOTHELIAL CELLS

In Chapter III, I set out to investigate how ECs integrate mechanical and ECM-specific cues. Through my research, I found that the ECM composition has a profound effect on the cellular response to tension on PECAM-1. I demonstrated that matrix-specific PKA activation and subsequent de-activation of RhoA influences EC response to force. I further extended these studies to the physiological stimulus of shear stress and the complex hemodynamic environment of the vessel. In this Chapter, I elaborate on our knowledge of matrix specific signaling in the endothelium and discuss PKA as a critical regulator of endothelial and cardiovascular biology.

Matrix-specific responses to force.

Matrix-specific signaling in the endothelium has been well documented in recent years. Fluid shear stress elicits integrin activation and ligation with the underlying ECM[43]. Therefore, activation of divergent integrin subtypes can influence downstream signaling cascades. For example, ECs on CL preferentially activate PKA[44] and eNOS[45] in response

to laminar shear stress, when compared to ECs on FN. Conversely, ECs adherent on FN display preferential activation of protein kinase C (PKC)[42], PAK[46], JNK[47, 48], and NF-κB[53]. Activation of distinct signaling cascades can have profound effects on the cellular phenotype. For instance, JNK and NF-κB are associated with pro-inflammatory signaling, indicating that FN-dependent signaling is correlated with inflammation and onset and progression of disease. Conversely, activation of eNOS is atheroprotective and anti-inflammatory.

In Chapter III, I demonstrated that ECs adherent on FN generate a mechanical response that includes stiffening and growth of focal adhesions in response to tension on PECAM-1, whereas ECs adherent on CL do not. This difference in mechanical phenotypes is due to CL-specific activation of PKA and inactivation of RhoA. Interestingly, other vascular cell types have also shown matrix-specific mechanical responses. For instance, mechanical force has been applied to FN and CL-binding integrins in vascular smooth muscle cells (VSMCs) using AFM[112]. In those studies, mechanical perturbation of FN-binding integrins induced a contractile response in VSMCs that is ROCK-dependent. Conversely, when tension is applied to CL-binding integrins, the contractile response is absent (although other signaling events such as increased calcium influx remain intact). Thus, there may be matrix-specific and force-dependent differences in RhoA activity in other vascular cell types as well.

The data presented in Chapter III indicate that the presence of FN promotes a stiffening phenotype, whereas adhesion to CL promotes a more compliant phenotype. Interestingly, increased vascular stiffness has been associated with increased permeability and leukocyte infiltration, both of which are correlated with inflammation and vascular dysfunction. Thus, my research also suggests that FN-dependent signaling promotes a pro-inflammatory phenotype, while CL-dependent signaling may provide atheroprotective cues in the endothelium.

PKA in vascular biology.

PKA is a multifunctional kinase that has many well-documented roles in cell biology. Importantly, the protein has also been implicated in numerous facets of vascular biology, including angiogenesis[113], anti-inflammatory signaling[44], and endothelial barrier function[114, 115]. Here, I will briefly summarize our knowledge of the role of PKA in vascular biology and summarize how my studies contribute to the field.

ECs are central to angiogenesis, the process by which a new blood vessel arises from pre-existing vessels. This process is tightly linked to cancer, as growth of new blood vessels not only provides oxygen and nutrients to the tumor, but also provides a means of escape during metastasis. Angiogenesis is a complicated process that relies on dynamic EC interactions with the surrounding microenvironment. Therefore, it is not surprising that integrins play a critical role in this process. Indeed, integrin-dependent regulation of PKA has been shown to influence angiogenesis. In the context of cancer, ligation of $\alpha5\beta1$ (a FN-binding integrin) suppresses PKA activation, which increases EC survival and promotes angiogenesis[113]. Data presented in Chapters II and III of this dissertation demonstrate that: 1) Tension on PECAM-1 elicits $\alpha5\beta1$ activation in ECs adherent on FN, and 2) ECs attached to FN do not activate PKA in response to force application on PECAM-1. Thus, ligation of $\alpha5\beta1$ downstream of mechanically activated PECAM-1 may also suppress PKA activation in the context of hemodynamic force.

Another well-studied process in the vascular system is inflammation; a cellular process that contributes to numerous diseases, including atherosclerosis. As previously mentioned, fluid shear stress plays a critical role in the development and progression of atherosclerosis, as flow-dependent and matrix-specific signaling have profound effects on pro/anti-inflammatory signaling in the endothelium. Furthermore, matrix-specific activation of PKA has been shown to influence EC inflammation. PKA is preferentially activated on CL in response to shear stress, and activation of the kinase inhibits pro-inflammatory signaling,

including activation of NF-κB. Previous work has demonstrated that inhibition of PKA *in vivo* promotes pro-inflammatory signaling in the regions of the aorta where CL predominates[44]. Conversely, administration of iloprost, a prostacyclin analog that enhances adenylyl cyclase activity, in the FN-rich aortic arch (a region that is susceptible to pro-inflammatory signaling), decreases inflammation *in vivo*. Thus, matrix-specific regulation of PKA activity has profound effects on EC inflammation *in vivo*.

The work presented in Chapter III suggests that hemodynamic and matrix-specific activation of PKA also contribute to EC compliance in the CL-rich descending aorta. Vascular stiffness positively correlates with increased permeability and decreased barrier function[55]. Therefore, activation of PKA and a more compliant cellular phenotype may serve as an atheroprotective mechanism that enhances barrier function. PKA has been shown to decrease permeability and increase EC barrier function in previous studies. Prostaglandin-mediated activation of the kinase enhances adherens junction formation and decreases permeability in a cAMP/PKA-dependent manner via regulation of the Rho GTPase, Rac1[114, 115]. Furthermore, PKA-dependent RhoA phosphorylation enhances barrier function and prostaglandin-mediated PKA activation protects against thrombin-induced Rho activation and increased phosphorylated myosin light chain (pMLC) in ECs. My data indicate that mechanically induced activation of PKA attenuates force-induced RhoA activation and promotes cell compliance, which may also influence EC barrier function and permeability *in vivo*.

INTEGRATING CHAPTERS II AND III: MECHANISMS AND CONSEQUENCES OF EC STIFFENING.

Shear stress and EC stiffness.

ECs are situated in a dynamic mechanical environment. Due to their unique location in the vessel, they are constantly exposed to hemodynamic forces produced by blood flow and must simultaneously regulate their own mechanical properties in order to resist shear forces. Several studies have used various techniques to address the question of how fluid shear stress influences EC stiffness, and it is clear that a dynamic relationship between shear stress and EC stiffness exists over various timescales. Using particle tracking of endogenous cellular vesicles, Dangaria et al demonstrated that laminar shear stress (10 dyn/cm^2) increases cytoplasmic compliance in as little as 30 sec, indicating that the cytoplasm softens upon exposure to shear[58]. However, this response is short-lived as compliance returns to pre-shear levels within minutes. However, one caveat of this study is that particle tracking of endogenous vesicles only provides insight in cytoplasmic stiffness, and therefore, excludes changes in mechanics of the cortical actin cytoskeleton.

Several studies have investigated cellular mechanics in response to shear stress over longer timescales. Experimental evidence suggests that ECs that have been exposed to shear stress (2 Pa = 20 dyn/cm^2) for 6 hours demonstrate similar mechanical properties as static ECs[116, 117]. However, ECs become more resistant to AFM indentation between 6-24 hours of laminar shear, indicating an increase in cellular stiffness[117]. Taken together, the literature suggests biphasic regulation of EC mechanics in response to fluid shear stress. ECs immediately soften upon exposure to shear, but compliance returns to pre-shear values upon minutes to hours flow stimulation. However, at timescales longer than 6hrs, ECs stiffen when compared to static cells.

Interestingly, flow-induced changes in EC stiffness coincide with shear-dependent changes in Rho activity and cytoskeletal reorganization. RhoA activity decreases within 5 minutes upon shear stress stimulation, and within this short window, there is a significant breakdown of actin filaments[43]. Interestingly, it is during this time that an increase in cellular compliance has been reported[58]. Furthermore, the timescale in which flow-induced increases in EC stiffness have been documented also coincide with the emergence of actin stress fibers that align in the direction of flow[43, 117, 118]. These data suggest that changes in RhoA activity and reorganization of the actin cytoskeleton may contribute to shear-dependent changes in EC mechanics. Therefore, future experiments investigating flow-dependent changes in RhoA activity and EC compliance may provide insights into the molecular mechanisms linking shear stress and EC mechanics.

Previous work has also highlighted a complex relationship between hemodynamic force and cellular stiffness. Effects on cellular stiffness are dependent on both shear stress magnitude and duration. For instance, ECs exposed to 10 dyn/cm^2 shear stress show little change in stiffness after 30 minutes of stimulation, but show a 3-fold increase in stiffness compared to static counterparts at later time points[119]. Conversely, high shear stress magnitudes (~85 dyn/cm^2) influence cellular stiffness in as little as 30-90 min, as ECs exposed to high shear stress magnitudes within this short time frame show a 4-fold increase in stiffness compared to static ECs[119]. Furthermore, shear-induced EC stiffness is anisotropic within a single cell, such that the downstream edge of the cell is more compliant than the upstream edge of the cell (albeit still stiffer than a static cell)[118]. Thus, while shear stress and EC mechanics are clearly related, the relationship between the two is complex and influenced by a number of dynamic variables.

While many studies have begun to address the relationship between shear and EC stiffness, many questions remain. For instance, the influence of the extracellular matrix has not yet been explored in shear-induced EC stiffness, as all of the studies

performed to date have investigated responses in EC adherent on FN. Furthermore, investigating shear-induced EC stiffness on other matrices may be important, as the data presented in this dissertation suggest that the ECM composition has a profound effect on EC responsiveness to hemodynamic force. In addition, studies to date have not yet investigated the influence of shear stress patterns (laminar vs. oscillatory) on EC stiffness, as all studies to date have compared EC stiffness in static cells versus ECs subjected to laminar shear. One may hypothesize that laminar or oscillatory shear stress may have different effects on EC mechanics. In support of this hypothesis, a recent study suggests that laminar and oscillatory shear stress have divergent effects on EC intracellular tension[120].

Finally, shear-induced effects on EC stiffness *in vivo* remain largely unexplored. One study performed in the late 1990s investigated how dynamic changes in shear stress influence focal adhesion components and cytoskeletal organization. In this study, hemodynamics were altered *in vivo* by restricting the diameter of the aorta via the surgical model of coarctation in guinea pigs. This surgery alters both shear stress patterns and magnitudes in the coarctation zone[121]. Interestingly, ECs in the coarctation zone displayed more prominent stress fibers and increased focal adhesion size and number[122]. While changes in EC stiffness were not evaluated in the study, my data suggest that increased focal adhesion size and number corresponds with EC stiffening[13].

Some studies have measured vessel wall stiffness in various regions of the vasculature using atomic force microscopy[57, 123]. However, using this method, it is difficult to isolate EC stiffness, as mechanical properties of the underlying layers of the vessel are the major contributors to the measured compliance. I used external microbead passive rheology in order to measure EC stiffness in freshly isolated aortas and demonstrated that PKA influences EC compliance in the CL-rich descending aorta. However, a comprehensive understanding of EC mechanics in the heterogeneous environment *in*

vivo remains elusive. Based on the findings in Chapter II and III, I hypothesize that ECs in the aortic arch (a region of the vasculature with high FN content) would be stiffer than ECs in the CL-rich descending aorta, and external microbead passive rheology will be used in future experiments in order to test this hypothesis. However, it is important to remember that the aortic arch and descending aorta also differ in their hemodynamic environment, which may confound interpretation of results. Thus, as previously noted, there is a need to understand the influence of shear stress patterns and ECM composition on EC mechanics *in vitro* in order dissect their respective contributions to EC stiffness *in vivo*.

EC stiffening and vascular pathologies.

While studies linking shear stress and EC stiffness *in vivo* are lacking, numerous studies have identified a link between EC stiffness and decreased cardiovascular health. For instance, EC stiffness (as well as overall vessel stiffness) often increases in hypertensive vessels. Stimulation of ECs with exogeneous extracellular sodium or aldosterone, a hormone that influences blood pressure by promoting sodium retention, induces an immediate and prolonged increase in EC stiffness[54, 124]. Interestingly, this increase in EC stiffness has a functional effect as well, as ECs stimulated with sodium or aldosterone exhibit decreased NO production *in vitro* and blunted flow-mediated dilation *in vivo*[54].

Increased EC stiffness has also been linked to hypercholesterolemia, a condition that contributes to vascular pathologies such as atherosclerosis and chronic inflammation. Vascular inflammation can be influenced by oxidative damage of low density lipoprotein (LDL), and increased levels of oxidized LDL (oxLDL) have been linked to endothelial dysfunction and atherosclerotic plaque formation[125]. OxLDL treatment increases EC stiffness *in vitro* and is associated with a concomitant increase in EC

intracellular force generation[126]. In addition, ECs isolated from hypercholesterolemic pigs (which display increased oxLDL levels) are stiffer than control ECs isolated from healthy pigs[126], suggesting that oxLDL also affects EC stiffness *in vivo*. Furthermore, increased cellular stiffness may also affect EC responsiveness to fluid shear stress. Previous studies have indicated that ECs treated with oxLDL and exhibiting increased stiffness: 1) do not change morphology when subjected to shear, 2) show significant detachment from the substrate, and 3) display a 30% decrease in intercellular tension when under fluid shear stress[127]. Therefore, EC stiffness may affect flow-mediated processes that are critical for vascular homeostasis.

Finally, age-related intimal stiffening has also been associated with increased EC permeability and leukocyte transendothelial migration[55]. Furthermore, stiffness-induced EC permeability is ROCK-dependent, and inhibition of the kinase restores EC barrier function *in vitro* and reduces leukocyte transendothelial migration *in vivo*. Interestingly, PECAM-1-mediated adaptive stiffening is also ROCK-dependent. Thus, it may be interesting to investigate if PECAM-1-mediated adaptive stiffening also influences EC permeability and leukocyte transendothelial migration *in vivo* in future studies.

Taken together, the literature clearly indicates that EC stiffness is associated with numerous pathologies and can be induced by various stimuli. My work suggests that PECAM-1-mediated mechanosignaling and fluid shear stress influence mechanical responsiveness to hemodynamic force and EC stiffness *in vitro* and *in vivo*. Previous studies have implicated hemodynamic force, extracellular matrix-specific signaling, and EC stiffness as contributors to cardiovascular disease. However, the molecular mechanisms connecting these factors have not been identified. My work highlights the EC mechanosensor PECAM-1 as a critical regulator of hemodynamic and ECM-specific EC stiffening *in vitro* and *in vivo*, thus providing a link to connect these three factors. Furthermore, the work presented here provides new insights into how mechanosensitive

signaling influences the EC phenotype and cardiovascular health and highlight PECAM-1-mediated mechanotransduction as a critical regulator of EC biology and cardiovascular physiology.

REFERENCES

1. Tan JL, Tien J, Pirone DM, Gray DS, Bhadriraju K, Chen CS. Cells lying on a bed of microneedles: An approach to isolate mechanical force. *Proc Natl Acad Sci U S A*. 2003;100:1484-1489

2. Liu Z, Tan JL, Cohen DM, Yang MT, Sniadecki NJ, Ruiz SA, Nelson CM, Chen CS. Mechanical tugging force regulates the size of cell-cell junctions. *Proc Natl Acad Sci U S A*. 2010;107:9944-9949

3. Wang N, Butler JP, Ingber DE. Mechanotransduction across the cell surface and through the cytoskeleton. *Science*. 1993;260:1124-1127

4. Guilluy C, Swaminathan V, Garcia-Mata R, Timothy O'Brien E, Superfine R, Burridge K. The rho gefs larg and gef-h1 regulate the mechanical response to force on integrins. *Nat Cell Biol*. 2011

5. Riveline D, Zamir E, Balaban NQ, Schwarz US, Ishizaki T, Narumiya S, Kam Z, Geiger B, Bershadsky AD. Focal contacts as mechanosensors: Externally applied local mechanical force induces growth of focal contacts by an mdia1-dependent and rock-independent mechanism. *J Cell Biol*. 2001;153:1175-1186

6. Na S, Collin O, Chowdhury F, Tay B, Ouyang M, Wang Y, Wang N. Rapid signal transduction in living cells is a unique feature of mechanotransduction. *Proc Natl Acad Sci U S A*. 2008;105:6626-6631

7. Matthews BD, Overby DR, Mannix R, Ingber DE. Cellular adaptation to mechanical stress: Role of integrins, rho, cytoskeletal tension and mechanosensitive ion channels. *J Cell Sci*. 2006;119:508-518

8. Balaban NQ, Schwarz US, Riveline D, Goichberg P, Tzur G, Sabanay I, Mahalu D, Safran S, Bershadsky A, Addadi L, Geiger B. Force and focal adhesion assembly: A close relationship studied using elastic micropatterned substrates. *Nat Cell Biol*. 2001;3:466-472

9. Chicurel ME, Singer RH, Meyer CJ, Ingber DE. Integrin binding and mechanical tension induce movement of mrna and ribosomes to focal adhesions. *Nature*. 1998;392:730-733

10. le Duc Q, Shi Q, Blonk I, Sonnenberg A, Wang N, Leckband D, de Rooij J. Vinculin potentiates e-cadherin mechanosensing and is recruited to actin-anchored sites

within adherens junctions in a myosin ii-dependent manner. *J Cell Biol*. 2010;189:1107-1115

11. Weber GF, Bjerke MA, DeSimone DW. A mechanoresponsive cadherin-keratin complex directs polarized protrusive behavior and collective cell migration. *Dev Cell*. 2012;22:104-115

12. Huveneers S, Oldenburg J, Spanjaard E, van der Krogt G, Grigoriev I, Akhmanova A, Rehmann H, de Rooij J. Vinculin associates with endothelial ve-cadherin junctions to control force-dependent remodeling. *J Cell Biol*. 2012;196:641-652

13. Collins C, Guilluy C, Welch C, O'Brien ET, Hahn K, Superfine R, Burridge K, Tzima E. Localized tensional forces on pecam-1 elicit a global mechanotransduction response via the integrin-rhoa pathway. *Curr Biol*. 2012;22:2087-2094

14. Chatzizisis YS, Coskun AU, Jonas M, Edelman ER, Feldman CL, Stone PH. Role of endothelial shear stress in the natural history of coronary atherosclerosis and vascular remodeling: Molecular, cellular, and vascular behavior. *J Am Coll Cardiol*. 2007;49:2379-2393

15. Davies PF, Mundel T, Barbee KA. A mechanism for heterogeneous endothelial responses to flow in vivo and in vitro. *J Biomech*. 1995;28:1553-1560

16. Davies PF, Civelek M, Fang Y, Fleming I. The atherosusceptible endothelium: Endothelial phenotypes in complex haemodynamic shear stress regions in vivo. *Cardiovasc Res*. 2013;99:315-327

17. Davies PF. Flow-mediated endothelial mechanotransduction. *Physiol Rev*. 1995;75:519-560

18. Sun J, Williams J, Yan HC, Amin KM, Albelda SM, DeLisser HM. Platelet endothelial cell adhesion molecule-1 (pecam-1) homophilic adhesion is mediated by immunoglobulin-like domains 1 and 2 and depends on the cytoplasmic domain and the level of surface expression. *J Biol Chem*. 1996;271:18561-18570

19. Sun QH, DeLisser HM, Zukowski MM, Paddock C, Albelda SM, Newman PJ. Individually distinct ig homology domains in pecam-1 regulate homophilic binding and modulate receptor affinity. *J Biol Chem*. 1996;271:11090-11098

20. Buckley CD, Doyonnas R, Newton JP, Blystone SD, Brown EJ, Watt SM, Simmons DL. Identification of alpha v beta 3 as a heterotypic ligand for cd31/pecam-1. *J Cell Sci*. 1996;109 (Pt 2):437-445

21. Newman PJ, Newman DK. Signal transduction pathways mediated by pecam-1: New roles for an old molecule in platelet and vascular cell biology. *Arterioscler Thromb Vasc Biol*. 2003;23:953-964

22. Muller WA, Weigl SA, Deng X, Phillips DM. Pecam-1 is required for transendothelial migration of leukocytes. *J Exp Med*. 1993;178:449-460

23. DeLisser HM, Christofidou-Solomidou M, Strieter RM, Burdick MD, Robinson CS, Wexler RS, Kerr JS, Garlanda C, Merwin JR, Madri JA, Albelda SM. Involvement of endothelial pecam-1/cd31 in angiogenesis. *Am J Pathol*. 1997;151:671-677

24. Gao C, Sun W, Christofidou-Solomidou M, Sawada M, Newman DK, Bergom C, Albelda SM, Matsuyama S, Newman PJ. Pecam-1 functions as a specific and potent inhibitor of mitochondrial-dependent apoptosis. *Blood*. 2003;102:169-179

25. Maas M, Stapleton M, Bergom C, Mattson DL, Newman DK, Newman PJ. Endothelial cell pecam-1 confers protection against endotoxic shock. *Am J Physiol Heart Circ Physiol*. 2005;288:H159-164

26. Privratsky JR, Paddock CM, Florey O, Newman DK, Muller WA, Newman PJ. Relative contribution of pecam-1 adhesion and signaling to the maintenance of vascular integrity. *J Cell Sci*. 2011;124:1477-1485

27. Ma L, Mauro C, Cornish GH, Chai JG, Coe D, Fu H, Patton D, Okkenhaug K, Franzoso G, Dyson J, Nourshargh S, Marelli-Berg FM. Ig gene-like molecule cd31 plays a nonredundant role in the regulation of t-cell immunity and tolerance. *Proc Natl Acad Sci U S A*. 2010;107:19461-19466

28. Wong MX, Hayball JD, Jackson DE. Pecam-1-regulated signalling thresholds control tolerance in anergic transgenic b-cells. *Mol Immunol*. 2008;45:1767-1781

29. Tzima E, Irani-Tehrani M, Kiosses WB, Dejana E, Schultz DA, Engelhardt B, Cao G, DeLisser H, Schwartz MA. A mechanosensory complex that mediates the endothelial cell response to fluid shear stress. *Nature*. 2005;437:426-431

30. Osawa M, Masuda M, Harada N, Lopes RB, Fujiwara K. Tyrosine phosphorylation of platelet endothelial cell adhesion molecule-1 (pecam-1, cd31) in mechanically stimulated vascular endothelial cells. *Eur J Cell Biol*. 1997;72:229-237

31. Osawa M, Masuda M, Kusano K, Fujiwara K. Evidence for a role of platelet endothelial cell adhesion molecule-1 in endothelial cell mechanosignal transduction: Is it a mechanoresponsive molecule? *J Cell Biol*. 2002;158:773-785

32. Chiu YJ, McBeath E, Fujiwara K. Mechanotransduction in an extracted cell model: Fyn drives stretch- and flow-elicited pecam-1 phosphorylation. *J Cell Biol*. 2008;182:753-763

33. Fleming I, Fisslthaler B, Dixit M, Busse R. Role of pecam-1 in the shear-stress-induced activation of akt and the endothelial nitric oxide synthase (enos) in endothelial cells. *J Cell Sci*. 2005;118:4103-4111

34. Liu Y, Collins C, Kiosses WB, Murray AM, Joshi M, Shepherd TR, Fuentes EJ, Tzima E. A novel pathway spatiotemporally activates rac1 and redox signaling in response to fluid shear stress. *J Cell Biol*. 2013;201:863-873

35. Chen Z, Tzima E. Pecam-1 is necessary for flow-induced vascular remodeling. *Arterioscler Thromb Vasc Biol*. 2009;29:1067-1073

36. Liu Y, Bubolz AH, Shi Y, Newman PJ, Newman DK, Gutterman DD. Peroxynitrite reduces the endothelium-derived hyperpolarizing factor component of coronary flow-mediated dilation in pecam-1-knockout mice. *Am J Physiol Regul Integr Comp Physiol*. 2006;290:R57-65

37. Chen Z, Rubin J, Tzima E. Role of pecam-1 in arteriogenesis and specification of preexisting collaterals. *Circ Res*. 2010;107:1355-1363

38. Harry BL, Sanders JM, Feaver RE, Lansey M, Deem TL, Zarbock A, Bruce AC, Pryor AW, Gelfand BD, Blackman BR, Schwartz MA, Ley K. Endothelial cell pecam-1 promotes atherosclerotic lesions in areas of disturbed flow in apoe-deficient mice. *Arterioscler Thromb Vasc Biol*. 2008

39. Goel R, Schrank BR, Arora S, Boylan B, Fleming B, Miura H, Newman PJ, Molthen RC, Newman DK. Site-specific effects of pecam-1 on atherosclerosis in ldl receptor-deficient mice. *Arterioscler Thromb Vasc Biol*. 2008

40. Stevens HY, Melchior B, Bell KS, Yun S, Yeh JC, Frangos JA. Pecam-1 is a critical mediator of atherosclerosis. *Dis Model Mech*. 2008;1:175-181; discussion 179

41. Jalali S, del Pozo MA, Chen K, Miao H, Li Y, Schwartz MA, Shyy JY, Chien S. Integrin-mediated mechanotransduction requires its dynamic interaction with specific extracellular matrix (ecm) ligands. *Proc Natl Acad Sci U S A*. 2001;98:1042-1046

42. Orr AW, Ginsberg MH, Shattil SJ, Deckmyn H, Schwartz MA. Matrix-specific suppression of integrin activation in shear stress signaling. *Mol Biol Cell*. 2006;17:4686-4697

43. Tzima E, del Pozo MA, Shattil SJ, Chien S, Schwartz MA. Activation of integrins in endothelial cells by fluid shear stress mediates rho-dependent cytoskeletal alignment. *EMBO J*. 2001;20:4639-4647

44. Funk SD, Yurdagul A, Jr., Green JM, Jhaveri KA, Schwartz MA, Orr AW. Matrix-specific protein kinase a signaling regulates p21-activated kinase activation by flow in endothelial cells. *Circ Res*. 2010;106:1394-1403

45. Yurdagul A, Jr., Chen J, Funk SD, Albert P, Kevil CG, Orr AW. Altered nitric oxide production mediates matrix-specific pak2 and nf-kappab activation by flow. *Mol Biol Cell*. 2013;24:398-408

46. Orr AW, Stockton R, Simmers MB, Sanders JM, Sarembock IJ, Blackman BR, Schwartz MA. Matrix-specific p21-activated kinase activation regulates vascular permeability in atherogenesis. *J Cell Biol*. 2007;176:719-727

47. Hahn C, Orr AW, Sanders JM, Jhaveri KA, Schwartz MA. The subendothelial extracellular matrix modulates jnk activation by flow. *Circ Res*. 2009;104:995-1003

48. Hahn C, Wang C, Orr AW, Coon BG, Schwartz MA. Jnk2 promotes endothelial cell alignment under flow. *PLoS One*. 2011;6:e24338

49. Knowles JW, Reddick RL, Jennette JC, Shesely EG, Smithies O, Maeda N. Enhanced atherosclerosis and kidney dysfunction in enos(-/-)apoe(-/-) mice are ameliorated by enalapril treatment. *J Clin Invest*. 2000;105:451-458

50. Wang J, An FS, Zhang W, Gong L, Wei SJ, Qin WD, Wang XP, Zhao YX, Zhang Y, Zhang C, Zhang MX. Inhibition of c-jun n-terminal kinase attenuates low shear stress-induced atherogenesis in apolipoprotein e-deficient mice. *Mol Med*. 2011;17:990-999

51. Feaver RE, Gelfand BD, Wang C, Schwartz MA, Blackman BR. Atheroprone hemodynamics regulate fibronectin deposition to create positive feedback that sustains endothelial inflammation. *Circ Res*. 2010;106:1703-1711

52. Malek AM, Alper SL, Izumo S. Hemodynamic shear stress and its role in atherosclerosis. *JAMA*. 1999;282:2035-2042

53. Orr AW, Sanders JM, Bevard M, Coleman E, Sarembock IJ, Schwartz MA. The subendothelial extracellular matrix modulates nf-kappab activation by flow: A potential role in atherosclerosis. *J Cell Biol*. 2005;169:191-202

54. Oberleithner H, Riethmuller C, Schillers H, MacGregor GA, de Wardener HE, Hausberg M. Plasma sodium stiffens vascular endothelium and reduces nitric oxide release. *Proc Natl Acad Sci U S A*. 2007;104:16281-16286

55. Huynh J, Nishimura N, Rana K, Peloquin JM, Califano JP, Montague CR, King MR, Schaffer CB, Reinhart-King CA. Age-related intimal stiffening enhances endothelial permeability and leukocyte transmigration. *Sci Transl Med*. 2011;3:112ra122

56. Chatzizisis YS, Giannoglou GD. Coronary hemodynamics and atherosclerotic wall stiffness: A vicious cycle. *Med Hypotheses*. 2007;69:349-355

57. Tracqui P, Broisat A, Toczek J, Mesnier N, Ohayon J, Riou L. Mapping elasticity moduli of atherosclerotic plaque in situ via atomic force microscopy. *J Struct Biol*. 2011;174:115-123

58. Dangaria JH, Butler PJ. Macrorheology and adaptive microrheology of endothelial cells subjected to fluid shear stress. *Am J Physiol Cell Physiol*. 2007;293:C1568-1575

59. Hoffman BD, Crocker JC. Cell mechanics: Dissecting the physical responses of cells to force. *Annu Rev Biomed Eng*. 2009;11:259-288

60. Choquet D, Felsenfeld DP, Sheetz MP. Extracellular matrix rigidity causes strengthening of integrin-cytoskeleton linkages. *Cell*. 1997;88:39-48

61. Martinez-Rico C, Pincet F, Thiery JP, Dufour S. Integrins stimulate e-cadherin-mediated intercellular adhesion by regulating src-kinase activation and actomyosin contractility. *J Cell Sci*. 2010;123:712-722

62. Tim O'Brien E, Cribb J, Marshburn D, Taylor RM, 2nd, Superfine R. Chapter 16: Magnetic manipulation for force measurements in cell biology. *Methods Cell Biol*. 2008;89:433-450

63. Garcia-Mata R, Wennerberg K, Arthur WT, Noren NK, Ellerbroek SM, Burridge K. Analysis of activated gaps and gefs in cell lysates. *Methods Enzymol*. 2006;406:425-437

64. Chretien ML, Zhang M, Jackson MR, Kapus A, Langille BL. Mechanotransduction by endothelial cells is locally generated, direction-dependent, and ligand-specific. *J Cell Physiol*. 2010;224:352-361

65. Raucher D, Stauffer T, Chen W, Shen K, Guo S, York JD, Sheetz MP, Meyer T. Phosphatidylinositol 4,5-bisphosphate functions as a second messenger that regulates cytoskeleton-plasma membrane adhesion. *Cell*. 2000;100:221-228

66. Pertz O, Hodgson L, Klemke RL, Hahn KM. Spatiotemporal dynamics of rhoa activity in migrating cells. *Nature*. 2006;440:1069-1072

67. Galbraith CG, Skalak R, Chien S. Shear stress induces spatial reorganization of the endothelial cell cytoskeleton. *Cell Motil Cytoskeleton*. 1998;40:317-330

68. Poh YC, Na S, Chowdhury F, Ouyang M, Wang Y, Wang N. Rapid activation of rac gtpase in living cells by force is independent of src. *PLoS One*. 2009;4:e7886

69. Wang Y, Botvinick EL, Zhao Y, Berns MW, Usami S, Tsien RY, Chien S. Visualizing the mechanical activation of src. *Nature*. 2005;434:1040-1045

70. Ilan N, Mahooti S, Rimm DL, Madri JA. Pecam-1 (cd31) functions as a reservoir for and a modulator of tyrosine- phosphorylated beta-catenin. *J Cell Sci*. 1999;112 Pt 18:3005-3014.

71. Ilan N, Cheung L, Pinter E, Madri JA. Platelet-endothelial cell adhesion molecule-1 (cd31), a scaffolding molecule for selected catenin family members whose binding is mediated by different tyrosine and serine/threonine phosphorylation. *J Biol Chem*. 2000;275:21435-21443

72. Tanaka Y, Albelda SM, Horgan KJ, van Seventer GA, Shimizu Y, Newman W, Hallam J, Newman PJ, Buck CA, Shaw S. Cd31 expressed on distinctive t cell subsets is a preferential amplifier of beta 1 integrin-mediated adhesion. *J Exp Med*. 1992;176:245-253

73. Varon D, Jackson DE, Shenkman B, Dardik R, Tamarin I, Savion N, Newman PJ. Platelet/endothelial cell adhesion molecule-1 serves as a costimulatory agonist receptor that modulates integrin-dependent adhesion and aggregation of human platelets. *Blood*. 1998;91:500-507

74. Lu TT, Yan LG, Madri JA. Integrin engagement mediates tyrosine dephosphorylation on platelet-endothelial cell adhesion molecule 1. *Proc Natl Acad Sci U S A*. 1996;93:11808-11813

75. Roca-Cusachs P, Gauthier NC, Del Rio A, Sheetz MP. Clustering of alpha(5)beta(1) integrins determines adhesion strength whereas alpha(v)beta(3) and talin enable mechanotransduction. *Proc Natl Acad Sci U S A*. 2009;106:16245-16250

76. Miyazaki H, Hayashi K. Atomic force microscopic measurement of the mechanical properties of intact endothelial cells in fresh arteries. *Med Biol Eng Comput*. 1999;37:530-536

77. Nigro P, Abe JI, Berk BC. Flow shear stress and atherosclerosis: A matter of site specificity. *Antioxid Redox Signal*. 2011

78. Ren XD, Kiosses WB, Schwartz MA. Regulation of the small gtp-binding protein rho by cell adhesion and the cytoskeleton. *EMBO J*. 1999;18:578-585

79. Wu CC, Li YS, Haga JH, Kaunas R, Chiu JJ, Su FC, Usami S, Chien S. Directional shear flow and rho activation prevent the endothelial cell apoptosis induced by micropatterned anisotropic geometry. *Proc Natl Acad Sci U S A*. 2007;104:1254-1259

80. Ohura N, Yamamoto K, Ichioka S, Sokabe T, Nakatsuka H, Baba A, Shibata M, Nakatsuka T, Harii K, Wada Y, Kohro T, Kodama T, Ando J. Global analysis of shear stress-responsive genes in vascular endothelial cells. *J Atheroscler Thromb*. 2003;10:304-313

81. Mammoto A, Connor KM, Mammoto T, Yung CW, Huh D, Aderman CM, Mostoslavsky G, Smith LE, Ingber DE. A mechanosensitive transcriptional mechanism that controls angiogenesis. *Nature*. 2009;457:1103-1108

82. Guilluy C, Swaminathan V, Garcia-Mata R, O'Brien ET, Superfine R, Burridge K. The rho gefs larg and gef-h1 regulate the mechanical response to force on integrins. *Nat Cell Biol*. 2011;13:722-727

83. Kuo JC, Han X, Hsiao CT, Yates JR, 3rd, Waterman CM. Analysis of the myosin-ii-responsive focal adhesion proteome reveals a role for beta-pix in negative regulation of focal adhesion maturation. *Nat Cell Biol*. 2011;13:383-393

84. Hirai T, Sasayama S, Kawasaki T, Yagi S. Stiffness of systemic arteries in patients with myocardial infarction. A noninvasive method to predict severity of coronary atherosclerosis. *Circulation*. 1989;80:78-86

85. Wang YX, Halks-Miller M, Vergona R, Sullivan ME, Fitch R, Mallari C, Martin-McNulty B, da Cunha V, Freay A, Rubanyi GM, Kauser K. Increased aortic stiffness assessed by pulse wave velocity in apolipoprotein e-deficient mice. *Am J Physiol Heart Circ Physiol*. 2000;278:H428-434

86. Guilluy C, Garcia-Mata R, Burridge K. Rho protein crosstalk: Another social network? *Trends Cell Biol*. 2011;21:718-726

87. Lang P, Gesbert F, Delespine-Carmagnat M, Stancou R, Pouchelet M, Bertoglio J. Protein kinase a phosphorylation of rhoa mediates the morphological and functional effects of cyclic amp in cytotoxic lymphocytes. *EMBO J*. 1996;15:510-519

88. Forget MA, Desrosiers RR, Gingras D, Beliveau R. Phosphorylation states of cdc42 and rhoa regulate their interactions with rho gdp dissociation inhibitor and their extraction from biological membranes. *Biochem J*. 2002;361:243-254

89. Ellerbroek SM, Wennerberg K, Burridge K. Serine phosphorylation negatively regulates rhoa in vivo. *J Biol Chem*. 2003;278:19023-19031

90. Mott RE, Helmke BP. Mapping the dynamics of shear stress-induced structural changes in endothelial cells. *Am J Physiol Cell Physiol*. 2007;293:C1616-1626

91. Davies PF, Robotewskyj A, Griem ML. Quantitative studies of endothelial cell adhesion. Directional remodeling of focal adhesion sites in response to flow forces. *J Clin Invest*. 1994;93:2031-2038

92. Hoffman BD, Massiera G, Van Citters KM, Crocker JC. The consensus mechanics of cultured mammalian cells. *Proc Natl Acad Sci U S A*. 2006;103:10259-10264

93. Wirtz D. Particle-tracking microrheology of living cells: Principles and applications. *Annu Rev Biophys*. 2009;38:301-326

94. Jin H, Garmy-Susini B, Avraamides CJ, Stoletov K, Klemke RL, Varner JA. A pka-csk-pp60src signaling pathway regulates the switch between endothelial cell invasion and cell-cell adhesion during vascular sprouting. *Blood*. 2010;116:5773-5783

95. Qiao J, Huang F, Lum H. Pka inhibits rhoa activation: A protection mechanism against endothelial barrier dysfunction. *Am J Physiol Lung Cell Mol Physiol*. 2003;284:L972-980

96. Birukova AA, Burdette D, Moldobaeva N, Xing J, Fu P, Birukov KG. Rac gtpase is a hub for protein kinase a and epac signaling in endothelial barrier protection by camp. *Microvasc Res*. 2010;79:128-138

97. Tkachenko E, Sabouri-Ghomi M, Pertz O, Kim C, Gutierrez E, Machacek M, Groisman A, Danuser G, Ginsberg MH. Protein kinase a governs a rhoa-rhogdi protrusion-retraction pacemaker in migrating cells. *Nat Cell Biol*. 2011;13:660-667

98. Howe AK, Juliano RL. Regulation of anchorage-dependent signal transduction by protein kinase a and p21-activated kinase. *Nat Cell Biol*. 2000;2:593-600

99. Howe AK, Hogan BP, Juliano RL. Regulation of vasodilator-stimulated phosphoprotein phosphorylation and interaction with abl by protein kinase a and cell adhesion. *J Biol Chem*. 2002;277:38121-38126

100. Whittard JD, Akiyama SK. Positive regulation of cell-cell and cell-substrate adhesion by protein kinase a. *J Cell Sci*. 2001;114:3265-3272

101. Yang B, Radel C, Hughes D, Kelemen S, Rizzo V. P190 rhogtpase-activating protein links the beta1 integrin/caveolin-1 mechanosignaling complex to rhoa and actin remodeling. *Arterioscler Thromb Vasc Biol*. 2011;31:376-383

102. Meiri D, Greeve MA, Brunet A, Finan D, Wells CD, LaRose J, Rottapel R. Modulation of rho guanine exchange factor lfc activity by protein kinase a-mediated phosphorylation. *Mol Cell Biol*. 2009;29:5963-5973

103. Saphirstein RJ, Gao YZ, Jensen MH, Gallant CM, Vetterkind S, Moore JR, Morgan KG. The focal adhesion: A regulated component of aortic stiffness. *PLoS One*. 2013;8:e62461

104. Matthews BD, Overby DR, Alenghat FJ, Karavitis J, Numaguchi Y, Allen PG, Ingber DE. Mechanical properties of individual focal adhesions probed with a magnetic microneedle. *Biochem Biophys Res Commun*. 2004;313:758-764

105. Bershadsky AD, Balaban NQ, Geiger B. Adhesion-dependent cell mechanosensitivity. *Annu Rev Cell Dev Biol*. 2003;19:677-695

106. Alenghat FJ, Nauli SM, Kolb R, Zhou J, Ingber DE. Global cytoskeletal control of mechanotransduction in kidney epithelial cells. *Exp Cell Res*. 2004;301:23-30

107. Ingber DE. Cellular mechanotransduction: Putting all the pieces together again. *FASEB J*. 2006;20:811-827

108. Hughes PE, Pfaff M. Integrin affinity modulation. *Trends Cell Biol*. 1998;8:359-364

109. Tengholm A, Meyer T. A pi3-kinase signaling code for insulin-triggered insertion of glucose transporters into the plasma membrane. *Curr Biol*. 2002;12:1871-1876

110. Hammond GR, Sim Y, Lagnado L, Irvine RF. Reversible binding and rapid diffusion of proteins in complex with inositol lipids serves to coordinate free movement with spatial information. *J Cell Biol*. 2009;184:297-308

111. Friedland JC, Lee MH, Boettiger D. Mechanically activated integrin switch controls alpha5beta1 function. *Science*. 2009;323:642-644

112. Sun Z, Martinez-Lemus LA, Hill MA, Meininger GA. Extracellular matrix-specific focal adhesions in vascular smooth muscle produce mechanically active adhesion sites. *Am J Physiol Cell Physiol*. 2008;295:C268-278

113. Kim S, Bakre M, Yin H, Varner JA. Inhibition of endothelial cell survival and angiogenesis by protein kinase a. *J Clin Invest*. 2002;110:933-941

114. Kobayashi K, Tsubosaka Y, Hori M, Narumiya S, Ozaki H, Murata T. Prostaglandin d2-dp signaling promotes endothelial barrier function via the camp/pka/tiam1/rac1 pathway. *Arterioscler Thromb Vasc Biol*. 2013;33:565-571

115. Birukova AA, Zagranichnaya T, Fu P, Alekseeva E, Chen W, Jacobson JR, Birukov KG. Prostaglandins pge(2) and pgi(2) promote endothelial barrier enhancement via pka- and epac1/rap1-dependent rac activation. *Exp Cell Res*. 2007;313:2504-2520

116. Sato M, Ohshima N, Nerem RM. Viscoelastic properties of cultured porcine aortic endothelial cells exposed to shear stress. *J Biomech*. 1996;29:461-467

117. Sato M, Nagayama K, Kataoka N, Sasaki M, Hane K. Local mechanical properties measured by atomic force microscopy for cultured bovine endothelial cells exposed to shear stress. *J Biomech*. 2000;33:127-135

118. del Alamo JC, Norwich GN, Li YS, Lasheras JC, Chien S. Anisotropic rheology and directional mechanotransduction in vascular endothelial cells. *Proc Natl Acad Sci U S A*. 2008;105:15411-15416

119. Sato M, Levesque MJ, Nerem RM. Micropipette aspiration of cultured bovine aortic endothelial cells exposed to shear stress. *Arteriosclerosis*. 1987;7:276-286

120. Hur SS, del Alamo JC, Park JS, Li YS, Nguyen HA, Teng D, Wang KC, Flores L, Alonso-Latorre B, Lasheras JC, Chien S. Roles of cell confluency and fluid shear in

3-dimensional intracellular forces in endothelial cells. *Proc Natl Acad Sci U S A*. 2012;109:11110-11115

121. Langille BL, Reidy MA, Kline RL. Injury and repair of endothelium at sites of flow disturbances near abdominal aortic coarctations in rabbits. *Arteriosclerosis*. 1986;6:146-154

122. Kano Y, Katoh K, Fujiwara K. Lateral zone of cell-cell adhesion as the major fluid shear stress-related signal transduction site. *Circ Res*. 2000;86:425-433

123. Hayenga HN, Trache A, Trzeciakowski J, Humphrey JD. Regional atherosclerotic plaque properties in apoe-/- mice quantified by atomic force, immunofluorescence, and light microscopy. *J Vasc Res*. 2011;48:495-504

124. Kliche K, Jeggle P, Pavenstadt H, Oberleithner H. Role of cellular mechanics in the function and life span of vascular endothelium. *Pflugers Arch*. 2011;462:209-217

125. Yla-Herttuala S, Palinski W, Rosenfeld ME, Parthasarathy S, Carew TE, Butler S, Witztum JL, Steinberg D. Evidence for the presence of oxidatively modified low density lipoprotein in atherosclerotic lesions of rabbit and man. *J Clin Invest*. 1989;84:1086-1095

126. Byfield FJ, Tikku S, Rothblat GH, Gooch KJ, Levitan I. Oxldl increases endothelial stiffness, force generation, and network formation. *J Lipid Res*. 2006;47:715-723

127. Wei D, Chen Y, Tang C, Huang H, Liu L, Wang Z, Li R, Wang G. Ldl decreases the membrane compliance and cell adhesion of endothelial cells under fluid shear stress. *Ann Biomed Eng*. 2013;41:611-618